

---

# Quantum dynamics of non-perturbative solutions

Andrei Kovtun

---



München 2022



---

# Quantum dynamics of non-perturbative solutions

Andrei Kovtun

---

Dissertation  
an der Fakultät für Physik  
der Ludwig-Maximilians-Universität  
München

vorgelegt von  
Andrei Kovtun  
aus Ischvsk

München, den 21.11.2022

Erstgutachter: Prof. Dr. Gia Dvali

Zweitgutachter: Prof. Dr. Dieter Lüst

Tag der mündlichen Prüfung: 12.12.2022

# Contents

<b>Zusammenfassung</b>	<b>ix</b>
<b>Abstract</b>	<b>x</b>
<b>1 Introduction</b>	<b>1</b>
<b>2 Quantum breaking</b>	<b>11</b>
2.1 Notion of semi-classical system . . . . .	11
2.2 Corpuscular picture of quantum breaking . . . . .	13
2.3 Quantum breaking from the entropy point of view . . . . .	14
2.4 Quantum breaking as a growth of quantum fluctuations . . . . .	15
2.5 Quantum breaking criterion . . . . .	17
<b>3 2PI effective action</b>	<b>19</b>
3.1 General description of 2PI formalism . . . . .	20
3.1.1 Definition . . . . .	20
3.1.2 Stationary conditions . . . . .	22
3.1.3 Renormalization . . . . .	26
3.1.4 Initial conditions and time-contour . . . . .	27
3.1.5 Generalized Ward-Takahashi identities . . . . .	32
3.2 Quantum breaking criterion using 2PI . . . . .	35
<b>4 Semi-classical theory of a stationary solutions</b>	<b>41</b>
4.1 Classical stable condensate . . . . .	42
4.1.1 Classical solution . . . . .	42
4.1.2 Stability of the condensate . . . . .	44
4.2 Initial conditions for the simulation . . . . .	46
<b>5 Quantum evolution of the stable condensate</b>	<b>51</b>
5.1 Numerical simulations . . . . .	51
5.2 Comparison with the perturbative expansion . . . . .	56

---

<b>6</b>	<b>Classically unstable condensate</b>	<b>61</b>
6.1	Fast quantum breaking . . . . .	61
6.2	Classical theory . . . . .	62
6.2.1	Condensate . . . . .	63
6.2.2	Bright Soliton . . . . .	64
6.2.3	Classical stability as the reflection of an interplay between two solutions	65
6.2.4	Saddle-point solution as the initial condition . . . . .	67
6.3	Numerical Simulations . . . . .	68
6.3.1	Evolution along the BEC trajectory . . . . .	70
6.3.2	Quantum break-time . . . . .	73
	<b>Conclusion</b>	<b>76</b>

# List of Figures

1.1	Here three types of trajectories are depicted. The green line shows all the possible states of the physical systems. The brown dots show stable stationary states, the purple dots show unstable stationary states, and blue lines show trajectories. . . . .	3
4.1	Energy $E_{BC}$ of a stable condensate as a function of charge $Q$ versus the energy of the collection of free particles with the same net charge. . . . .	44
4.2	Field values for saddle-point and 1-loop approximations for $\lambda = 1$ , $m = 1$ , $L = 10 m^{-1}$ . . . . .	49
5.1	Time dependence of the classical and full charges for $\omega = 3$ and $\lambda = 0.5$ . . . . .	52
5.2	Time dependence of $Q_q$ for different frequencies $\omega$ . . . . .	52
5.3	Time dependence of $Q_{cl}$ normalized by the initial value for different frequencies $\omega$ . . . . .	53
5.4	Quantum break-time as a function of the full charge . . . . .	55
5.5	Quantum break-time as a function of period of initial classical oscillations . . . . .	55
5.6	Behaviour of the classical and quantum charge for long time. Conservation of charge is showed. Here $\omega = 1.1$ , $\lambda = 0.5$ . . . . .	56
5.7	Perturbative expansion compared with fully resummed 2PI for $\lambda = m^2$ and $\omega = 1.1 m$ . . . . .	59
6.1	Bright soliton solution for different frequencies $\omega$ and length $L = 4\pi m^{-1}$ . . . . .	64
6.2	Energy versus charge behaviour of condensate and soliton. Here $L = 4\pi m^{-1}$ and $\lambda = 2m^2$ . . . . .	67
6.3	Time dependence of the classical charge for different frequencies in the strong coupling regime. . . . .	69
6.4	Time dependence of the classical charge for different frequencies in the weak coupling regime. . . . .	69
6.5	Time evolution of the classical energy $E_{cl}(t)$ as a function of $Q_{cl}(t)$ for different $\omega \in (.90, \omega_{cr})$ (each with a different marker). Here the evolution follows the classical condensate trajectory. . . . .	71

---

6.6	Time evolution of the classical energy $E_{cl}(t)$ as a function of $Q_{cl}(t)$ for different $\omega \in (.81, \omega_{cr})$ (each with a different marker). The failure of the simulation is apparent as $\omega$ decreases. . . . .	72
6.7	Quantum breaking time dependence on $\omega$ compared to analytical estimation. Solid lines are functions $\log Q(\omega, \lambda)/\text{Im}(\gamma_-(p_1))$ for different couplings and triangles are quantum breaking times extracted from simulations . . . . .	75



# Zusammenfassung

Ziel dieser Arbeit ist es, ein kürzlich eingeführtes Phänomen namens Quantenbruch zu untersuchen. Dieses Phänomen steht für die Zerstörung der makroskopischen Gesamtdynamik des halbklassischen Systems aufgrund der Quanteneffekte und drückt sich in der Erfassung des Unterschieds zwischen der klassischen Evolution und ihrer wahren (oder vollständigen) Quantenevolution aus. Hier möchte ich einige Punkte ansprechen.

In erster Linie geht es darum, einen einheitlichen Formalismus für die Berechnung der ungefähren Quantenevolution einzuführen, um nicht triviale dynamische Effekte zu erfassen. Dies scheint unerlässlich zu sein, da alle bisher in der Literatur betrachteten Ansätze besonderen Merkmalen der betrachteten Systeme unterworfen waren und sich voneinander unterschieden. Es ist also immer praktisch, einen Ansatz zu haben, der eine breite Anwendbarkeit ermöglicht. Dieser Ansatz bewältigt zwei Probleme: die Berechnungsmethode der Evolution und das allgemeine Kriterium zur Identifizierung der Zeitskala, die mit dem Quantenbruch verbunden ist.

Das zweite Ziel besteht darin, die Quantenevolution tatsächlich zu simulieren und Quantenbrüche für mehrere relativistische Systeme zu erkennen, die in der Theorie des komplexen Skalarfelds auftauchen, und diese Ergebnisse mit denen zu vergleichen, die bereits in früheren Forschungen erzielt wurden.

Die hier betrachteten Systeme sind stabile und instabile Bose-Einstein-Kondensate, die in der komplexen Skalarfeldtheorie entstehen. Die Evolution wurde in beiden Fällen berechnet, indem eine irreduzible effektive Aktion mit zwei Teilchen verwendet wurde, die mit der Integrationskontur "*in-in*" ausgestattet war. Anhand des neu eingeführten Kriteriums wurden Zeitskalen des Quantenbruchs identifiziert und mit bereits in der Literatur erhaltenen verglichen.



# Abstract

The goal of this work is to study a recently introduced phenomenon called quantum breaking. This phenomenon stands for the destruction of the overall macroscopic dynamics of the semi-classical system due to the quantum effects, and is expressed in the capturing the difference between the classical evolution, and its true (or full) quantum evolution. Here, I would like to address several points.

The first and foremost, is to introduce a unified formalism for computing approximate quantum evolution to capture non-trivial dynamical effects. It seems to be essential to do that, because all the approaches considered in the literature so far were subjected to peculiar features of the systems under consideration, and were different from one another. So, it is always handy to have an approach allowing for broad applicability. This approach manages two problems: the method of computation of the evolution, and the general criterion to identify timescale associated with quantum breaking.

The second goal, is to actually simulate quantum evolution and detect quantum breaking for several relativistic systems emerging in the theory of the complex scalar field, and compare these results to the ones already obtained in previous research.

The systems that are considered here are stable and unstable Bose-Einstein condensates emerging in the complex scalar field theory. The evolution was computed in both cases by using two-particle irreducible effective action equipped with “*in-in*” integration contour. Timescales of the quantum breaking were identified on the basis of the newly introduced criterion, and compared to those obtained in literature already.



# Chapter 1

## Introduction

In the most general terms, there are two types of problems that bother the minds of physicists. The first one is the structure of the physical body, namely, what it is composed of? The second problem is the evolution of the physical system, which is no less essential than the first one because our knowledge serves nothing if we cannot make predictions. But the evolution of the physical system could be also of several types. A system can evolve as a whole, meaning that it moves in space and time without changing its structure, in which case the structure can be ignored. Another possibility is the internal evolution when the structure of the system itself is going through transformations. And, surely, we can combine both, and consider all the subtleties of the full evolution, which is usually incredibly cumbersome. In the best case, we would like to be able to describe both, its structure and its dynamics. Nevertheless, depending on circumstances, we could ignore either one to make our job easier. For instance, in mechanics if a body is rigid enough we could not care less about its structure, and focus on its macroscopic trajectory. Or, in considering crystals, we can keep the whole body resting and study its internal structure. We do this because in the real life we lack capabilities to describe the system with infinite precision. Therefore, we always must be aware up to what degree we can neglect some particular characteristics of a system in favour of others, more relevant ones. In this work, I would like to ask precisely this question, namely, how long we can ignore not only the internal structure in favour of macroscopic dynamics of a physical system, but for how long we can ignore the quantumness, or in other words, quantum nature of this structure. But before we come to that, let me set up some terminology in order to discuss dynamical properties of physical systems.

When we study evolution, the starting point usually is the initial conditions. We choose from which state system will start to evolve. Hence, it makes sense to classify possible sets of initial conditions because different initial conditions will lead to different trajectories, and trajectories themselves can be united into similarity classes, or classified. To clarify this, let me introduce the general term of trajectory. When we talk about a trajectory, we mean the sequence of states which the system is going through when time passes by. And trajectories could be of two types, namely, stationary and non-stationary. Stationary trajectory is such that the system is reproducing itself over some period of time, or remains the same. If it

remains the same, it is called static, but we can still consider it as a stationary trajectory with infinitely small period. And the rest of the trajectories are non-stationary meaning that leaving the initial state system never comes back, and undergoes sequence of changes which leads to the uncontrollable deviation from initial state. The kind of trajectory the system chooses depends on the initial conditions. As physicists, we can think of initial conditions as of the initial assembling of the system. So, it is a configuration that we build, and then let go to evolve. Now, once we have assembled initial state it can evolve either trivially, namely, the trajectory is stationary or static, or it can get away from the initial state. In general, of course we are interested to explore all the possibilities, but practically if we want to build something we wish it to remain in the same state as long as we need. Hence, the question arises. What kind of initial configurations will provide us trivial evolution? If we look at this from a purely mathematical point of view, then we can determine with infinite precision some set of initial conditions which will provide us trivial evolution. And other initial conditions will lead to the evolution which will take us further away from initial state. We will refer to the first type of initial conditions as stable ones, and the other as unstable ones. All possible initial conditions can be found in the so-called phase space of the theory, which is the space of all possible configurations of the system. And when we choose initial conditions, it means that we choose some point in the phase space. So, we can classify the points of the phase space as the stable and unstable.

Here we must pause and mention that it is time we draw a distinction between classical and quantum physics. Of course, what does concern us the most is the situation in quantum physics, although I would like to make a detour and elaborate on the issue of stability in the classical physics first.

As I have mentioned already, we pick initial conditions from the phase space of the theory. After we have done that, the system follows the trajectory defined by the initial point. At the level of classical physics, we can classify all such points with regard to the trajectory along which the system evolves after starting at a given point. These trajectories can be called stable, and unstable [1].

The stable trajectories are those starting from which the system remains at the same spot in the phase space, in other words has a static evolution, or evolves along cyclic trajectory meaning has a stationary trajectory. The same goes for the pseudo-stable points, but with one important distinction. Truly stable points are like wells where if we move our system a little from the stable point the trajectory while being non-trivial will remain in the vicinity of the static trajectory, and never departures too far from it, always remaining close to the static trajectory. The same goes for the points leading to stationary evolution. However, it may happen that some particular point in the phase space could be such that it leads to the static or stationary trajectory if the system is put there with infinite precision, but uncontrollable departure from this point happens even if there is an infinitely small displacement from this point. These points are called unstable, although the exact infinitely precise trajectory is static or stationary. And, the other points are truly unstable, meaning that system being put even at the exact this point will immediately start to depart and not coming back.

We can illustrate all this situation using the example of a material dot. You can

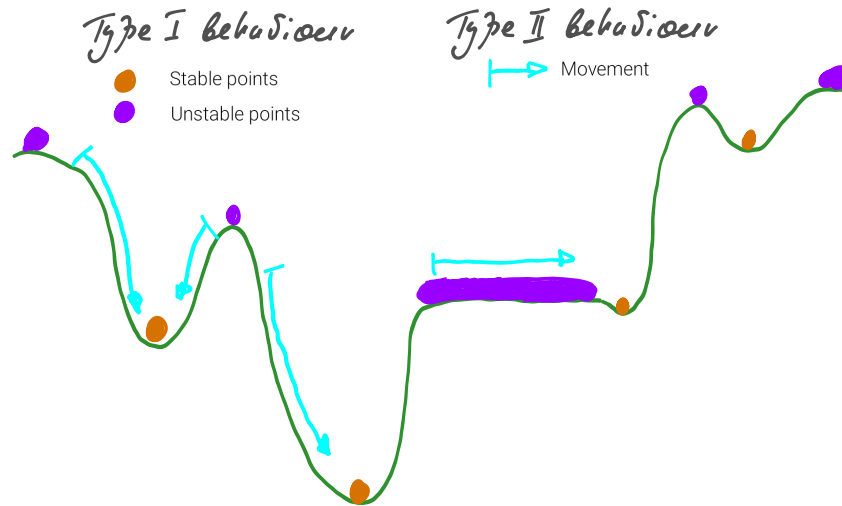


Figure 1.1: Here three types of trajectories are depicted. The green line shows all the possible states of the physical systems. The brown dots show stable stationary states, the purple dots show unstable stationary states, and blue lines show trajectories.

see that depending on the initial placement, material dot can experience different types of behaviour, which are depicted in Fig. 1.1. The same holds for compound system. We can assemble it in several ways some of which can be stable, and as a result of this assembling the compound system preserves its state or at least remains at the vicinity of the assembled configuration, or it can break. For instance, we can consider a conducting ball where we have initially distributed electric charge homogeneously across the whole ball [2]. Apparently, this configuration will not hold, and the charge will start instantly redistributing itself along the surface of the ball, namely, it will be redistributed on a sphere.

In classical physics there is a way to determine if the particular point in the phase space, or some set of points, trajectory, is stable. This method is called Lyapunov stability analysis [3]. Within this analysis we look for a particular point in phase space and then analyse small perturbations around this point. In this way we can say if the system is stable.

So, classically, we know how to figure out if the system will sustain its state without significant external intrusion. Now, assume we achieved this stability. And at this point, we let quantum mechanics come into play. Once we are finished with our assembly of classical system, we can ask ourselves what is going to happen when we take into account the quantum nature of our system.

Quantum mechanics changes the phase space of a system meaning it becomes quantized [4], and continuing with another fact that some new trajectories that were previously prohibited may appear [5].

Some examples we can give right away. For a starter, recall false vacuum decay [6, 7]. The system penetrates the potential barrier from the point where it classically rests. Although, this process is exponentially long, it still drives the system away from the point where it was classically stable.

Another example which is of similar nature is the systems with instantons [8, 9, 10, 11]. When we think of a classical system, say material dot again, it can occupy only point in the phase space at a given moment of time. But in the case of a dot in double well potential in quantum mechanics, we encounter that it can exist in several points of phase space simultaneously. Similar degeneracy exists in the field theory, e.g., for the instantons in gauge theories, where due to tunnelling between different classical vacua a quantum superposition arises as a new combined vacuum state [12, 13].

Thus, due to tunnelling processes, we can see that classical stability is jeopardized by the laws of quantum physics. However, let us ask a question, are the tunnelling process which take exponential time to kick in the only way to disturb classical stability? Can the quantum mechanical nature of the system let us know about itself way earlier than  $e^S$  time provided by tunnelling? The answer is *yes*, and it can happen precisely for systems that are compound. Look at the material dot. Intuition tells us that there are only two ways it can be actually disturbed, either it is kicked out of the well by hand (or by leg), or it can tunnel through a potential barrier. But the reason for that is the ridiculous simplicity of this system, namely there is no degeneracy of this state which leads to little, or even absent entropy. Now, if we think of the compound system it is apparent that there could be plenty of configurations, or in other words, plenty of ways to assemble it in such fashion that all the assemblies are degenerate or nearly degenerate and occupy the same space in the phase space of the theory. But classically, it could happen that a system being assembled in one domain of space can not change its configuration to the other version of assemblies. Here, we come to the point when it is evident that huge degeneracy can arise due to large amount of components. Therefore, it makes sense to look for a faster way of quantum laws disturbing the classical stability within the systems that are assembled from large amount of constituents. Namely, we can consider breakdown of a compound system comprised out of numerous constituents. This is something that we call quantum breaking. This is the breaking of the system which is semi-classical, namely, large enough (in terms of large number of its constituents), so, it could live long enough without letting us know about its quantum nature. And, in this work, I will study systems within the framework of Quantum Field Theory that could be subjected to this kind of breakdown.

Among all possible configurations being studied in Quantum Field Theory, there is a class of solutions establishing the bond between quantum and classical field theory, namely the semi-classical non-perturbative solutions. The current understanding of these objects in Quantum Field Theory is somewhat problematic because the quantum field is an assembly of infinitely many degrees of freedom, which usually makes it impossible to find eigenstates of the Hamiltonian governing the dynamics of the quantum field. However, there are several exceptions presented by integrable models. But if we start from the classical solution to field equations, there is no general method that allows us to build the corresponding quantum state, that is the eigenstate of the quantum Hamiltonian (if there



is one at all). These kinds of configurations that we are talking about are very versatile, and not all of them apparently can exhibit breaking.

First, let me clarify what is meant by semi-classical configuration in quantum field theory. Let us assume that we have some field classical field  $\phi$ . If we know the field function, we can compute classical action of this field configuration  $S[\phi]$ . This configuration is called semi-classical if condition

$$S[\phi] \gg \hbar$$

is satisfied [14].

Then we are interested if this configuration is classically stable. In order to figure this out, we check if this configuration is a stationary point of the action

$$\frac{\delta S[\phi]}{\delta \phi} = 0,$$

and study Lyapunov stability of this configuration by looking at the small perturbations  $\delta\phi$  around the configuration that we are considering  $\phi$ . Then, if it is indeed a stable stationary point of the action we can feel safe about this configuration in classical theory, and move to the analysis of the quantum mechanical picture.

There are plenty of different semi-classical solutions in quantum field theory. Two main groups are solitons [15], and condensates [16, 17]. Solitons are configurations of the field having finite size and energy that can exist in the infinite space volume. Among these solutions, there are two big classes, topological [18, 19] and non-topological solitons [20, 21]. However, solitons are not the most suitable object for the analysis of quantum stability because many of them do not really have internal structure, and in spite of them being treated as finite-size (even a large size) semi-classical objects their configurations are usually particle-like anyway and do not exhibit significant degeneracy, especially this concerns topological solitons. Condensates are a bit more interesting in this regard. These are configurations of the field confined within the finite volume, and if described from the field theoretical point of view usually have either large occupation numbers, or large global quantum numbers. Also, condensates in field theory are usually considered as homogeneous solutions. Thereby, it is a very suitable set of systems in quantum field theory to study their fate determined by their inherent quantumness. Now, let us dig deeper in what does quantum breaking actually means.

Quantum breaking is the idea that a given semi-classical solution, due to its quantum nature, might not be eternally faithful in describing the evolution of a system. In fact, due to quantum effects, a system might deviate in time from the semi-classical trajectory and significantly change its structure, therefore making the aforementioned mean-field approximation eventually unreliable. The concept that macroscopic objects can lose their classicality and become more “quantum” after a certain critical timescale was first introduced and developed in a series of papers [22, 23, 24, 25] motivated by a microscopic composite picture of a black hole, and it was later generalized to various systems, such as inflationary cosmologies and axion field [26, 27]. The outcome of these studies was that certain macroscopic systems, that are usually assumed to be well-described classically, in reality, exhibit a rather short quantum break-time.

One way to address the problem of the quantum fate of semi-classical solutions has been addressed in [23, 28, 26] where explicit corpuscular models were built. In these works, the classical solution is explicitly constructed as a coherent state of weakly coupled free quanta, and, because this state is not an eigenstate of the full non-linear interacting hamiltonian, due to unitary evolution, the system will depart from its initial configuration. Since in these realizations the quanta are weakly coupled, perturbative estimates can be made regarding the timescale after which the system will deviate significantly from its initial coherent state structure. Such a timescale has been named *quantum break time*  $t_{qb}$  [24, 27] and it is generically set by the strength of the interaction coupling  $\lambda$  and some classical timescale naturally embedded in the system

$$t_{qb} \sim \frac{t_{cl}}{\lambda}. \quad (1.1)$$

Even though the coherent state point of view has proved fruitful as it gave interesting insights on many different topics such as black hole evaporation and information paradox, eternal inflation and cosmic axion [28, 24, 27], it only provides estimates for the quantum break time and, therefore, further investigation of this issue is needed. Nevertheless, there is one work where detailed numerical investigation of the quantum breaking for Bose-Einstein condensate was performed. Namely, in [29] the connection between phenomena of quantum breaking and chaos was established and it was argued that a many-body macroscopic system can undergo a maximally fast quantum breaking and become chaotic, provided it possesses a Lyapunov exponent  $\gamma$ , with the following formula for quantum break-time:

$$t_{qb} \sim \gamma^{-1} \log N, \quad (1.2)$$

where  $N$  is a certain macroscopic particle number (e.g., the number of off-shell gravitons in the black-hole case, or the particle number in a non-relativistic BEC). In [29], this equation was explicitly checked on an example of a 1+1 dimensional system with Lyapunov exponent, namely a non relativistic unstable BEC. The above mentioned quantity was derived by means of entanglement arguments. Moreover it was also suggested that quantum breaking and chaos represent the microscopic mechanisms behind the so-called phenomenon of quantum information scrambling and that the existence of Lyapunov exponent is crucial for a system to saturate the logarithmic bound on the fast scrambling time proposed in [30]. It is argued that these kinds of systems are the ones which break the fastest<sup>1</sup>.

However, as we can see all these studies approach the problem from different sides, and with different degree of qualitiveness meaning they lack conventional or, so to say, unified approach. Hence, I deem it is important to fill this gap, and introduce some method which will not rely on peculiarities of particular system, and is equally applicable to the relativistic and non-relativistic fields. So, let's figure out how can we reach this goal.

There are several ingredients that give us a hint to the way we can pursue this matter. First, the properties of the system itself, namely, its classicality. The most handy approach, which is known for treating semi-classical systems, is the mean-field method [31]. This

<sup>1</sup>There are systems where  $t_{qb} \propto \hbar^{-1}$  c.f. [22], which is much longer than (1.2)

approach, also tells us the most convenient tool for computations, which is path integral. The only thing that we have to figure out is how we could treat evolution in the finite time-range via path integral. Here, we could use a help from the side of out-of equilibrium quantum field theory [32, 33]. We push the semiclassical treatment beyond the saddle point approximation by using the two-particle-irreducible (2PI) effective action [34, 35, 36, 37, 38, 39, 40].<sup>2</sup> This effective action treats both the expectation value of the field and the connected propagator as independent variables and correspondingly takes into account their mutual interaction, thus allowing us to account for back-reactions on the background and vice-versa. Using this approach we can resolve the quantum dynamics of the system integrating the equations of motion derived as the stationarity condition of the 2PI effective action functional [41, 42, 43, 44]. In order to obtain a real time evolution and observe the departure from the initial classical state (quantum breaking) explicitly, we integrate the equations of motion in the so called Schwinger-Keldysh (or *in-in*) formalism. This choice simplifies our task for two reasons: first, only the initial state needs to be specified as opposed to the *S-matrix* formalism, where also an asymptotic out state is required. Secondly, solving the integro-differential set of equations becomes numerically affordable, as the evolution is guaranteed to be causal.

After describing the tools for studying the evolution of classical solutions, we are ready to specify a particular system we are going to work with. We consider a Bose-Einstein condensate [45, 46]. There are several reasons for this choice. Firstly, BEC's appear in a various different branches of physics, not only in the condensed matter [17, 47, 48, 49] but also in high energy physics (such as for corpuscular black holes [28], de Sitter [26, 50], dark matter description [51, 52, 53, 54, 55], inflation [56, 57, 58], etc.). Secondly, there is an extremely simple way to assemble a condensate on field theory, namely, homogeneous, which simplifies the analysis significantly. And, the last but no the least is that there are several works where BEC configurations have been already studied from the point of view of quantum breaking, and it is essential to have a comparison of the results when implementing a novel approach.

The model we are going to focus on is the simplest one: namely a homogeneous relativistic BEC in  $1+1$  dimensions described by a  $SO(2)$  symmetric scalar theory [59, 20, 60] with a quartic self-interaction. Moreover, the analysis will be done for both types of the quartic interaction, repulsive and attractive, both demonstrating versatile behaviour [61, 62]. This allows to comprehend several aspects of the quantum breaking phenomenon, namely, different scaling of quantum break-time with the  $\hbar$ . In fact, for this system, it was possible to resolve explicitly its causal evolution as well as its departure from the classical trajectory.

To obtain all this, we work in the semi-classical framework of 2PI effective action. In fact, with this method we are able to study the unitary Minkowski-time evolution of a quantum coherent state mimicking a relativistic Bose-Einstein condensate. In turn, this allows us to check how the system dynamically deviates from the mean-field condensate

---

<sup>2</sup>The advantage of the semi-classical treatment, which is especially evident in light of the corpuscular approach, is that it does not rely on the corpuscular structure, though it still provides an instrument to capture some interesting quantum effects.

solution. To do so, we introduce a criterion which can be easily applied for identifying the timescale associated to quantum breaking for various semi-classical systems well-described within mean-field approach [63, 64]. Namely, we look at the dynamical evolution of the conserved integral quantity constraining the system i.e., charge<sup>3</sup>. This quantity is exactly conserved due to Nöther's theorem, so, it is not directly evident how we can use it to define quantum breaking. To understand that we have to take into account that a quantum field is an object having infinitely many degrees of freedom, and charge is a composite quantity, which can contain all possible degrees of freedom. Invoking general knowledge of the corpuscular structure of the condensate coming from Bogolyubov theory [65], we treat mean-field as the assembly of zero modes, which results into non-zero expectation value, or we can also approach this issue from the coherent state point of view, and construct Bose-Einstein condensate as a coherent state [66, 67, 68, 69, 70], namely, an eigenstate of a zero-momentum annihilation operator  $\hat{a}_0$ . Hence, zero-mode contribution is the semi-classical one, and the rest can be regarded as quantum, as it represents quantum fluctuations above the background mean-field. Thus, we see that there is a distinction between classical charge coming from large occupation number of one particular mode, and small occupation numbers of all the other modes. But all the contributions combine must provide conservation of the charge anyway. If we were studying this system in the S-matrix formalism, then we would fix asymptotic state, and, therefore, would not manage to capture significant deviation from the status quo. However, since we are working within the 2PI framework, such composite quantity receives two contributions from the one- and the two-point expectation values respectively (note that these quantities balance each other out because of the above-mentioned symmetry to each order in loop-expansion in case of an  $\hbar$  expansion [71]). We will refer to the mean-field contribution coming from large zero-momentum mode occupation as classical charge  $Q_{cl}$ , and to the contribution coming from the connected part of the two-point Green's function as quantum charge  $Q_q$ . Then, we will study their evolution along closed *in-in* contour in Schwinger-Keldysh formalism. At the beginning of the evolution, the ratio between  $Q_{cl}$  and  $Q_q$  is fixed by the initial conditions. As one would expect, for a coherent or vastly occupied by single mode state describing a classical configuration, we have that  $Q_{cl} \gg Q_q$ . However, as the system evolves, this needs not be the case any more. It is therefore natural to define quantum breaking as the timescale when the two above-mentioned quantities become comparable. A great advantage from this criterion is obtained, as there is no need to deal with rescattering effects at the microscopic level, although one could infer it from the diagrams retained within a given 2PI expansion scheme. It is worth mentioning that in principle different integral quantities could serve as a mean to estimate the quantum break time as long as their conservation constrains the dynamics of the system. For example, one could equally use energy or, in the case of a non-relativistic system, the actual occupation number of all the modes, namely, the particle number. In the present work, however, our main focus is charge since, as we will see below, the contributions from the 1- and the 2-point expectation values, split in a

---

<sup>3</sup>We would like to remark that one could choose any other conserved integral quantity provided that it is possible to split it in a certain way, which we will later name as *quantum* and *classical* contributions.

---

very clear and manageable manner, which very straightforward as the charge is bilinear, as well as 2-point Green's function, and cluster decomposition dictates

$$\langle\phi(x)\phi(y)\rangle_{\text{full}} = \langle\phi(x)\rangle\langle\phi(y)\rangle + \langle\phi(x)\phi(y)\rangle_{\text{connected}}.$$

And this property is very efficiently captured by 2PI formalism.

Before we proceed with the treatment, let me encounter the main steps of the whole enterprise.

First, I will discuss in the very detail the nature of semi-classicality, and provide an intuitive picture of the phenomenon of quantum breaking. Then, I will summarize all the approaches known so far in the literature to the computation of the quantum break-time.

Second, I will describe mathematical formalism that fits for the approach I have chosen, and set all definitions to proceed along this way.

After that, I will describe the system to be considered in the very detail, and provide the initial conditions for the quantum evolution.

Then, we will come to the most important part – the computation itself, and compare naive perturbative analysis with the 2PI approach. It will be shown, that perturbative analysis is insufficient for capturing true quantum evolution during a long timescale.

In the end, I will wrap everything up in the short summary, and prospects of the following research.



# Chapter 2

## Quantum breaking

### 2.1 Notion of semi-classical system

A physical world yields a variety of different instances which we call “systems”, and there is no way one could come up with a single unified classification of all possible systems. A physicist can encounter individual particles as elementary excitations of a field, or bound states of several particles, resonances. Also, there are solitons, condensates and any other countless physical instances. All of them are endowed with vast versatility of distinguishable traits, and we can divide them into categories of all different sorts. But there is one trait that neatly separates physical objects into two categories, namely, their belonging to the classical or the quantum physics. We know that internally any system is quantum in its nature because the laws of quantum mechanics are the underlying laws, but for a large variety of systems we can ignore the underlying nature, and pay attention only to the relevant laws governing their “visible”, or macroscopic, or classical dynamic<sup>1</sup>. Therefore, the following question arises: *Is it possible to see underlying laws of quantum mechanics to reveal themselves, and actually affect macroscopic dynamics?*

During the course of the development of the physics community adopted terms as microscopic and macroscopic to talk about intricacies of small, and large compound systems. Now, instead of using these terms, which refer to the size of the physical system, we can quantitatively draw the difference by using the Planck’s constant in the equations describing physical systems to evaluate the degree of “quantumness” [72, 73]. In other words, we can evaluate how distinguishable quantum properties of the system by analysing the way Planck’s constant enters to different physical quantities.

Let’s take a close look at this by analysing magnetic field in a ferromagnet [74]. Every atom or molecule generates a dipole moment proportional to Bohr’s magneton

$$\mu_B = \frac{e\hbar}{2mc}$$

---

<sup>1</sup>I use here word “classical”, but, of course, as we are aware of quantum mechanical laws as the underlying set of physical laws, the actual term must be “semi-classic”. Because there are no purely classical objects.

which is proportional to the Planck's constant. And, magnetic field in a ferromagnet in the absence of the external field goes as the sum of individual magnetic momenta

$$\vec{H}_{\text{ferr.}} = \alpha \sum_i \vec{\mu}_i,$$

where  $\alpha$  simply reflects susceptibility of the material.

Hence, if a large amount of individual dipoles are aligned, the average amplitude of the field is proportional to the macroscopic number of individual magnetic dipoles

$$\langle \vec{H}_{\text{ferr.}} \rangle \sim \alpha N \langle \vec{\mu} \rangle.$$

From this formula we see that despite every individual dipole moment is small (or even vanishes in the  $\hbar \rightarrow 0$  limit), when we have the number of dipoles  $N$  large enough, the resulting magnetic field is macroscopic.

Using this ancient example, it is easy to define what is meant by classical limit when one keeps track of quantum mechanical trace.

We will call a physical observable  $Q$  classical (semi-classical), if it survives in the limit

$$Q \xrightarrow{\hbar \rightarrow 0} \text{const} \neq 0 \tag{2.1}$$

It goes in the same way with an exchange energy coming from spin interaction in a ferromagnet described by Heisenberg Hamiltonian [75, 76, 77]. But the key feature is that once we encountered a macroscopic magnetic field we do not really care about its internal nature, in other words, microsporic fields of individual dipoles average out, and become the “mean-field”. So, classicality of a physical object implies that there is no need to identify its internal degrees of freedom in order to predict its overall, macroscopic, or classical properties, because quantum interactions are sub-leading when compared to the classical dynamics [78, 79, 80, 81, 82].

Now, as we understand what does it mean for a physical system to be classical, or more precisely semi-classical, we can ask a natural question, that is: *will it remain in the semi-classical state, or it will evolve into something different?*

For instance, we can take something very feasible and intuitive, such as a table. There is no doubt it is classical as it follows Newtonian laws, and if you drop it from a roof it will fall down according to equations of motion deduced from the second Newton's law. This is classical evolution.

But let us be less harsh with a table. And, ask what happens if we just let it rest. A resting table also classically evolves, but it evolves trivially, in other words, nothing changes for a table if we do not act upon it. If we consider it to be a closed system, we can ask ourselves if something will happen to it. We know that actual evolution of a physical system is subjected to the laws of quantum physics. So, how long does it take them to enter the game, and how soon internal degrees of freedom will let us know about their existence. Namely, *how long a table will remain a table?*

In order to answer this question, we have to introduce the notion of collective coupling.



Collective coupling is the product of number of constituents  $N$  and coupling constant  $\alpha$ , that reflects the interaction strength of individual constituents among each other. For instance, if we take a gas of molecules the main interaction would be a rapidly decaying van der Waals force between them, which means that distant molecules do not affect each other's existence. But if the interaction strength is strong enough to engage plenty of constituents to “feel” each other, it's natural to use a notion of the collective coupling.

Hence, we can define it as

$$\alpha_{\text{coll.}} = \alpha N, \quad (2.2)$$

where  $N$  is amount of interacting constituents and  $\alpha$  is the interaction strength of individual degrees of freedom.

As long as the interaction between constituents, namely the collective coupling, is much smaller than unity, quantum breaking matters on very long timescales. *This is why we do not observe quantum breaking in everyday life!* And, why a table remains a table for a very long time. Molecules comprising one leg of a table know nothing about molecules comprising another leg. But if the collective coupling is not negligible, the situation can change dramatically. Indeed, with non-negligible collective coupling (in which the system is said to be critical), quantum (internal) dynamics might lead to substantial deviations from the classical description. This leads us to the introduction of the notion of *quantum breaking*.

In a nutshell, the conception of quantum breaking reflects the deviation of true quantum evolution from the classical one meaning described by classical equations. The quantum breaking happens when interaction between internal degrees of freedom accumulate enough influence to disturb the system as a whole. As we figured out, for this to happen, a collective coupling of a particular system must be large enough. We will call such systems *critical*.

Intuitively, the picture of quantum breaking is simple: it is due to critical or close-to-critical interacting quantum constituents, which with time invalidate the tree-level description as the system becomes more and more quantum. When this happens, the system is said to have undergone quantum breaking. But there is a huge amount of different quantum mechanical systems that are semi-classical, hence a natural question to ask is whether there is a way to quantify quantum breaking generically, regardless of the particular details of a given system.

This question is the one that I address in this thesis. Now, before we proceed further, let us gain a little more intuition about quantum breaking by looking at this concept from different angles.

## 2.2 Corpuscular picture of quantum breaking

As particle physicists, we tend to look at things by studying scattering processes. One excellent example to illustrate the concept of the quantum breaking by invoking scattering is the picture developed in [27] for cosmic axion<sup>2</sup>, which can serve as a hypothetical

---

<sup>2</sup>Scalar axion originated as a solution to strong CP problem [83]

candidate to explain dark matter [84, 85, 86].

In [27] condensate of axions is treated as a coherent state of weakly interacting bosons. Hence, mean field is some classically oscillating function  $\phi(x) = A \cos(mt)$ . Axions in condensate have zero-momentum, therefore, ordinary tree-level elastic scattering does not happen there, but what can happen is decay.

The lowest order process in this theory that involves decay happens due to  $\phi^6$  interaction. It happens when four particles with zero-momentum decay into two particles with momenta of the order of the mass of a free particle. This process gradually leads to depletion of the condensate, and corresponding thermalization.

When substantial part of the particles initially comprising condensate depleted, we can say that breaking occurred and the dynamics will no longer remain coherent. Moreover, a decay process like that is genuinely quantum, hence the decay rate constant  $\Gamma$  will be proportional to the  $\hbar$ . So, in order to evaluate breaking time of such coherently assembled condensate we just have to wait for long enough time and quantum break-time then will be  $t_{\text{qb}} \sim N/\Gamma$ , where  $\hbar$  factor comes from decay constant and  $N$  is the number of constituents to decay which is of order of amount of axions in condensate.

This example not only illustrates the scattering picture of quantum breaking, but also introduces polynomial scaling of quantum breaking with time. It usually happens for classically stable systems [27, 63] that quantum-break time scales as

$$t_{\text{qb}} \sim \frac{1}{\hbar^p}, \quad p \in \mathbb{N}. \quad (2.3)$$

### 2.3 Quantum breaking from the entropy point of view

Another approach developed to understand quantum breaking is deeply intertwined with the so-called scrambling phenomenon, which is considered to be also the microscopic mechanism behind the quantum breaking. When saying scrambling I mean the process of thermalization described by the reduced density matrix (defined on a subset of the Hilbert space) which leads to the scrambling of information and growth of entropy. The timescale associated to this process is called scrambling time, and in [29] this timescale was associated with quantum breaking as well. In fact, in Ref. [29], the initial state is chosen to be macroscopically occupied with zero-momentum modes, and the subsequent evolution leads to a significant smearing of this distribution. As one can see, this definition is purely informational, and the entropy growth can be computed by evaluating the unitary evolution of the reduced density matrix. However, one must take into account that systems subjected to scrambling may not be initially macroscopic or coherently assembled (namely “classical like”). Therefore, the so-called scrambling phenomenon does not always imply actual decoherence or a substantial deviation from the semi-classical trajectory. More precisely, it stands for thermalization of the reduced density matrix<sup>3</sup>. This means that scrambling does not always imply quantum breaking. However, the opposite is supposed to be true.

---

<sup>3</sup>We remark this because unitary evolution may not lead to significant deviations from the initial state, even if the latter is macroscopic and is not a pure eigenstate of the Hamiltonian.

Looking at quantum breaking as the process leading to significant deviation from an initial macroscopic state, we can say that quantum breaking has occurred when information about such initial state is substantially lost. This can be reflected in the observation that the notion of initial degrees of freedom or information about the way they were assembled within the initial state is lost (or dramatically long time is needed for this information to be retrieved). In other words we can say that if quantum breaking takes place, the system necessarily scrambled, i.e.,

$$\text{quantum breaking} \subset \text{scrambling}.$$

A more elaborate discussion of the relation between quantum breaking and scrambling can be found in [29].

However, it is quite apparent that the estimation of the scrambling time poses significant difficulties, as it requires the knowledge of the object microscopic structure, which is not always accessible. Indeed, resolving the inner structure in terms of off-shell degrees of freedom for most of the known semi-classical systems is not possible (or at the very least extremely difficult). Although, the previous example of the scattering picture shows that for the case of very weak interaction strength corpuscular picture is qualitatively very useful and leads explicit results. We can also assume that we have encoded some message in the condensate of axions. But after the cascade of decays driving our system out of coherence the message will be destroyed by the redistribution of momenta between comprising particles, and after most of the particles re-scattered it is no longer can be retrieved.

## 2.4 Quantum breaking as a growth of quantum fluctuations

Both pictures outlined before nicely describe evolution leading to quantum breaking for particular cases and give a neat intuitive picture of what it is. But as soon as both descriptions rely on particular computational strategies, they are not handy for general description of quantum breaking. The question I would like to address is: *how to describe this process without relying on given circumstantial features of a system under consideration?*

As soon as quantum breaking is generally referring to de-classicalization or, so to say, departure from semi-classical evolution, it would be nice to establish a picture which specifically relies on nothing but availability of semi-classical description of the system.

The method I propose naturally arises within standard semi-classical treatment of non-perturbative solutions in quantum field theory. Let me illustrate it here.

Consider some correlation function for an arbitrary system, say

$$\langle \Psi | \hat{O} | \Psi \rangle, \tag{2.4}$$

where  $|\Psi\rangle$  refers to some semi-classical state.

In general this correlator is some function of  $\hbar$ , namely

$$\langle \Psi | \hat{O} | \Psi \rangle = O(\hbar). \quad (2.5)$$

If the system is semi-classical, it admits mean-field approximation which we can be expressed in the following way

$$\langle \Psi | \hat{O} | \Psi \rangle = O_{\text{mf}} + f(\hbar), \quad (2.6)$$

$$\begin{aligned} f(\hbar) &\xrightarrow{\hbar \rightarrow 0} 0, \\ \frac{\partial O_{\text{mf}}}{\partial \hbar} &= 0, \end{aligned} \quad (2.7)$$

and, surely, it must be satisfied that

$$O_{\text{mf}} \gg f(\hbar) \quad (2.8)$$

Here,  $O_{\text{mf}}$  is the mean-field contribution that does not vanish in the  $\hbar \rightarrow 0$  limit and  $f(\hbar)$  stands for quantum fluctuation at the top of mean-field contribution.

An example of such correlator that pops up in mind right away is the energy and the way we compute it for solitons, condensates, and other non-perturbative solutions. There is always splitting on classical energy  $E_{\text{cl}}$  (mean-field contribution) computed from the classical energy functional, and quantum corrections computed from the functional determinant  $\delta E_{qc}$ . Then, first approximation to the full energy is

$$\langle \Psi | \hat{H} | \Psi \rangle = E_{\text{cl}} + \hbar \delta E_{qc} + \mathcal{O}(\hbar^2). \quad (2.9)$$

This illustrates the fact that if we fix our boundary conditions to keep the given non-perturbative solution as the asymptotic state at  $T \rightarrow \pm\infty$  then the main contribution to the energy is classical, and sub-leading contribution is described by quantum fluctuations.

But if we would like to compute actual evolution, we have to investigate a more involved thing, which is true quantum evolution of this operator. Then, all the initial contributions become time-dependent,

$$O_{\text{mf}} + f(\hbar) \xrightarrow{\hat{U}(t,t_0)} O_{\text{mf}}(t) + f(\hbar, t), \quad (2.10)$$

where  $\hat{U}(t, t_0)$  is the unitary operator of evolution.

So, both mean-field contribution and quantum fluctuations will evolve and become intertwined. Then, at some point condition (2.8) will be violated, and we can safely say that when there is no clear distinction between contributions coming from mean-field and quantum fluctuations, then quantum breaking occurred. We see from this that in order to catch quantum breaking, we have to employ some technique to compute the evolution of the correlation function at some finite timescale. Notice, that energy is the conserved quantity which means that its expectation value is conserved as well, but it doesn't mean that both contributions to the initial state which are classical energy and contribution from quantum fluctuations are conserved as well, this is only their sum that remains the same.

Therefore, the issue is to understand if it's possible to compute somehow evolution of correlation function such that it could be decomposed in a way prescribed by eq. (2.10).

## 2.5 Quantum breaking criterion

In this work, I will pick the last option as a framework to describe the whole picture of quantum breaking, and formulate a criterion of determining the time of a quantum-breakdown.

In this section, I will omit details of the precise computational approach, and focus only on the general concept. After all, I will present the method as whole in the subsequent analysis.

In order to determine quantum break-time of the system based on analysis of the correlation functions, and their splitting discussed in the previous section, we must have several ingredients, which are

1. A physical observable that is conserved, and reflects semi-classicality of the system
2. A way to compute evolution
3. A proper initial conditions for the evolution such that they comply with semi-classicality
4. A criterion which determines quantum break-time

let us break it down in details.

A *conserved physical observable*  $\mu$  is the first and very essential ingredient, as it will help to determine mutual influence of “quantum” and “classical” contributions to the evolution. Of course as any physical observable in quantum theory,  $\mu$  is represented by some unitary operator, and the quantity of interest is its expectation value taken in the brackets of our semi-classical state  $|\text{SC}\rangle$

$$\langle \text{SC} | \hat{\mu} | \text{SC} \rangle := \mu, \quad \frac{d\mu}{dt} = 0. \quad (2.11)$$

Of course, as a conserved quantity, the expectation value of  $\mu$  does not evolve along dynamical flow. But later we will see that some information can be extracted anyway if it is broken down to pieces that make each other up to provide conservation.

Next thing is that  $\mu$  must reflect *semi-classicality* of the system. This means that the following limit must hold up

$$\mu \xrightarrow{\hbar \rightarrow 0} \text{const} \neq 0, \quad (2.12)$$

meaning, this observable survives exact classical limit.

There are plenty of observable quantities of such sort. For instance, one can take the rest energy as the most apparent one, or charge. Although, it’s better if this quantity is characteristic to the system, namely, covariant. In this work I will focus on Bose-Einstein condensate which has both these quantities at disposal. However, one could argue that energy is not covariant quantity, it is well-suited for the homogeneous condensate put in the box with periodical boundary conditions. In this case there are no space-time transformations which actually change energy as the frame is fixed once and for all.

Another remark I would like to do concerns the way Planck's constant enters the physical quantities, and the way classical limit is taken.

Recall the energy of the system. If the system is classical, then the notion of the classical energy is well-established as it's directly measurable observable. For a semi-classical system it survives the  $\hbar$  limit and nothing dramatic happens. But let us take a closer look at quantization of the angular momentum in 2-dimensional system with  $SO(2)$  symmetry. For such system operator  $\hat{L}$  is quantized, and has a set of eigenvalues  $\hbar l$ , where  $l \in \mathbb{Z}$  and  $l$  is apparently dimensionless. Therefore, in order to have semi-classical rotation, one can see that dimensionless operator  $\hat{l}$  must have its mean value  $\langle \hat{l} \rangle$  to blow up in  $\hbar \rightarrow 0$  limit. So, the mean-coordinate (or mean-field in field theory) value of a dimensionless operator  $\langle \hat{l} \rangle \sim 1/\hbar$  is inversely proportional to the  $\hbar$  in order to have semi-classical behavior. At the same time, the dimensional quantity  $\langle \hat{L} \rangle = \hbar \langle \hat{l} \rangle$  survives the classical limit. This is important to keep in mind because in our case angular momentum is the direct analogue of  $U(1)$  global charge. It is natural to have eigenvalues of charge operator  $\hat{Q}$  as integer values, but then it means that the mean-field value of charge blows up in the classical limit  $\langle \hat{Q} \rangle \rightarrow \infty$ ,  $\hbar \rightarrow 0$  but the dimensional quantity  $\hbar \langle \hat{Q} \rangle$  survives.

So, actually we must distinguish between these two quantities, keeping in mind that the actual system of units matters for taking the classical limit. However, along the course of this work I will keep working in units  $\hbar = 1$ , so I won't be making the difference between mean-field value  $\langle \hat{Q} \rangle$  and actual classical charge  $Q_{cl} = \hbar \langle \hat{Q} \rangle$  calling both quantities "classical".

Let's now get back on the course of determining quantum break-time of a system. Next thing, we must have is *the way we compute time-dependence of a given observable*. In other words, we have to have an instrument for computing time-evolution. If it's accomplished we have to split a conserved quantity of interest  $\mu$  on the contributions to which we will refer to as classical and quantum,

$$\mu = \mu_{cl}(t) + \mu_q(t). \quad (2.13)$$

Both contributions time-evolve but make each other up to the conserved quantity.

We separate this contributions out such that in the beginning of evolution they comply with semi-classicality, namely

$$\begin{cases} \mu_{cl}(0) \xrightarrow{\hbar \rightarrow 0} \text{const} \neq 0 \\ \mu_q(0) \xrightarrow{\hbar \rightarrow 0} 0 \end{cases}. \quad (2.14)$$

Then, we can formulate **a quantum breaking criterion** which states that when following quantum evolution two contributions become balanced quantum breaking occurred, and the quantum break-time is given by the solution of the following equation

$$\mu_{cl}(t_{qb}) \simeq \mu_q(t_{qb}). \quad (2.15)$$

Using this criterion, we can extract interesting timescale. And, the only thing left is to pick up a tool to be able to proceed with the actual computation.

# Chapter 3

## 2PI effective action

In order to compute evolution of a non-trivial solution, a non-trivial method is required. That is why, for this particular problem, methods from out-of-equilibrium field theory are particularly handy. In the subsequent analysis, I will use so-called 2PI effective action equipped with *in-in* (closed in time) integration contour to compute an evolution of the Bose-Einstein condensate.

One might wonder why is there a necessity to use such sophisticated approach. There are several reasons for that.

Firstly, usual ways of computing non-equilibrium processes such as using Feynman perturbation theory or ordinary 1PI effective action proved to be insufficient [87, 88, 89, 90] as they do not handle a problem of secular evolution, hence, they make sense only on the very short time-span. One can find a neat explanation of how exactly 2PI expansion makes things better, and provides much more reasonable approximation by infinite re-summation of certain terms in perturbation theory in order to render better approximation to the true evolution in the introduction to [91]. It is shown there how non-linear expansion scheme provided by nPI-effective actions renders the error of approximation to be confined in a certain range during the course of whole evolution and not only for the small time-range. Moreover, latter we will make a comparison of the evolution computed by means of ordinary perturbation theory, and using 2PI. As a result, we will see that ordinary perturbation theory miserably fails to capture a quantum breaking phenomenon.

Secondly, we use this formalism because it provides us a neat framework to embed a criterion to indicate quantum breaking. As it was already told we will use a  $U(1)$  charge as the main tool to capture quantum breaking, and we will have to split it to the classical and quantum contributions which is straightforwardly done within 2PI-effective action treatment.

So, words aside, and let's move to the explanation of this powerful formalism.

## 3.1 General description of 2PI formalism

### 3.1.1 Definition

The original approach to the n-PI effective actions was developed in the series of papers [36] and [37] where definitions were put, and it was shown that these functionals appear to be generating functionals for n-particle irreducible diagrams. Recall that diagram is called *n-particle irreducible*, when one needs to cut at least  $n+1$  internal lines to split the diagram in two separate ones. Later in [40] efficient formalism for computing was established by analogy with standard 1PI effective action [92].

Let's follow this procedure and construct 2PI functional.

In the usual 1PI effective action we introduce Legendre transform only with respect to one-point classical source  $J(x)$  and then compute effective action as a newly generating functional of conjugated variable  $\phi(x)$ . Here, we will go further and introduce also 2-particle source  $K(x, y)$ . Then, generating functional of the full quantum theory becomes

$$Z[J, K] = \int \mathcal{D}\varphi_a \exp \left( i \left( S[\varphi_a] + \int \int d^d x \varphi_a(x) J_a(x) + \frac{1}{2} \int d^d x \int d^d y \varphi_a(x) K_{ab}(x, y) \varphi_b(y) \right) \right), \quad (3.1)$$

where  $S[\phi_a]$  is the action of underlying theory

$$S[\phi_a] = \int d^d x \mathcal{L}(\phi_a, \partial\phi_a) \quad (3.2)$$

in  $d$  dimensions.

Here, we do not specify boundary conditions for the path integral. It will be taken care of later.

Using this functional for generic Green's functions, we can also define in the usual fashion a generating functional for connected Green's functions

$$W[J, K] = -i \log Z[J, K]. \quad (3.3)$$

Now, we can immediately demonstrate a huge advantage that provides introduction of the additional source.

Let's introduce conjugated variables  $\phi_a(x)$  and  $G_{ab}(x, y)$

$$\begin{cases} \frac{\delta W[J, K]}{\delta J_a(x)} = \phi_a(x), \\ \frac{\delta W[J, K]}{\delta K_{ab}(x, y)} = \frac{1}{2} (\phi_a(x) \phi_b(y) + G_{ab}(x, y)), \end{cases} \quad (3.4)$$

The definition for  $\phi_a(x)$  is already familiar to everyone, so, let's take a closer look at the definition of  $G_{ab}(x, y)$ .



When we take functional derivatives with respect to  $K$  and  $J$  we get the following set of equalities

$$\frac{\delta^2 W[J, K]}{\delta J_a(x) \delta J_b(y)} = i \frac{\delta W[J, K]}{\delta J_a(x)} \frac{\delta W[J, K]}{\delta J_b(y)} - i \frac{1}{Z[J, K]} \frac{\delta^2 Z[J, K]}{\delta J_a(x) \delta J_b(y)} \quad (3.5)$$

$$\frac{\delta W[J, K]}{\delta K_{ab}(x, y)} = -i \frac{1}{Z[J, K]} \frac{\delta Z[J, K]}{\delta K_{ab}(x, y)} \quad (3.6)$$

$$\frac{\delta Z[J, K]}{\delta K_{ab}(x, y)} = i \frac{\delta^2 Z[J, K]}{\delta J_a(x) \delta J_b(y)} \quad (3.7)$$

where it follows that the new variable  $G_{ab}(x, y)$  is nothing but connected part of the full 2-point function

$$G_{ab}(x, y) = i \frac{\delta^2 W[J, K]}{\delta J_a(x) \delta J_b(y)} = -i \langle \hat{T} \{ \phi_a(x) \phi_b(y) \} \rangle_{\text{connected}}. \quad (3.8)$$

So, here connected part of the Green's function or what we call quantum fluctuations is an independent variable in the functional formalism, and will have its own equation of motion. Precisely this trick allows us to separate quantum evolution from classical one.

Let's proceed with Legendre transformation further by introducing a new functional

$$\Gamma[\phi, G] = W[J, K] - \int d^d x \frac{\delta W[J, K]}{\delta J_a(x)} J_a(x) - \frac{1}{2} \int d^d x \int d^d y \frac{\delta W[J, K]}{\delta K_{ab}(x, y)} K_{ab}(x, y), \quad (3.9)$$

which is called 2-particle irreducible effective action.

Derivatives of  $\Gamma[\phi, G]$  with respect to  $\phi$  generate 2-particle irreducible Feynman diagrams where  $G_{ab}(x, y)$  is the propagator along the internal line. I shall remind that graphs are called 2-particle irreducible if they can not be split in two separate graphs by cutting one or two internal lines, it requires cutting at least three lines in the best case.

Next, we can take functional derivatives of 2PI effective action with respect to its variables

$$\left\{ \begin{array}{l} \frac{\delta \Gamma[\phi, G]}{\delta \phi_a(x)} = -J_a(x) - \int d^d y K_{ab}(x, y) \phi_b(y) \\ \frac{\delta \Gamma[\phi, G]}{\delta G_{ab}(x, y)} = -K_{ab}(x, y) \end{array} \right. \quad (3.10)$$

Hence, if we set original sources to be zero then we get stationary conditions determining exact Green's functions

$$\left\{ \begin{array}{l} \frac{\delta \Gamma[\phi, G]}{\delta \phi_a(x)} = 0, \\ \frac{\delta \Gamma[\phi, G]}{\delta G_{ab}(x, y)} = 0. \end{array} \right. \quad (3.11)$$

Solving this stationary conditions, we resolve full quantum theory and find connected one- and two-point functions as a result, and by computing functional derivatives we can compute any other correlation functions.

Notice, however, that we could start from putting  $K_{ab}(x, y) = 0$ , then we can resolve  $G_{ab}(x, y)$  from the second condition in (3.11), say

$$\left. \frac{\delta\Gamma[\phi, G]}{\delta G_{ab}(x, y)} \right|_{G=G(\phi)} = 0,$$

then we can put it back to  $\Gamma[\phi, G]$  and get

$$\Gamma[\phi, G(\phi)] = \Gamma^{1PI}[\phi], \quad (3.12)$$

meaning standard effective action. So, we see that if one manages somehow to get a full solution, then there is no difference between the results inferred from effective action of any type. But as soon as such a stunt is impossible to pull out, we employ more sophisticated technique provided by 2PI effective action in order *to get a better approximation!*

### 3.1.2 Stationary conditions

Now, as we have got a grasp of the definition of the action, we shall proceed to computing it. To do so, I follow a technique developed in [40] for evaluating 2PI effective action.

As it was mentioned, this functional is a generating functional for 2-particle irreducible graphs, so the procedure for computing the functional itself is even simpler compared to widely used 1PI effective action.

The whole functional can be written as follows

$$\Gamma[\phi, G] = S[\phi] + \frac{i}{2}\text{tr} \ln G^{-1} + \frac{i}{2}\text{tr} (G_0^{-1}G) + \Gamma_2[\phi, G]. \quad (3.13)$$

Let's break it down into pieces, and illustrate computational procedure using  $\lambda|\phi|^4$  theory.

The first part of this expression is, naturally, classical action of the theory (2-component real scalar in our case)

$$S[\phi_a] = \int d^d x \left( \frac{1}{2} (\partial_\mu \phi_a)^2 - \frac{1}{2} m^2 \phi_a^2 - \frac{\lambda}{4} ((\phi_a)^2)^2 \right).$$

Then, there is an analogue of functional determinant term

$$\frac{i}{2}\text{tr} \ln G^{-1}$$

which is actually similar but not exactly the same because  $G$  now is an independent variable, not a function of classical field  $\phi$ . However, next term

$$\frac{i}{2}\text{tr} (G_0^{-1}G) \quad (3.14)$$

draws the connection between the two.

Here,  $G_0$  is defined as

$$G_{0,ab}^{-1}(x,y) = -i \frac{\delta^2 S[\phi]}{\delta\phi_a(x)\delta\phi_b(y)}, \quad (3.15)$$

and is called auxiliary propagator, which shape one immediately recognizes from the propagator used to compute ordinary 1PI effective action [92].

Let me illustrate this.

If we stop at this point, and drop  $\Gamma_2$  term in (3.13) then we get

$$\Gamma_{(1)}[\phi, G] = S[\phi] + \frac{i}{2} \text{tr} \ln G^{-1} + \frac{i}{2} \text{tr} (G_0^{-1} G).$$

Then, applying stationary conditions (3.11) to this functional we derive from the stationary condition for propagator

$$\begin{aligned} \frac{\delta\Gamma_{(1)}[\phi, G]}{\delta G_{ab}(x, y)} = 0 &\Rightarrow -\frac{i}{2} G_{ab}^{-1}(x, y) + \frac{i}{2} G_{0,ab}^{-1}(x, y) = 0 \\ &\Rightarrow G_{ab}^{-1}(x, y) = -i \frac{\delta^2 S[\phi]}{\delta\phi_a(x)\delta\phi_b(y)}. \end{aligned}$$

We can plug it back to  $\Gamma_{(1)}[\phi, G]$  and get

$$\Gamma_{(1)}[\phi, G(\phi)] = S[\phi] + \frac{i}{2} \text{tr} \log \left( \frac{\delta^2 S[\phi]}{\delta\phi_a(x)\delta\phi_b(y)} \right) + \text{const},$$

which is ordinary 1PI effective action computed at one loop approximation, or Coleman-Weinberg potential if we take  $\phi = \text{const}$ .

Although, this similarity does not hold true any more when we start to compute higher loops. And, this is the part when we consider the most intricate and important part of eq. (3.13), namely,  $\Gamma_2[\phi, G]$ .

According to [40]  $\Gamma_2[\phi, G]$  is the sum of all 2PI diagrams.  $\Gamma_2[\phi, G]$  starts from the two-loop diagrams, and goes further because as we have seen right away one loop contribution is already taken care of. So, expansion of  $\Gamma_2[\phi, G]$  starts actually from the second order in  $\hbar$ .

Let me illustrate a computation procedure of  $\Gamma_2[\phi, G]$ .

First of all, we have to find vertices to determine Feynman rules for computing expansion of  $\Gamma_2$ . These vertices are given by a standard interaction term coming from the expansion of the classical action

$$S_{\text{int}}[\phi, \varphi] = S[\phi + \varphi] - S[\phi] - \int d^d x \frac{\delta S[\phi]}{\delta\phi_a(x)} \varphi_a(x) - \int \int d^d x d^d y \frac{1}{2} \varphi_a(x) \frac{\delta^2 S[\phi]}{\delta\phi_a(x)\delta\phi_b(y)} \varphi_b(y), \quad (3.16)$$

where  $\phi(x)$  is the variable (background field) of the 2PI effective action, and  $\varphi$  is the quantum field with respect to which we compute.

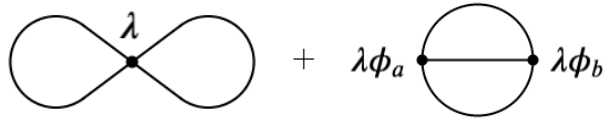
In the case of theory we are going to consider interaction part follows as

$$S_{\text{int}}[\varphi, \phi] = \int d^d x \left( \frac{\lambda}{2} \phi_a \varphi_a (\varphi_b)^2 + \frac{\lambda}{4} ((\varphi_a)^2)^2 \right), \quad (3.17)$$

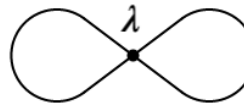
where  $\varphi_a(x)$  is the integration variable in path integral, and  $\phi_a(x)$  is the background field, which is the variable of 2PI functional defined in (3.4).

Then using vertices derived from interaction we compute Feynman diagrams with the only difference that now propagator is given by a full propagator of the theory, namely,  $G$ .

To illustrate this, let's compute the first two two-loop diagrams, which contribute in  $\hbar^2$  order of  $\Gamma_2$  expansion.

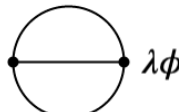
$$\Gamma_2^{(2)}[\phi, G] = \text{Diagram 1} + \lambda \phi_a \text{Diagram 2} \lambda \phi_b + \mathcal{O}(\hbar^3) \quad (3.18)$$


The first diagram comes from the  $\varphi^4$  vertex of the interaction (3.17). Using propagator  $G_{ab}(x, y)$  to compute it, we derive

$$\text{Diagram 1} = i \frac{\lambda}{16} \int d^d x (2G_{ab}(x, x)G_{ab}(x, x) + (G_{aa}(x, x))^2). \quad (3.19)$$


This diagram apparently presents local contribution, as it depends on only one point in space and time.

The next diagram is more involved and requires combination of cubic vertices from (3.17) to get it

$$\lambda \phi_a \text{Diagram 2} \lambda \phi_b = - \frac{\lambda^2}{16} \int d^d x \int d^d y (G_{ab}(x, y) \phi_a(x) \phi_b(y) G_{cd}(x, y) G_{cd}(x, y) + 2 \phi_a(x) G_{ab}(x, y) G_{bc}(x, y) G_{cd}(x, y) \phi_d(y)) \quad (3.20)$$


So, we see that this one depends on two points in space and time, and, also, on the background field which eventually leads to capturing non-trivial effects.

To sum up, the two-loop approximation to the effective action becomes

$$\begin{aligned} \Gamma[\phi, G] = & \int d^d x \left( \frac{1}{2} (\partial_\mu \phi_a)^2 - \frac{1}{2} m^2 \phi_a^2 - \frac{\lambda}{4} ((\phi_a)^2)^2 \right) + \frac{i}{2} \text{tr} \log G_{ab}(x, y) + \\ & \frac{i}{2} \text{tr} \left( i \left( \left( \partial_x^2 + m^2 + \frac{\lambda}{4} \phi_a^2 \right) \delta_{ab} + \frac{\lambda}{2} \phi_a \phi_b \right) G_{ab}(x, y) \right) - \\ & \frac{\lambda}{16} \int d^d x (2G_{ab}(x, x)G_{ab}(x, x) + (G_{aa}(x, x))^2) + \\ & i \frac{\lambda^2}{16} \int_C dx \int dy (G_{ab}(x, y) \phi_a(x) \phi_b(y) G_{cd}(x, y) G_{cd}(x, y) + \\ & 2 \phi_a(x) G_{ab}(x, y) G_{bc}(x, y) G_{cd}(x, y) \phi_d(y)) + \mathcal{O}(\hbar^3) \quad (3.21) \end{aligned}$$

As we have learned how to use loop approximation for the 2PI effective action in practice, it is time now to turn to stationary conditions.

The stationary conditions are given by (3.11), and applying them to (3.13) we get

$$\begin{cases} \frac{\delta S[\phi]}{\delta \phi_a(x)} + \frac{i}{2} \text{tr} \left( \frac{\delta G_0^{-1}}{\delta \phi_a(x)} G \right) + \frac{\delta \Gamma_2[\phi, G]}{\delta \phi_a(x)} = 0, \\ G_{ab}^{-1}(x, y) - G_{0ab}^{-1}(x, y) + 2i \frac{\delta \Gamma_2[\phi, G]}{\delta G_{ab}(x, y)} = 0. \end{cases} \quad (3.22)$$

Here, the second equation resolves propagator  $G$  as a function of field  $G = G(\phi)$ . And, the non-trivial piece coming from higher-loop diagrams we call *self-energy*. Let me introduce a special notation for this piece

$$\Sigma_{ab}(x, y) = 2i \frac{\delta \Gamma_2[\phi, G]}{\delta G_{ab}(x, y)}. \quad (3.23)$$

Note, that when I was computing two-loop approximation to  $\Gamma_2$  I have called the first diagram a local one, and another one a non-local one. Using this fact, we can split self-energy in two parts, namely,

$$\Sigma_{ab}(x, y) = M_{ab}(x) \delta^{(d)}(x - y) + \Sigma_{ab}^{(non-local)}(x, y). \quad (3.24)$$

Contribution from  $M_{ab}(x)$  to the full self-energy is apparently local and depends only on one point in space-time in general, although in particular case of the condensate it's coordinate-independent at all. We can pull out this contribution from  $\Sigma$  by differentiating (3.18) and picking only those parts that multiply by delta function. Hence, we derive

$$M_{ab}^2(x) = m^2 \delta_{ab} + \frac{\lambda}{4} (\phi_c^2(x) + G_{cc}(x, x)) \delta_{ab} + \frac{\lambda}{2} (\phi_a(x) \phi_b(x) + G_{ab}(x, x)). \quad (3.25)$$

One can see that if we pick homogeneous background  $\phi = \text{const}$ , then propagator becomes transitionally invariant meaning  $G_{ab}(x, y) = G_{ab}(x - y)$ . Thus, it is apparent that

in these settings  $M_{ab}^2(x) = M_{ab}^2$  does not depend on  $x$ , and introduces nothing but constant mass shift. But this happens to be the case only if we drop the second diagram, which is non-local.

Let's turn finally to this non-local contribution. It is given by

$$\begin{aligned} \Sigma_{ac}^{non-local}(x, z) = & -\frac{\lambda^2}{8} (G_{df}(x, z)G_{df}(x, z)\phi_a(x)\phi_c(z) + 2\phi_d(x)G_{df}(x, z)\phi_f(z)G_{ac}(x, z) + \\ & 2\phi_a(x)G_{fc}(x, z)G_{fd}(x, z)\phi_d(z) + 2\phi_f(x)G_{fd}(x, z)G_{ad}(x, z)\phi_c(z) + \\ & 2\phi_f(x)G_{fc}(x, z)G_{ad}(x, z)\phi_d(z)). \end{aligned} \quad (3.26)$$

We see that it depends on two coordinate points in space and time. This is precisely the feature that makes the Green's function non-trivial, and eventually leads to intricate effects.

With the help of all these notations, we can rewrite now stationary conditions (3.22) as

$$\left\{ \begin{aligned} -\frac{\delta S[\phi]}{\delta \phi_a(x)} + \frac{\lambda}{4} (G_{dd}(x, x)\delta_{ab} + 2G_{ab}(x, x)) \phi_b(x) &= \frac{\delta \Gamma_2[\phi, G]}{\delta \phi_a(x)} \\ (\partial^2 \delta_{ac} + M_{ac}^2(x)) G_{cb}(x, y) + i \int dz \Sigma_{ac}^{non-local}(x, z) G_{cb}(z, y) &= -i\delta_{ab}\delta(x - y) \end{aligned} \right. , \quad (3.27)$$

where the only part to unfold is the functional derivative of  $\Gamma_2$  with respect to  $\phi$  which is given by

$$\begin{aligned} \frac{\delta \Gamma_2[\phi, G]}{\delta \phi_a(x)} = & \frac{i\lambda^2}{8} \int_c dy (G_{cd}(x, y)G_{cd}(x, y)G_{ab}(x, y)\phi_b(y) + \\ & 2G_{ab}(x, y)G_{cb}(x, y)G_{cd}(x, y)\phi_d(y)). \end{aligned} \quad (3.28)$$

To sum up, our main goal is to solve equations (3.27). But in order to do that, we miss several more important ingredients. These are renormalization, initial conditions, boundary conditions, and contour of integration.

Let's first start from the renormalization, as it is the simplest issue in our case.

### 3.1.3 Renormalization

In general, renormalization of the 2PI effective action is extremely difficult and intricate procedure. The first steps for finite temperature systems were made in a series of articles by van Hees and Knoll [93, 94, 95], and later others developed general techniques for treating renormalization [96], [97].

Even for ordinary scalar  $\phi^4$  theory renormalization at two loops is very cumbersome, and require solving non-linear integral equations to renormalize coupling constant [97], which is an expected difficulty, because the approach itself involves solution of non-linear equations even when one employs approximation, it would be strange to expect that renormalization

could be somehow simpler than that. Imagine only a difficulty of renormalizing at two loops when the background field is non-trivial (one can feel a taste of this looking up the procedure for the case of three-loop diagram at  $\phi = 0$  in [97]).

However, things are not very dramatic for the theory considered in this work, because it inhabits in 1+1 dimensions where things are simple and handy. It is very well-known that coupling constant doesn't require renormalization here as well as the field strength. The only part of renormalization is the mass, which is trivially renormalizable at any order.

In order to handle the mass renormalization, the only thing that we have to do is to substitute  $m^2$  with  $m^2 + \delta m^2$  in eq. (3.27) and eq. (3.25), where

$$\delta m^2 = -\frac{\lambda}{L} \sum_{n=-\infty}^{+\infty} \frac{1}{2\sqrt{p_n^2 + m^2}} \quad (3.29)$$

simply renders  $M_{ab}^2(x) = m^2$  when  $\phi = 0$ .

### 3.1.4 Initial conditions and time-contour

So far, we have just established equations for the Green's function that we have to solve. If one will consider asymptotic boundary conditions, namely, when field approaches to one stationary at  $T \rightarrow -\infty$ , and the same configuration at  $T \rightarrow +\infty$ , then we will get nothing but results of the scattering theory. In this fashion we can compute the propagator at the top of our semi-classical solution, then, compute corrections to the energy, and so on... Also, notice that if we will try to solve eq. (3.27) for the infinite time-line then we have to solve them in the whole space-time simultaneously due to the fact that equations are differential-integral. This is apparently not the simplest task to accomplish. However, here we attempt to solve actual evolutionary problem, in other words, we would like to solve the real-time evolution. Therefore, we need to come up with the better idea for treating integration along the time direction. Here, closed time path-contour bails us out.

Let me explain how does it emerge.

First of all, we always start from the general formulation of the generating functional in the form of the path integral for a certain theory. And, for the path integral we have to specify boundary conditions meaning field configurations at the initial and final times

$$\mathcal{Z}[J] = \int_{\phi(t_{in}, \vec{x}) = \varphi_1(\vec{x})}^{\phi(t_{out}, \vec{x}) = \varphi_2(\vec{x})} \mathcal{D}\phi \exp \left( i S[\phi] - i \int_{\mathcal{T}} dt \int d\vec{x} J(x) \phi(x) \right). \quad (3.30)$$

From this expression we see that integration goes along a time-contour  $\mathcal{T}$  which starts at time  $t = t_{in}$  and finishes at  $t = t_{out}$ . Also, we have fixed field configurations in the very beginning as  $\varphi_1(\vec{x})$  and in the very end  $\varphi_2(\vec{x})$ . If we considered scattering process in the vacuum, then these conditions would become  $\varphi_1(\vec{x}) = \varphi_2(\vec{x}) = 0$ , and  $t_{in} \rightarrow -\infty$ ,  $t_{out} \rightarrow +\infty$  meaning that asymptotically we approach vacuum. Otherwise, if we had treated scattering at the top of some non-perturbative semi-classical background, we would have

chosen  $\phi_1(\vec{x}) = \phi_2(\vec{x}) = f(\vec{x})$ , and  $t_{in} \rightarrow -\infty$ ,  $t_{out} \rightarrow +\infty$ . In this case,  $f(\vec{x})$  is the solution of non-linear classical equations of motion. Then, we would treat quantum fluctuations assuming that background does not really change by performing a  $\phi(x) = f(\vec{x}) + \delta\phi(x)$  substitution where  $\delta\phi(x)$  are quantum fluctuations (shifted variable in path integral). In this approach we fix background by hand, but what we would like to do in this work is to study the evolution of the background field itself! This means that either  $\varphi_1(\vec{x})$  and  $\varphi_2(\vec{x})$  must be different which is not very convenient because we set up  $\varphi_1(x)$  as an initial condition, but we do not know  $\varphi_2(x)$ , which is the configuration we would like to come to as the result of the evolution. To accomplish that we could, for instance, take various  $\phi_2(\vec{x})$ 's that we could possibly imagine, evaluate path integral, and compare amplitudes. However, this enterprise seems to be extremely cost computationally, if not impossible.

Nevertheless, there is a trick that allows to resolve this problem, and set up an actual initial-value problem for the equations (3.27). This trick employs closed time-path contour.

We can choose it in the following way  $\mathcal{T}_{cl} = \lim_{\epsilon \rightarrow 0^+} \{[0 + i\epsilon, t + i\epsilon] \cup [t - i\epsilon, 0 - i\epsilon]\}^1$  which means that we start from  $t = 0$  slightly above real time, and then go back slightly below it. This means that we get back to where we have started. It helps to satisfy suitable integration limits for path integral, namely, we set them equal each other as in any other semi-classical treatment but at the same time we can track down what happens in between.

So, path integral at this point becomes

$$\mathcal{Z}[J] = \int_{\phi(t_0+i0^+, \vec{x})=\varphi(\vec{x})}^{\phi(t_0-i0^+, \vec{x})=\varphi(\vec{x})} \mathcal{D}\phi \exp \left( i S[\phi] - i \int_{\mathcal{T}_{cl}} dt \int d\vec{x} J(x) \phi(x) \right). \quad (3.31)$$

The remaining step is to rewrite equations (3.27) in the suitable form, so, we could take advantage of the closed path integration.

To do so, we have to rewrite the full correlation function using time ordering with respect to the closed time-contour. We start from one-point function because it is the most apparent one

$$\langle \Psi | \hat{T}_{\mathcal{T}_{cl}} \{ \hat{\phi}(x) \} | \Psi \rangle = \langle \Psi | \hat{\phi}(x) | \Psi \rangle \quad (3.32)$$

which is self-evident, and recall that by  $\hat{T}_{\mathcal{T}}$  I mean time-ordering along contour  $\mathcal{T}$ . More interesting situation happens for the two-point function.

$$\langle \Psi | \hat{T}_{\mathcal{T}} \{ \hat{\phi}(x) \hat{\phi}(y) \} | \Psi \rangle \quad (3.33)$$

Usually, we write it down as

$$\langle \Psi | \hat{T}_{\mathcal{T}} \{ \hat{\phi}(x) \hat{\phi}(y) \} | \Psi \rangle = \theta(x^0 - y^0) \langle \Psi | \hat{\phi}(x) \hat{\phi}(y) | \Psi \rangle + \theta(y^0 - x^0) \langle \Psi | \hat{\phi}(y) \hat{\phi}(x) | \Psi \rangle \quad (3.34)$$

but now we have to indicate that this theta function  $\theta(x^0 - y^0)$  should become a theta function along a closed time-contour which I denote in the following way

$$\text{Theta function along closed time-path contour} \equiv \theta_{\mathcal{T}_{cl}}(x^0 - y^0). \quad (3.35)$$

<sup>1</sup>Here, subscript *cl* refers to term closed, do not confuse it with *cl* denoting classical.



Using this definition we can rewrite two-point function in a very convenient form, namely,

$$G_{ab}(x, y) = F_{ab}(x, y) + \frac{i}{2} \text{sgn}_{\mathcal{T}_{cl}}(x^0 - y^0) \rho_{ab}(x, y). \quad (3.36)$$

I have introduced here new notations

$$\left\{ \begin{array}{l} G_{ab}(x, y) \equiv \langle \Psi | \hat{T}_{\mathcal{T}_{cl}} \{ \hat{\phi}_a(x) \hat{\phi}_b(y) \} | \Psi \rangle \\ F_{ab}(x, y) \equiv \langle \Psi | \{ \hat{\phi}_a(x), \hat{\phi}_b(y) \} | \Psi \rangle \\ \rho_{ab}(x, y) \equiv \langle \Psi | [ \hat{\phi}_a(x), \hat{\phi}_b(y) ] | \Psi \rangle \end{array} \right. , \quad (3.37)$$

where  $\{ , \}$  and  $[ , ]$  denote anti-commutator and commutator correspondingly.

$G_{ab}(x, y)$  in these equations is the full propagator of the theory, and this is precisely the second functional variable of 2PI effective action. Using this decomposition, we can rewrite equations (3.27) such that they will become equations defining the initial-value problem.

Recall that in equations (3.27) we have non-local self-energy term  $\Sigma_{ab}(x, y)$ . This term appears to be function of  $\phi_a(x)$  and  $G_{ab}(x, y)$  itself. But as soon as there are no any other contributions it can be represented in the same form as  $G_{ab}(x, y)$  in equation (3.36). We decompose it in the same fashion

$$\Sigma_{ab}^{non-local}(x, y) = \Sigma_{ab}^F(x, y) - \frac{i}{2} \text{sgn}_{\mathcal{T}_{cl}}(x^0 - y^0) \Sigma_{ab}^\rho(x, y). \quad (3.38)$$

To get an explicit expression of  $\Sigma^F$  and  $\Sigma^\rho$  one can notice from (3.26) that  $\Sigma^{non-local}$  is actually a function of two products, namely,  $G_{ab}(x, y)G_{cd}(x, y)$  and  $\phi_a(x)\phi_b(y)$

$$\Sigma^{non-local}(x, y) = \Sigma^{non-local}(G_{ab}(x, y)G_{cd}(x, y), \phi_a(x)\phi_b(y)). \quad (3.39)$$

Using this property it follows that both parts of the decomposition (3.38) can be expressed as

$$\Sigma_{ab}^F(x, y) = \Sigma^{non-local} \left( F_{ab}(x, y)F_{cd}(x, y) - \frac{1}{4} \rho_{ab}(x, y)\rho_{cd}(x, y), \phi_a(x)\phi_b(y) \right), \quad (3.40)$$

$$\Sigma_{ab}^\rho(x, y) = \Sigma^{non-local} \left( F_{ab}(x, y)\rho_{cd}(x, y) + \rho_{ab}(x, y)F_{cd}(x, y), \phi_a(x)\phi_b(y) \right). \quad (3.41)$$

Next, we have to sort out  $\delta\Gamma_2/\delta\phi(x)$  contribution from the first equation of system (3.27). We can rewrite this function as

$$\frac{\delta\Gamma_2}{\delta\phi_a(x)} = \int d^d y \Sigma_{ab}^\phi(x, y)\phi_b(x). \quad (3.42)$$

Then,

$$\begin{aligned} \Sigma_{ab}^\phi(x, y) = \frac{\lambda^2}{8} & \left( \left( F_{cd}^2(x, y) - \frac{1}{4} \rho_{cd}^2(x, y) \right) \rho_{ab}(x, y) + 2F_{cd}(x, y) \rho_{cd}(x, y) F_{ab}(x, y) + \right. \\ & 2\rho_{ad}(x, y) F_{cd}(x, y) F_{cb}(x, y) + 2F_{ad}(x, y) \rho_{cd}(x, y) F_{cb}(x, y) + \\ & \left. 2F_{ad}(x, y) F_{cd}(x, y) \rho_{cb}(x, y) - \frac{1}{4} \rho_{ad}(x, y) \rho_{cd}(x, y) \rho_{cb}(x, y) \right). \end{aligned} \quad (3.43)$$

Finally, let's recall that we have also local part of the self-energy which is simply

$$M_{ab}^2(x) = (m^2 + \delta m^2) \delta_{ab} + \frac{\lambda}{4} (\phi_c^2(x) + F_{cc}(x, x)) \delta_{ab} + \frac{\lambda}{2} (\phi_a(x) \phi_b(x) + F_{ab}(x, x)). \quad (3.44)$$

Using all these notations we can rewrite equations (3.27) in the following form

$$\left\{ \begin{aligned} -\frac{\delta S[\phi]}{\delta \phi_a(x)} + \frac{\lambda}{4} F_{cc}(x, x) \phi_a(x) + \frac{\lambda}{2} F_{ab}(x, x) \phi_b(x) &= \int_0^{x^0} dy^0 \int_0^L dy^1 \Sigma_{ab}^\phi(x, y) \phi_b(y), \\ (\partial^2 \delta_{ab} + M_{ab}^2(x)) F_{bc}(x, y) &= \int_0^{y^0} dz^0 \int_0^L dz^1 \Sigma_{ab}^F(x, z) \rho_{bc}(z, y) - \\ & \int_0^{x^0} dz^0 \int_0^L dz^1 \Sigma_{ab}^\rho(x, z) F_{bc}(z, y) \\ (\partial^2 \delta_{ab} + M_{ab}^2(x)) \rho_{bc}(x, y) &= - \int_0^{x^0} dz^0 \int_0^L dz^1 \Sigma_{ab}^\rho(x, z) \rho_{bc}(z, y), \end{aligned} \right. \quad (3.45)$$

We have exchanged two equations for  $\phi$  and  $G$  for three equations for  $\phi$ ,  $G$ , and  $\rho$  but in exchange we have got clearly posed initial-value problem for three functions<sup>2</sup>.

These equations are second order in time because of  $\partial^2$  in each of them. Therefore, we need two initial conditions for each function.

Firstly, we discuss initial conditions for  $\rho_{ab}(x, y)$  because these are most obvious ones. Initial condition for  $\rho_{ab}(x, y)$  actually are not defined by us but by the properties of the quantum mechanics itself. Recall from (3.37) that it is nothing but commutator of fields. Due to this fact we easily determine initial conditions for  $\rho_{ab}(x, y)$  using equal-time commutation relations for the scalar field

<sup>2</sup>I do not account here that functions here actually have indices, as  $\phi_a(x)$  is 2-dimensional vector, and  $G_{ab}(x, y)$  is 2-dimensional matrix. So actually, we have exchanged six equations for 10.

$$\left\{ \begin{array}{l} [\phi_a(t, x), \dot{\phi}_b(t, y)] = -i \delta_{ab} \delta(x - y) \\ [\dot{\phi}_a(t, x), \dot{\phi}_b(t, y)] = 0 \\ [\phi_a(t, x), \phi_b(t, y)] = 0 \end{array} \right. \Rightarrow \left\{ \begin{array}{l} \lim_{y^0 \rightarrow x^0} \partial_{x^0} \rho_{ab}(x^0, x; y^0, y) = \delta_{ab} \delta(x - y) \\ \lim_{y^0 \rightarrow x^0} \partial_{x^0} \partial_{y^0} \rho_{ab}(x^0, x; y^0, y) = 0 \\ \rho_{ab}(x^0, x; x^0, y) = 0 \end{array} \right. \quad (3.46)$$

Then we set  $x^0 = 0$  and get initial conditions. Due to this fact  $\rho_{ab}(x, y)$  is called the spectral part of the Green's function of the theory because it reflects characteristics of the theory regardless particular initial settings.

Next, we will determine initial conditions for  $F_{ab}(x, y)$  which is called statistical part of the Green's function because it depends on the actual initial state that we choose to evolve. Thus, as soon as there are no generic settings to choose three conditions

$$\left\{ \begin{array}{l} F_{ab}(0, \vec{x}; 0, \vec{y}) = \mathcal{F}_{ab}^{(0)}(\vec{x}, \vec{y}), \\ \lim_{t \rightarrow 0} \partial_t F_{ab}(t, \vec{x}; 0, \vec{y}) = \mathcal{F}_{ab}^{(1)}(\vec{x}, \vec{y}), \\ \lim_{\substack{t \rightarrow 0 \\ \tau \rightarrow 0}} \partial_t \partial_\tau F_{ab}(t, \vec{x}; \tau, \vec{y}) = \mathcal{F}_{ab}^{(2)}(\vec{x}, \vec{y}), \end{array} \right. \quad (3.47)$$

we will keep then for a time being.

The last but not least are the initial conditions for the background field which are simply

$$\left\{ \begin{array}{l} \phi_a(0, \vec{x}) = \varphi^{(0)}(\vec{x}) \\ \lim_{t \rightarrow 0} \partial_t \phi_a(t, \vec{x}) = \varphi^{(1)}(\vec{x}) \end{array} \right. \quad (3.48)$$

This is the complete set of initial conditions for the differential-integral system of equations (3.45).

As I have already stated we still have to define initial conditions for  $F$  and  $\phi$ . I will choose them based on the semi-classical quantization of choosen non-perturbative solution. Namely, I will take classical expectation value of the field inferred from solving classical equations of motion, and initial conditions for  $F$  I will get from the Green's function computed in the background of my classical field, which is nothing but  $G_0$  defined as inverse of the second derivative of the action in (3.15).

First of all, it is the second order in time which makes it simple to set the initial-value problem. Second of all, the most difficult non-linear part of these equations provided by (3.26) contributes to (3.45) through memory integrals. It means that everything that happens in the future depends cumulatively on everything that has happened in the past. This is probably challenging task to solve analytically but evidently very straightforward problem for a numerical integration.

Adopting all these advantages of 2PI effective action and closed time-contour of integration we can simulate initial value problem for any semi-classical background. This is the approach I undertake in current work.

But before we come to that there are still a few things to discuss.

### 3.1.5 Generalized Ward-Takahashi identities

Another important ingredient of the approach I am taking in this work is the generic global symmetry of the theory I am about to consider. As it is well-known, there are conserved currents, and conserved charges corresponding to these currents according to Nöther's theorem. At the classical level it states that in case theory is invariant under the action of the global symmetry group  $\mathcal{G}$ , such that if we take an element of  $\mathcal{G}$  linked to the unity element of the group

$$g \in \mathcal{G}, \quad g_a^b = \delta_a^b + (\tau_p)_a^b \epsilon^p + \mathcal{O}(\epsilon^2), \quad (3.49)$$

where  $(\tau_p)_a^b$  are generators which span tangent space to the unity element and  $\epsilon^p$  are coordinates at this space, then field transforms as

$$\phi_a(x) \xrightarrow{g} g_a^b \phi_b(x). \quad (3.50)$$

As a result we get conserved currents

$$\mathcal{J}_p^\mu = \frac{\partial \mathcal{L}}{\partial \partial_\mu \phi_a} (\tau_p)_a^b \phi_b. \quad (3.51)$$

In the sense that

$$\partial_\mu \mathcal{J}_p^\mu = 0, \quad \text{for all } p. \quad (3.52)$$

Then we can extract conserved current under two possible assumptions. Namely, either fields must vanish at space-like infinity, or they must satisfy periodic boundary conditions. The last one is the case, which appears to provide conserved currents in the model we are intended to consider. Taking into account of these assumptions, we integrate by parts classical conservation law (3.52), and deduce

$$\mathcal{C}_p = \int d\vec{x} \frac{\partial \mathcal{L}}{\partial \partial_t \phi_a} (\tau_p)_a^b \phi_b, \quad (3.53)$$

where  $\mathcal{C}_p$  are classical charges.

However, as we know classical conservation laws are not always smoothly getting transferred to the quantum theory, although this is certainly the case if no gauge fields involved. Nevertheless, we have to establish an analogue of the classical conservation laws in terms of 2PI effective action variables.

Let's notice that 2PI formalism depends on two variables, hence, to the usual transformation property of the field given by (3.50) we have added the transformation of the

connected part of the 2-point Green's function. Then, 2PI effective action should remain invariant under following set of transformations

$$\begin{cases} \bar{\phi}_a(x) = g_a^b \phi_b(x) \\ \bar{G}_{ab}(x, y) = g_a^c g_b^d G_{cd}(x, y) \end{cases} \Rightarrow \Gamma[\phi, G] = \Gamma[\bar{\phi}, \bar{G}], \quad (3.54)$$

if the global symmetry holds true when field theory promoted to quantum level.

The statement of eq. (3.54) remains legitimate for any approximation of  $\Gamma[\phi, G]$  that is consistent with the symmetry. Applying, transformation (3.54) to the two-loop contributions (3.19) and (3.20) that we have derived before, invariance of the loop approximation becomes apparent as well.

Although, we haven't yet established that symmetry is consistent with quantum mechanics. In order to do so, let us take generating functional (3.1) and perform a local transformation

$$\phi_x(a) \xrightarrow{g} \phi_a(x) + \delta\phi_a(x), \quad \delta\phi_a(x) = (\tau_p)_a^b \epsilon_b(x) + \mathcal{O}(\epsilon^2), \quad (3.55)$$

where coordinates on the tangent space of unity element of the group were promoted to be space-coordinate functions. This transformation leaves invariant generating functional, hence, we get

$$\begin{aligned} 0 = \int \mathcal{D}\phi \left( \int d^d x \left( \frac{\delta S[\phi]}{\delta \phi_a(x)} - J^a(x) \right) (\tau_p)_a^b \phi_b(x) \epsilon_p(x) + \right. \\ \left. \int d^d y \left( (\tau_p)_a^{\bar{a}} \delta_b^{\bar{b}} + (\tau_p)_b^{\bar{b}} \delta_a^{\bar{a}} \right) K_{\bar{a}\bar{b}}(x, y) \phi_a(x) \phi_b(y) \epsilon_p(x) \right) \\ \exp \left( i \left( S[\varphi_a] + \int \int d^d x \varphi_a(x) J_a(x) + \right. \right. \\ \left. \left. \frac{1}{2} \int d^d x \int d^d y \varphi_a(x) K_{ab}(x, y) \varphi_b(y) \right) \right). \quad (3.56) \end{aligned}$$

Notice, that this holds true for arbitrary variations of parameters  $\epsilon_p(x)$ , therefore we are left with

$$\begin{aligned} 0 = \int \mathcal{D}\phi \left( \left( \frac{\delta S[\phi]}{\delta \phi_a(x)} - J^a(x) \right) (\tau_p)_a^b \phi_b(x) + \right. \\ \left. \int d^d y \left( (\tau_p)_a^{\bar{a}} \delta_b^{\bar{b}} + (\tau_p)_b^{\bar{b}} \delta_a^{\bar{a}} \right) K_{\bar{a}\bar{b}}(x, y) \phi_a(x) \phi_b(y) \right) \\ \exp \left( i \left( S[\varphi_a] + \int \int d^d x \varphi_a(x) J_a(x) + \right. \right. \\ \left. \left. \frac{1}{2} \int d^d x \int d^d y \varphi_a(x) K_{ab}(x, y) \varphi_b(y) \right) \right). \quad (3.57) \end{aligned}$$

Now we can recall that according to Nöther theorem relation

$$\frac{\delta S[\phi]}{\delta \phi_a(x)} (\tau_p)_a^b \phi_b(x) = \partial_\mu j_p^\mu \quad (3.58)$$

holds true in general, namely, it doesn't rely upon equations of motion to be satisfied. Using this together with (3.10), and recalling definitions of  $\phi_a(x)$  and  $G_{ab}(x, y)$  given by (3.4) we derive from (3.57) the following property

$$-i \langle \partial_\mu j_p^\mu(x) \rangle = \frac{\delta \Gamma[\phi, G]}{\delta \phi_a(x)} (\tau_p)_a^b \phi_b(x) + \int d^d y \frac{\delta \Gamma[\phi, G]}{\delta G_{ab}(x, y)} \left( (\tau_p)_a^{\bar{a}} \delta_b^{\bar{b}} + (\tau_p)_b^{\bar{b}} \delta_a^{\bar{a}} \right) G_{\bar{a}\bar{b}}(x, y), \quad (3.59)$$

where expectation value of the conserved current is given by standard path integral expression

$$\langle j_p^\mu(x) \rangle = \frac{1}{Z} \int \mathcal{D}\phi \left( \partial_\mu \phi_a(x) (\tau_p)_a^b \phi_b(x) \right) \exp \left( i \left( S[\varphi_a] + \int \int d^d x \varphi_a(x) J_a(x) + \frac{1}{2} \int d^d x \int d^d y \varphi_a(x) K_{ab}(x, y) \varphi_b(y) \right) \right). \quad (3.60)$$

Equation (3.59) provides the most general quantum conservation law due to global symmetries even with non-trivial source  $J$  and  $K$  but if we decide to satisfy stationary conditions (3.11) as well, then we truly get quantum global conserved current

$$\partial_\mu \langle \hat{j}_p^\mu(x) \rangle = 0, \quad (3.61)$$

which can be easily expressed using 2PI variables

$$\partial_\mu \langle \hat{j}_p^\mu(x) \rangle = \partial_\mu \left\langle \partial_\mu \hat{\phi}_a(x) (\tau_p)_a^b \hat{\phi}_b(x) \right\rangle = \partial_\mu \left( \partial_\mu \phi_a(x) (\tau_p)_a^b \phi_b(x) + (\tau_p)_a^b \lim_{y \rightarrow x} \frac{\partial G_{ab}(x, y)}{\partial x^\mu} \right). \quad (3.62)$$

In order to infer conserved current for this expression we just have to assume  $\phi$  and  $G$  to have vanishing at infinity, or periodic in the box boundary conditions. As soon as we do that we can make use of quantum conserved charges deduced by integration by parts

$$Q_p = \int d\vec{x} \left( \partial_{x^0} \phi_a(x) (\tau_p)_a^b \phi_b(x) + (\tau_p)_a^b \lim_{y \rightarrow x} \frac{\partial G_{ab}(x, y)}{\partial x^0} \right). \quad (3.63)$$

One can notice that we can deduce the same relations for currents and charges treating 2PI effective action as a classical functional of two variables, and establishing Nöther currents as the consequence of symmetry (3.54). Also, if one derives equation (3.63) in this way, it becomes apparent that it holds not only as a general property but at the level of a different approximation schemes as well if these schemes are consistent with the symmetry.

## 3.2 Quantum breaking criterion using 2PI

Now, we turn to the most essential part of the current work, namely, establishing a working approach to determining quantum-break-time.

The goal of this work is to study the dynamical evolution of a classical BEC. Within the 2PI approach, both correlators  $\phi_a(x)$  and  $G_{ab}(x, y)$  have their own mutually-interacting dynamics. It is natural to ask what is a good indicator to determine whether a significant departure from the classical trajectory took place, namely, how to understand when decoherence, which is associated with quantum breaking, happened. Since the initial classical-like configuration consists of coherently excited zero-momentum modes, we define quantum-breaking as the moment after which most of these quanta no longer contribute to the 1-point expectation value  $\phi_a(x)$ . This is due to re-scattering effects that, with time, lead to the occupation of non-zero momentum modes. The latter quantity is encoded in the propagator  $G_{ab}(x, y)$ . Now, I will describe a way to infer quantum break-time using the full power of out-of-equilibrium QFT tools.

It is well known that classical solutions are commonly described within background-field treatment. Namely, a coherent field configuration is described in terms of mean-field expectation value  $\phi_a(x)$ , solving classical equations of motion. Using saddle-point approximation or ordinary 1PI effective action, one can compute quantum corrections and Green's function in the background of this configuration. However, within these approaches, quantum fluctuations are just functions of a given stationary background. On the opposite side, within 2PI treatment, quantum fluctuations, which are encoded in the exact propagator  $G_{ab}(x, y)$ , follow their own interacting evolution, which is of course intertwined with the evolution of the expectation value  $\phi_a(x)$  according to Eq. (3.11). Therefore, both quantities mutually interact and simultaneously evolve. Our criterion for quantum breaking is based on the validity of the semi-classical approximation, implying the existence of a quantity  $\mu$  satisfying conditions described in Sec. 2.5. We will fulfil these conditions by employing semi-classical character of the solution, and using generalized ward-Takahashi identities in 2PI formalism, or more precisely, quantum conserved charges (3.63) derived from them. We discuss here both things simultaneously.

As a useful tool for determining quantum break-time, we will use conserved charge coming from  $SO(2)$  symmetry of the theory. This charge arises due to symmetry transformation

$$\varphi_a \rightarrow R_{ab}(\alpha)\varphi_b, \quad (3.64)$$

that leaves classical action invariant.  $R_{ab}(\alpha)$  is ordinary matrix of the rotations in two dimensions. For this group, transformation generators are simply given by  $i\sigma_2$  Pauli matrix, or in other words 2-dimensional Levi-Civita tensor  $\epsilon_{ab}$ . Then, classical conserved charge is given by

$$Q_{cl}(x^0) = \int_0^L d\vec{x} \lim_{y \rightarrow x} \epsilon_{ab} \partial_{x^0} \phi_a(x) \phi_b(y) = \int_0^L d\vec{x} \left( \dot{\phi}_1(x) \phi_2(x) - \dot{\phi}_2(x) \phi_1(x) \right), \quad (3.65)$$

Although,  $Q_{cl}$  usually scales as  $1/\lambda$  where  $\lambda$  is the dimensionless coupling of the theory the situation is a bit more involved for Bose condensates because  $Q$  is charge not the particle number, and there emerge one more dimensionless parameter that must be controlled in order to properly ensure consistency of semi-classical approximation. But take it as a promise, that we will take care of it later, and for the time being let grant ourselves that classical charge is actually large, meaning<sup>3</sup>

$$Q \xrightarrow{\hbar \rightarrow 0} \text{const}, \text{ and } Q/\hbar \gg 1, \quad (3.66)$$

which is a good start as it complies with the first demand for quantum breaking criterion formulated in Sec. 2.5. Then, let's recall that we can compute quantum fluctuations, as they do really contribute to the charge as well. The contribution of quantum fluctuations to the charge is given by the connected part of the 2-point function which is in terms of 2PI variables becomes

$$\int d\vec{x} \lim_{y \rightarrow x} \epsilon_{ab} \partial_{x^0} \left\langle \hat{\phi}_a(x) \hat{\phi}_b(x) \right\rangle_{\text{connected}} = \int d\vec{x} \lim_{y \rightarrow x} \epsilon_{ab} \partial_{x^0} G_{ab}(x, y). \quad (3.67)$$

Then, let us employ decomposition of the connected Green's function to the statistical, and spectral contributions (3.36). In terms of this decomposition, we get

$$\begin{aligned} \int d\vec{x} \lim_{y \rightarrow x} \epsilon_{ab} \partial_{x^0} \left\langle \hat{\phi}_a(x) \hat{\phi}_b(x) \right\rangle_{\text{connected}} &= \int d\vec{x} \lim_{y \rightarrow x} \epsilon_{ab} \partial_{x^0} G_{ab}(x, y) = \\ &= \int d\vec{x} \lim_{y \rightarrow x} \epsilon_{ab} \partial_{x^0} F_{ab}(x, y) + \text{Infinite constant}, \end{aligned} \quad (3.68)$$

where infinite constant is nothing but

$$\int d\vec{x} \lim_{y \rightarrow x} \epsilon_{ab} \partial_{x^0} (\text{sgn}(x^0 - y^0) \rho_{ab}(x, y)) = \delta(0) \quad (3.69)$$

due to canonical commutation relations. Using this decomposition we will define quantum charge as

$$Q_q(x^0) = \int_0^L d\vec{x} \lim_{y \rightarrow x} \epsilon_{ab} \partial_{x^0} F_{ab}(x, y) \quad (3.70)$$

We safely drop this term, and consider statistical part  $F_{ab}(x, y)$ . We can compute it from the 2-point function in the background of our semi-classical solution from  $G_{0 ab}(x, y)$  defined by eq. (3.15). But using general properties of semi-classical systems  $F_{ab}(x, y) \sim \mathcal{O}(\lambda^0)$ . Therefore, it is apparent that classical charge computed for mean-field (3.65) is bigger compared to quantum charge (3.70)

$$Q_{cl} \gg Q_q \text{ when semi-classics holds.} \quad (3.71)$$

---

<sup>3</sup>Here, I have assumed  $\hbar$  to be restored in all equations



Moreover, let's recall that we have deduced full quantum expression for the conserved charge (3.63) which in terms of the decomposition (3.36) of the connected 2-point Green's function becomes

$$Q = \int d\mathbf{x} \lim_{y \rightarrow x} \epsilon_{ab} \partial_{x^0} (\phi_a(x) \phi_b(y) + F_{ab}(x, y)), \quad (3.72)$$

or in other words

$$Q = Q_{cl}(x^0) + Q_q(x^0). \quad (3.73)$$

Now, we can really see that we have found a quantity which satisfies all the necessary criteria to become the mean to measure departure from classicality. Let's summarize all of it

1. We have a quantity  $Q$  which is conserved

$$\frac{dQ}{dx^0} = 0$$

2. It can be decomposed into two contributions one of which is mean-field dominated and another is expressed in terms of quantum fluctuations

$$Q = Q_{cl}(x^0) + Q_q(x^0) = \int d\mathbf{x} \lim_{y \rightarrow x} \epsilon_{ab} \partial_{x^0} (\phi_a(x) \phi_b(y) + F_{ab}(x, y))$$

3. This quantity satisfies semi-classicality condition

$$\begin{cases} Q_{cl} \xrightarrow{\hbar \rightarrow 0} \text{const} \\ Q_q \xrightarrow{\hbar \rightarrow 0} 0 \end{cases}$$

4. If use closed time-contour described in Sec. 3.1.4 then full charge remains conserved but its composites  $Q_{cl}$  and  $Q_q$  become time dependent

$$Q = Q_{cl}(t) + Q_q(t). \quad (3.74)$$

Hence, the initial conditions computed for stationary configuration still satisfy

$$Q_{cl}(t=0) \gg Q_q(t=0)$$

but this does not necessarily holds true for subsequent evolution.

Based on all these properties we can eventually formulate criterion for quantum breaking which states that when both contributions become comparable, namely

$$Q_q(t_{qb}) \simeq Q_{cl}(t_{qb}), \quad (3.75)$$

breaking occurs. And, the time when it happens  $t_{qb}$  we call *quantum break-time*.

It should be noted that in the theory endowed with  $SO(2)$  symmetry there is a globally conserved charge, which is a bilinear function of the field operators. This is a key factor from which the emergence of such a clear decomposition of the full charge (3.63) in classical (3.65) and quantum (3.70) components emerges. However, if the system is not endowed with such a conserved quantity, a different quantity should be used. In fact, every fundamental relativistic system is by default endowed with integrals of motion connected to the Poincaré group. Therefore, another possibility would be to use the full energy functional, which can also be split into quantum and classical contributions: the classical part stands for the classical energy, namely an expression in terms of the 1-point correlation function and the remaining part is quantum since it depends on the 2-point function. In this case, however, the quantum part is a function of both  $G(x, y)$  and  $\phi(x)$ , although it inevitably holds true that in the  $\hbar \rightarrow 0$  limit quantum contribution vanishes. So, despite way more intricate dependency of energy on 2PI variables, it is nevertheless possible to make a distinction between classical and quantum contributions.

## Some additional remarks

Let me finish this chapter by making a few minor comments.

One could ask us whether it's essential at all to use charge as a mean for measuring departure from classical evolution. Why couldn't we just use directly mean-field and connected parts of the 2-point Green's function to study the evolution and encounter quantum breaking. Indeed, we could, but it would be way more messy and not really illustrative. By using charge we study two well-defined scalar functions of time, imagining if we had to compare two 2 by 2 matrices, each of which depends on two time and two space variables. This sounds not very practical, and we have to anyway come up with some norm to compare these tensor objects. In this regard, the combination of observable integrated over space to give charge gives a great measure and actually is a truly scalar quantity with respect to all symmetries of the theory, both local and global.

Another issue which has to be mentioned is the validity of the expansion. As long as we start from a semi-classical solution, we have to know whether the expansion we are using is valid or not. Usually, validity of semi-classical approximation can be demonstrated as following. We can re-scale fields for the case of 1+1 dimensions,

$$\phi_a \rightarrow \frac{m}{\sqrt{\lambda}} \phi_a, \quad x_\mu \rightarrow mx_\mu. \quad (3.76)$$

Which helps to pull out dimensionless factor

$$S[\phi] = \frac{m^2}{\lambda} \tilde{S}[\tilde{\phi}], \quad (3.77)$$

where  $\tilde{S}[\tilde{\phi}]$  is dimensionless and independent of any coupling. Thus, we have a factor of  $m^2/\lambda$  in front of the dimensionless action, validating the semi-classical approximation for a small value of the coupling constant. This is what indicates naive analysis.

---

However, the situation with Bose-Einstein condensates is a bit more involved. For relativistic condensate, there is another independent dimensionless parameter. This parameter is collective coupling  $\tilde{\lambda}Q$ , where  $\tilde{\lambda} = \lambda/m^2$ . Thus, a dimensionless field  $\tilde{\phi}$  is anyway a function of another dimensionless parameter  $\tilde{\lambda}Q$ . In this situation, to ensure validity of semi-classical approximation, we have to actually keep collective coupling fixed. It could easily happen that collective coupling is smaller than one, but even in this case as long as it is fixed we can render self-interaction coupling  $\tilde{\lambda}$  to be small enough to ensure  $Q \gg 1$  or to make generating functional semi-classical by setting  $S[\phi] \gg 1$ .



# Chapter 4

## Semi-classical theory of a stationary solutions

Now, it is the time to discuss the actual system that we are going to study. I have chosen Bose-Einstein condensate as one of the simplest possible non-perturbative solution to consider. A Bose-Einstein condensate in the context of the quantum field theory can be viewed as a homogeneous stationary solution of the equations of motion. This solution's simplicity is encompassed in its homogeneity. And classically, it is just a function of time. However, of course, we would like to go beyond that by studying this system in its full glory, and, hence, looking at quantum mechanical evolution of excitations and all the other non-trivial degrees of freedom encoded in excitations above the background as well. But as a first step, let's begin with the consideration of the classical theory.

We are going to consider a complex scalar field with  $SO(2)$  symmetry and quartic self-interaction for both signs of quartic coupling. The reason we choose quartic self-interaction is that it is the simplest possible analytical interaction, preserving the symmetry. Also, it's more convenient to keep the scalar field real here, because in the end of the day the study of its evolution is conducted numerically, which is essentially simpler when working with two scalar functions instead of one complex.

Next, we put this system in the box of size  $L$ , and impose periodic boundary conditions for the scalar field, and I would like to remind that we consider this theory on a ring, so there is one time and one space dimension as well. As it is common for field theory, notation  $x$  implies the whole 2-vector in 1+1 dimensional Minkowski space, namely,  $x = (x^0, x^1)$ . The action of such theory is

$$S[\varphi_a] = \int_0^T dx^0 \int_0^L dx^1 \left( \frac{1}{2} (\partial_\mu \varphi_a)^2 - \frac{1}{2} m^2 \varphi_a^2 - \frac{\lambda}{16} (\varphi_a^2)^2 \right), \quad (4.1)$$

where  $m$  is the mass of the scalar field, and  $\lambda$  is quartic coupling. Here, I put “+” sign in front of the coupling, but I want you to remember that eventually we will consider both cases.

We impose periodic boundary conditions in space which are

$$\varphi_a(x^0, x^1) = \varphi_a(x^0, x^1 + L). \quad (4.2)$$

Using these conditions, we can derive classical equations of motion varying functional (4.1) with respect to a scalar field

$$\partial^2 \phi_a + m^2 \phi_a(x) + \frac{\lambda}{4} (\phi_b(x))^2 \phi_a(x) = 0. \quad (4.3)$$

Recall that the action of this theory is invariant under the  $SO(2)$  transformation

$$\phi_a(x) \rightarrow \phi_a(x) + \alpha \epsilon_{ab} \phi_b(x) + \mathcal{O}(\alpha^2), \quad (4.4)$$

where  $\alpha$  is small parameter, and  $\epsilon_{ab}$  is 2-dimensional Levi-Civita tensor. This invariance combined with periodic boundary conditions (4.2) leads to the global conserved charge

$$Q = \int_0^L dx^1 \lim_{y \rightarrow x} \epsilon_{ab} \partial_{x^0} \varphi_a(x) \varphi_b(y) = \int_0^L dx^1 (\dot{\varphi}_1(x) \varphi_2(x) - \dot{\varphi}_2(x) \varphi_1(x)), \quad (4.5)$$

where  $\dot{\varphi}_a(x) = \partial_{x^0} \varphi_a(x^0, x^1)$ .

Besides the  $SO(2)$ -charge there are usual integrals of motions such as energy, and momentum. We will recall here solely the energy integral because during the whole study we will keep momentum conserved and set to be zero as it is irrelevant for us due to the fact that we would like to study homogeneous system.

The energy of the scalar field in the box is

$$E^{(cl)} = \int_0^L dx^1 \left( \frac{1}{2} \left( \frac{\partial \varphi_a}{\partial t} \right)^2 + \frac{1}{2} \left( \frac{\partial \varphi_a}{\partial x} \right)^2 + \frac{1}{2} m^2 \varphi_a^2 + \frac{\lambda}{16} (\varphi_a^2)^2 \right). \quad (4.6)$$

Now, equipped with this knowledge, we can study classical solution of this theory. And we start from the case of the positive self-interaction  $+\lambda\phi^4$  to study a stable condensate.

## 4.1 Classical stable condensate

### 4.1.1 Classical solution

A family of classical solution of the equations of motion (4.3) can be expressed by using following ansatz

$$\varphi_a(t) = 2v R_{ab}(\omega t) \vec{e}_b, \quad (4.7)$$

where  $\vec{e}_b$  is a constant vector of the unit length,  $v$  is the amplitude of the scalar field, and

$$R_{ab}(\alpha) = \begin{pmatrix} \cos(\alpha) & \sin(\alpha) \\ -\sin(\alpha) & \cos(\alpha) \end{pmatrix}, \quad (4.8)$$

with  $\alpha = \omega t$ .

Thus our field is nothing but a homogeneous function of time. and we have to parameters to define, namely, amplitude  $v$  and frequency of rotation  $\omega$ . To get an equation for amplitude we simply put ansatz (4.7) to the equations of motion (4.3), had come to

$$\frac{d^2v}{dx^2} + (\omega^2 - m^2)v + \lambda v^3 = 0 \quad (4.9)$$

as the vector part factors out, and we are left only with scalar equation. This equations is elementary to solve as  $v$  does not depend on  $x$ , so, it's just an ordinary non-linear equation. Hence, classical amplitude of the field is nothing but

$$v(x) = \sqrt{\frac{(\omega^2 - m^2)}{\lambda}}. \quad (4.10)$$

In this equation frequency lies in the range  $\omega \in (m, +\infty)$  where we have excluded case  $\omega = m$  because in this case  $v = 0$  and we simply get a vacuum which we do not care about right now because the condensate itself sort of plays the role of the vacuum, but in the sector of a fixed charge.

Now, we have to figure out the role of the new dimensional parameter  $\omega$ . This is simply done by computing charge (4.5) of the classical configuration (4.7), where  $v$  is given by (4.10)

$$Q = \frac{4\omega L(\omega^2 - m^2)}{\lambda}. \quad (4.11)$$

We can see that charge actually defines  $\omega$ .

Let's simplify the matter and analyze charge for the case of  $\omega \gg m$

$$\omega \simeq m \left( \frac{1}{4mL} \right)^{1/3} \left( \frac{\lambda Q}{m^2} \right)^{1/3}, \quad (4.12)$$

and for  $\omega \ll m$

$$\omega \simeq m \left( 1 + \frac{1}{8mL} \frac{\lambda Q}{m^2} \right) \quad (4.13)$$

and we see that  $\omega$  is actually a function of dimensionless collective coupling  $\lambda Q/m^2$  and dimensionless size  $mL$ . Hence, using this formula we can express field  $\varphi_a(x)$  just as a function of  $m, Q$ , and  $\lambda$ . One can look at the  $\omega$  versus  $Q$  exchange as at the dimensional transmutation where it is not really dimensional completely because the additional parameter arising in theory can be viewed as  $\omega/m$  which is dimensionless as well.

As a last step we compute classical energy as well. From (4.6) we get

$$E = \frac{L}{\lambda} (3\omega^4 - m^4 - 2m^2\omega^2). \quad (4.14)$$

We can express classical energy as a function of charge, which is depicted in Fig. 4.1, and observe that the energy of a classical condensate in the sector of fixed charge is always larger than the energy of free particles  $E_{BC}(Q) > mQ$

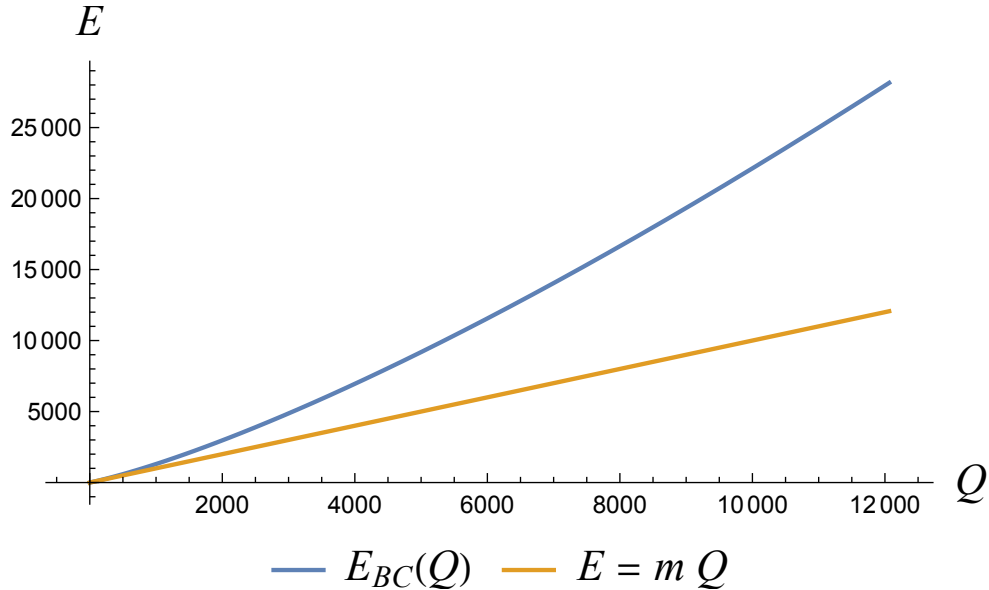


Figure 4.1: Energy  $E_{BC}$  of a stable condensate as a function of charge  $Q$  versus the energy of the collection of free particles with the same net charge.

### 4.1.2 Stability of the condensate

The aim of this work is to consider a true quantum evolution of the Bose-Einstein condensate. However, one must recall that classical evolution occurs as well, and we have to carefully separate it from the quantum one. It might be the case that already at the classical level solution breaks fast enough for some reasons, and as a result there is even no necessity to consider influence of quantum laws onto breaking of our system. For instance, in [27] two kinds of evolution were compared, and the difference between classical, and quantum breaking was drawn. However, for condensate made up from cosmic axion the condensate solution was not the full solution of classical non-linear equations of motion, but it was just a solution of the linear part of equations of motion. Hence, the departure happens due to kick in of the non-linearity. The case considered in this work is a bit more intricate. Here, we have exact solution of non-linear classical equations of motion. Thus, the only departure that can lead to substantial deviations from this solution is due to external influence of the systems. For instance, one can disturb a condensate and excite it, which brings into play the spectrum of linear excitations, and in order to figure out if non-trivial evolution is possible at the classical level we have to analyse the spectrum of small perturbations of a given solution. If this spectrum contains only those normal modes that just oscillate in time it means that the system is stable, and we have nothing to worry about, but if one excites an exponentially growing modes we can be in trouble, because then system departs from the exact solution exponentially fast. This is the reason before going to the analysis of quantum evolution, we have to figure out if the system is classically stable, meaning we have to analyse the spectrum of linear perturbations.



In order to compute the spectrum of linear perturbations, we simply expand equations of motion (4.3) around the classical solution (4.7) and linearize them. It's done by means of substitution

$$\phi_a(x) \rightarrow \phi_a^{(cl)}(x) + \delta\phi_a(x), \quad (4.15)$$

where  $\phi_a^{(cl)}(x)$  is the classical solution and  $\delta\phi_a(x)$  are the small perturbations. Then equations for  $\delta\phi_a(x)$  follow as

$$\int d^2y \left. \frac{\delta^2 S[\phi]}{\delta\phi_a(x)\delta\phi_b(y)} \right|_{\phi=\phi_{cl}} \delta\phi_b(y) = 0, \quad (4.16)$$

or in the explicit form

$$\left( \left( \partial^2 + m^2 + \frac{\lambda}{4} \phi_a^{(cl)2}(t) \right) \delta_{ab} + \frac{\lambda}{2} \phi_a^{(cl)}(t) \phi_b^{(cl)}(t) \right) \delta\phi_b(x) = 0 \quad (4.17)$$

These equations are actually time dependent due to the fact that the classical solution is time-dependent, which doesn't allow solving the eigenvalue problem for  $\delta\phi_a(x)$  right away.

But we can perform a change of variables

$$\delta\bar{\phi}_a(x) = R_{ab}(\omega t) \delta\phi_b(x), \quad (4.18)$$

then equations for small perturbations become linear and time-independent at the expense of appearance of the linear time derivative

$$\left( (\partial^2 - \omega^2 + \frac{\lambda}{4} v^2) \delta_{ab} + 2\omega\epsilon_{ab}\partial_t + \frac{\lambda}{2} v^2 e_a e_b \right) \delta\bar{\phi}_b(t, x) = 0. \quad (4.19)$$

We recall that vector  $e_a$  is just a constant unit vector, hence, we can freely rotate it to be  $e_a = (1, 0)$ .

We can solve this equations by using ansatz

$$\delta\bar{\phi} = \sum_n (a_n \exp(ip_n x) \cos(\gamma_n t) + b_n \exp(ip_n x) \sin(\gamma_n t)), \quad p_n = \frac{2\pi n}{L}, \quad n \in \mathbb{Z}/\{0\}. \quad (4.20)$$

After solving equations (4.19) by employing ansatz (4.20), we find two sets of eigenvalues, which we denote  $\gamma_+$  and  $\gamma_-$

$$\gamma_{\pm}^2 = p_n^2 + \omega^2 + m^2 + \lambda v^2 \pm \sqrt{4(p_n^2 + m^2)\omega^2 + 16\lambda v^2 \omega^2 + \lambda^2 v^4}. \quad (4.21)$$

Here the zero mode is excluded as it is the mode that comprises the condensates itself and this is precisely the zero mode overpopulation that is regarded as a condensation.

One can see by putting the explicit expression for  $v$  given in (4.10), that for  $\omega \in (m, +\infty)$  these eigenvalues are always positive, which ensures classical stability of the condensate with positive quartic coupling. It gives assurance that upon small disturbances this solution will be close enough to its exact form.

Hence, this analysis ensures the triviality of the stationary evolution of the Bose-Einstein condensate composed out of scalar field with positive quartic self-interaction. Now, as we discussed the theory at the classical level, we can complete the discussion about initial conditions.

## 4.2 Initial conditions for the simulation

In this section, we will derive initial conditions for the statistical part of the Green's function and for the field expectation value. We extract the initial conditions from the 1-loop approximation of the 2PI effective action. Namely, we are going to solve here equations (4.26). Within this order, the evolution of the system is trivial because the first loop contains only a functional determinant, which gives the contribution to the local part of self-energy. Hence, the solution we will be looking for is stationary, and doesn't have non-trivial time evolution. Therefore, we can use it as an initial condition.

We start the discussion about initial conditions from summarizing all the functions we will be computing.

The first one is the expectation value  $\phi_a(x)$ . We could take the classical solution as an initial condition for the expectation value, namely,

$$\begin{cases} \phi_a(0, x^1) = \phi_a^{(cl)}(0, x^1) \\ \dot{\phi}_a(0, x^1) = \dot{\phi}_a^{(cl)}(0, x^1) \end{cases}, \quad (4.22)$$

but instead we will go a bit further, and put the one-loop quantum corrected expectation value by solving stationary conditions for 2PI effective action at one loop level.

Next, we have the 2-point connected Green's function,  $G_{ab}(x, y)$  which we split up on the two components  $F_{ab}(x, y)$  and  $\rho_{ab}(x, y)$  using the decomposition (3.36). We know that initial conditions for  $\rho$  are fixed due to commutation relation of the relativistic scalar field theory (3.46), but  $F$  so far remained unfixed. There are no prior restriction for some specific choice of  $F$ , because it is dictated by the initial state (or choice of the initial density matrix). Hence, we have to pick it somehow in the same fashion we chose initial conditions for expectation value of the field.

The initial condition for  $F$  also comes naturally in our analysis. Remember that we would like to study the departure from the mean-field trajectory, and this trajectory is nothing but a local minimum of the classical action. We have already made sure that this configuration realizes local minimum by studying the spectrum (4.21) of the small perturbations (4.15) around the classical mean-field solution. Thus, we know that classically, we are in the safe spot. Now, as we know that fluctuations assure field to be the local minimum configuration, the only thing that could drive it away is the kick-in of quantum evolution.

Hence, to make sure that saddle-point configuration remains saddle-point one, we also set up  $F$  to get its initial value from the solution of 2PI effective action at one-loop level.

In order to get one-loop 2PI effective action, we drop all the contributions which are higher or equal  $\hbar^2$  order. That means basically dropping all the non-trivial part  $\Gamma_2[\phi, G]$ . In this case, functional becomes

$$\Gamma_{(1)}[\phi, G] = S[\phi] + \frac{i}{2} \text{tr} \ln G^{-1} + \frac{i}{2} \text{tr} (G_0^{-1} G). \quad (4.23)$$

Let me show one more time that this is nothing but ordinary effective action imposing stationary condition on  $G$

$$\frac{\delta\Gamma_{(1)}[\phi, G]}{\delta G_{ab}(x, y)} = 0 \Rightarrow \int d^2z G_{0ac}^{-1}(x, z) G_{cb}(z, y) = \delta_{ab}\delta^2(x - y). \quad (4.24)$$

Thus, we see that

$$G_{ab}(x, y) = G_{0,ab}(x, y), \quad (4.25)$$

where  $G_0$  defines leading order Green's function in the mean-field background (3.15), and effective action becomes The stationary conditions in this case are

$$\begin{cases} G_{0,ab}^{-1}(x, y) = G_{ab}^{-1}(x, y), \\ \frac{\delta S}{\delta\phi_a(x)} + \frac{i}{2}\text{tr}\frac{\delta G_0^{-1}}{\delta\phi_a}G = 0, \end{cases} \quad (4.26)$$

where, from the definition (3.15) and the action (4.1) it follows that

$$G_{0,ab}^{-1}(x, y) = i \left( \left( \partial^2 + m^2 + \frac{\lambda}{4}\phi_a^2 \right) \delta_{ab} + \frac{\lambda}{2}\phi_a\phi_b \right) \delta^{(2)}(x - y). \quad (4.27)$$

One can notice that after evaluating the first stationary condition in (4.26), we can plug the result back into the effective action (4.23), and derive

$$\Gamma_{(1)}[\phi, G[\phi]] = S[\phi] + \frac{i}{2}\text{tr}\ln G_0^{-1} \equiv \Gamma[\phi]_{1PI},$$

which is the 1-particle irreducible effective action at one-loop order.

The condensate solution of equations (4.26) can be picked up by using ansatz

$$\begin{cases} \phi_a(x) = R_{ab}(\omega x^0)f_b, \\ G_{ab}(x, y) = R_{ac}(\omega x^0)R_{bd}(\omega y^0)\tilde{G}_{cd}(x - y), \end{cases}, \quad (4.28)$$

where  $f_a$  is the constant vector, and  $R_{ab}(\alpha)$  was defined in (4.8).

One can actually see that after plugging in this ansatz, 2PI effective action admit a homogeneous non-trivial solution for the field expectation value while still preserving time and space translation-invariance as explicit time dependence fully factors out.

Hence, after plugging the ansatz (4.28) in the equations (4.26), we get

$$\begin{cases} \left( \left( \omega^2 + \gamma^2 - p_n^2 - m^2 - \frac{\lambda}{4}f_d^2 \right) \delta_{ac} - 2i\omega\gamma\epsilon_{ac} - \frac{\lambda}{2}f_a f_c \right) \tilde{G}_{cb}(\gamma, p_n) = i\delta_{ab} \\ \left( \left( -\omega^2 + m^2 + \delta m^2 + \frac{\lambda}{4}f_d^2 \right) \delta_{ab} + \frac{\lambda}{4} \left( \tilde{G}_{dd}(0, 0)\delta_{ab} + 2\tilde{G}_{ab}(0, 0) \right) \right) f_b = 0 \end{cases}, \quad (4.29)$$

where

$$\tilde{G}_{ab}(x - y) = \frac{1}{L} \int \frac{d\gamma}{2\pi} \sum_{n=-\infty}^{+\infty} e^{-i\gamma(x^0 - y^0) + ip_n(x^1 - y^1)} \tilde{G}_{ab}(\gamma, p_n) \Big|_{p_n = \frac{2\pi n}{L}}$$

and

$$\delta m^2 = -\lambda \sum_{n=-\infty}^{+\infty} \frac{1}{2\sqrt{p_n^2 + m^2}} \quad (4.30)$$

is the counterterm taken from the free theory, which is natural since the true vacuum of the theory is intact and well-defined.

We can find the solution of the first equation, because we simply have to invert the background dependent constant matrix.

To solve the system (4.29) we have to figure out, when the linear operator acting on  $\tilde{G}$  in the first equation is invertible. It turns out that this is the case when the following condition is fulfilled,

$$\sqrt{f_a^2} > v \quad (4.31)$$

where  $v$  is defined in (4.10). Thus, we see that actually the modulus of the field must be bigger than its saddle-point value. Next, keeping in mind this condition, we can invert  $\tilde{G}_0^{-1}$  and find  $\tilde{G}_{ab}$ , which is

$$\tilde{G}_{ab}(\gamma, p_n) = \frac{i \left( \left( \omega^2 + \gamma^2 - p_n^2 - m^2 - \frac{\lambda}{4} v^2 \right) \delta_{ac} + 2i\omega\gamma\epsilon_{ac} - \frac{\lambda}{2} v^2 e_a e_c \right)}{\left( \gamma^2 - \gamma_+^2(p_n) i 0^+ \right) \left( \gamma^2 - \gamma_-^2(p_n) + i 0^+ \right)}, \quad (4.32)$$

where  $i 0^+$  indicates the usual Feynman boundary conditions,  $\epsilon_{ab}$  is 2-dimensional Levi-Civita tensor and the excitation energies are defined by

$$\gamma_{\pm}^2 = p_n^2 + \omega^2 + m^2 + \frac{\lambda}{2} f^2 \pm \sqrt{4(p_n^2 + m^2)\omega^2 + 8\lambda f^2 \omega^2 + \frac{1}{4}\lambda^2 f^4}, \quad (4.33)$$

which are exactly the same as (4.21) with the exception that we will use here quantum corrected expectation value of the scalar field.

Then, we just plug everything into the first equation of the system (4.29), and get the non-linear equation to find  $f_a$ , which depends only on its modulus. So, employing  $SO(2)$  symmetry, we choose this vector to be

$$f_a = \begin{pmatrix} f \\ 0 \end{pmatrix}, \quad (4.34)$$

and the equation to define  $v$  becomes

$$-\omega^2 + m^2 + \frac{\lambda}{4} f^2 + \left( \frac{3\lambda}{4} \tilde{G}_{11}(0,0) + \frac{\lambda}{4} \tilde{G}_{22}(0,0) + \frac{\lambda}{2} \tilde{G}_{12}(0,0) + \delta m^2 \right) = 0. \quad (4.35)$$

The solution to these equations is actually a stationary condition for the Coleman-Weinberg potential of the Bose-Einstein condensate. The first equation in the system (4.29) defines a Green's function in the background of the condensate, and the second one

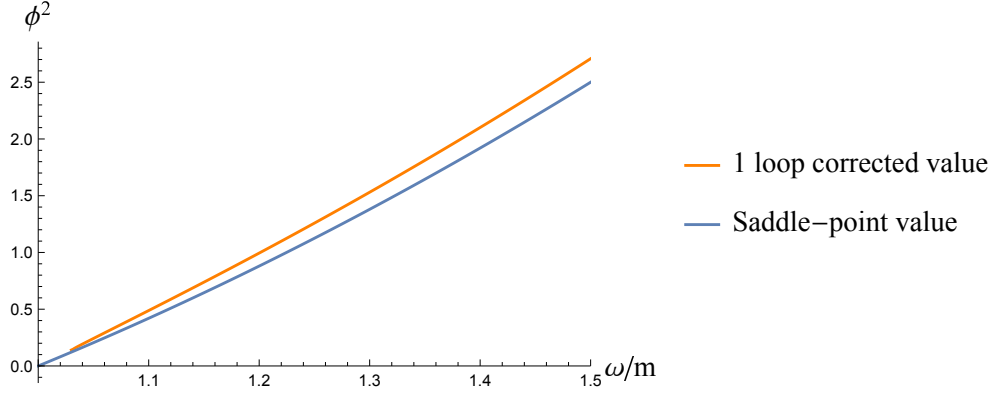


Figure 4.2: Field values for saddle-point and 1-loop approximations for  $\lambda = 1$ ,  $m = 1$ ,  $L = 10 m^{-1}$

is giving an expectation value. The  $\mathcal{O}(\hbar^0)$  part of the second equation are just the classical equations of motions, while the  $\mathcal{O}(\hbar)$  gives the one-loop correction.

By solving the equation (4.35) numerically, we can find the modulus of the field and compare this with the saddle-point value  $v(\omega)$  given by the equation (4.10). This comparison is presented in Fig. 4.2 for specific parameters. We took here  $\lambda = m^2 = 1$  for illustrative purposes, though, one can see that even in this case the corrections to the modulus are quite small. One can also observe that in the 1-loop case, for some  $\omega > m$ , a solution to equation (4.35) does not exist. This is in contrast with the classical case which admits a solution for all frequencies bigger than the mass of the free boson  $m$ .

Another point which is worth mentioning is the invertibility of the operator in (4.29) acting on the Green's function. We have made an a priori assumption about its invertibility given by (4.31) and now explicitly checked that for the solutions of (4.35) this inequality is indeed fulfilled.

Now, we have an expectation value  $f$ , which we can plug in to the Fourier image of the Green's function (4.32), and using the decomposition of the propagator (3.36) we can extract the initial condition for  $F$ .

We perform integration over  $\gamma$ , and separating to terms in the same way as in (3.36) we extract the statistical component of  $G$

$$F_{ab}^0(x, y) = \frac{1}{L} \sum_{n=-\infty}^{+\infty} R(\omega t) \left( \frac{1}{4\gamma_+} \left( e^{-i\gamma_+(x^0-y^0)} \tilde{G}(\gamma_-, p_n) + e^{i\gamma_+(x^0-y^0)} \tilde{G}(-\gamma_+, p_n) \right) - \frac{1}{4\gamma_-} \left( e^{-i\gamma_-(x^0-y^0)} \tilde{G}(\gamma_-, p_n) - e^{i\gamma_-(x^0-y^0)} \tilde{G}(-\gamma_-, p_n) \right) \right) R^T(\omega \tau) \frac{e^{i p_n(x^1-y^1)}}{(\gamma_+^2 - \gamma_-^2)}, \quad (4.36)$$

which will serve as initial condition.

Setting  $x^0 = y^0$  we get an initial condition for  $F_{ab}(x, y)$ . Hence, we have the set of initial conditions that define the initial state of the system. These are

$$\left\{ \begin{array}{l} \phi_a(0, x) = R_{ab}(0)f_b, \\ \dot{\phi}_a(0, x) = \lim_{t \rightarrow 0} \dot{R}_{ab}(\omega t)f_b, \end{array} \right. , \quad (4.37)$$

$$\left\{ \begin{array}{l} \lim_{\substack{x^0 \rightarrow 0 \\ y^0 \rightarrow 0}} F_{ab}(x, y) = \lim_{\substack{x^0 \rightarrow 0 \\ y^0 \rightarrow 0}} F_{ab}^0(x, y), \\ \lim_{\substack{x^0 \rightarrow 0 \\ y^0 \rightarrow 0}} \partial_{x^0} F_{ab}(x, y) = \lim_{\substack{x^0 \rightarrow 0 \\ y^0 \rightarrow 0}} \partial_{x^0} F_{ab}^0(x, y), \\ \lim_{\substack{x^0 \rightarrow 0 \\ y^0 \rightarrow 0}} \partial_t \partial_\tau F_{ab}(x, y) = \lim_{\substack{x^0 \rightarrow 0 \\ y^0 \rightarrow 0}} \partial_{x^0} \partial_{y^0} F_{ab}^0(x, y), \end{array} \right. \quad (4.38)$$

where  $F_{ab}^0(x, y)$  is given by (4.36), and  $f_a = (f, 0)^T$  with  $f$  being defined by the numerical solution of eq. (4.35).

Also, we recall from the equation (3.46) the initial conditions for  $\rho$  following from the canonical commutation relations

$$\left\{ \begin{array}{l} \lim_{y^0 \rightarrow x^0} \partial_{x^0} \rho_{ab}(x, y) = \delta_{ab} \delta(x^0 - y^0) \\ \lim_{y^0 \rightarrow x^0} \partial_{x^0} \partial_{y^0} \rho_{ab}(x, y) = 0 \\ \rho_{ab}(x^0, x; x^0, y) = 0 \end{array} \right. . \quad (4.39)$$

At this point, we have everything to inspect the quantum evolution of the stable Bose-Einstein condensate: the equations (3.45) to solve, the initial conditions (4.37), (4.39) to start from, and the only remaining thing is the finite-difference scheme for numerical integration of the equations, which I will describe in the next section.

# Chapter 5

## Quantum evolution of the stable condensate

In this chapter, I will present numerical solution of the stationary conditions of the effective action, and discuss the results from the point of view of the quantum breaking.

### 5.1 Numerical simulations

Equations (3.45) accompanied by initial conditions (4.37) and (4.39), have been solved numerically using a Newtonian finite difference scheme for derivatives and a trapezoidal rule for memory integrals. Both the size of the box and the spacing and the time step have been varied to ensure the reliability of the simulation by verifying the total charge conservation. Moreover, it was explicitly checked that for what follows, effects due to the box-size are irrelevant as long as  $L \gg m^{-1}$ ; from now on the setting  $L = 10 m^{-1}$  is used.

Since it is possible to rescale the action as in (3.76), it is reasonable to set  $m = 1$  and work in units of mass. Then, in order to explore the properties of the quantum breaking two parameters can be varied: namely the coupling  $\lambda$ , fixing the interaction strength, and the condensate frequency  $\omega$ , determining the initial field amplitude, or charge, because  $Q = Q(\omega)$ . Moreover, it should be noted that at  $t = 0$  we have  $Q_{cl} \gg Q_q$  as the classical one scales as  $\lambda^{-1}$ , and the quantum charge as  $\lambda^0$ , and the difference between full and classical charges at the beginning of the evolution is of order  $\mathcal{O}(\lambda^0)$ , so taking this into account we will not distinguish the initial classical charge from the full charge.

The first results I want to present are showed in Figure 5.1. It is shown how the classical charge  $Q_{cl}(t)$  decreases with time. This quantity is roughly constant during a rather long timescale (approximately 10 inverse masses), mimicking the classical tree level solution, and dramatically changes thereafter at an almost exponential speed; this is the essence of quantum breaking. Moreover, the total charge (blue line) is shown to be conserved, therefore ensuring the reliability of the simulation. This feature holds true also in figure 5.3, although not displayed explicitly. Here, the dynamics of the breaking is shown for different  $\omega$ 's (or, equivalently, different charges) and, as one can see, they all seem to break

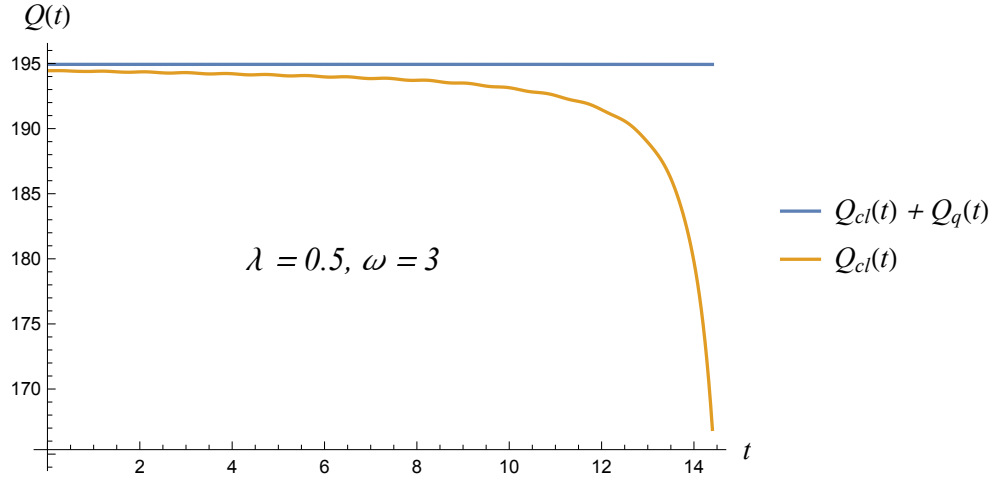


Figure 5.1: Time dependence of the classical and full charges for  $\omega = 3$  and  $\lambda = 0.5$ .

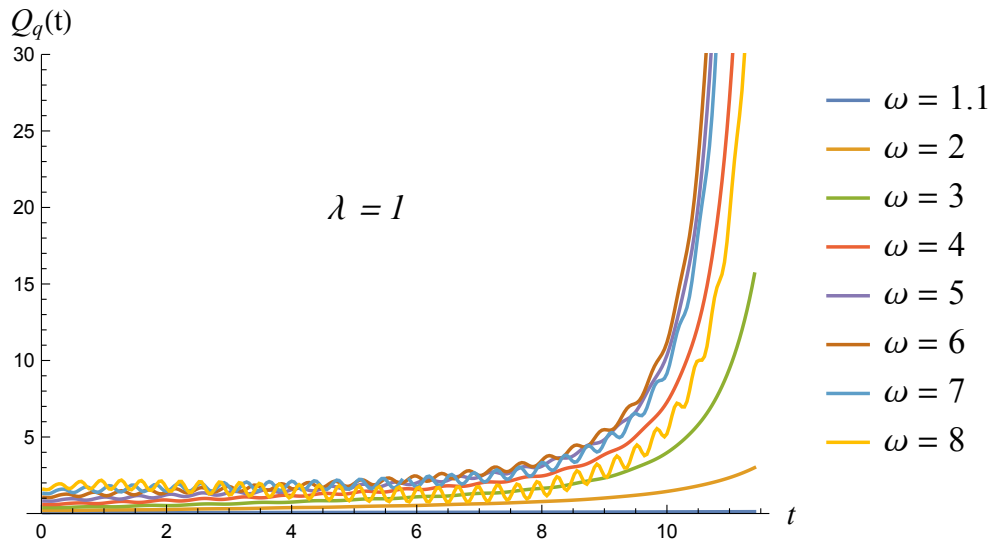


Figure 5.2: Time dependence of  $Q_q$  for different frequencies  $\omega$ .



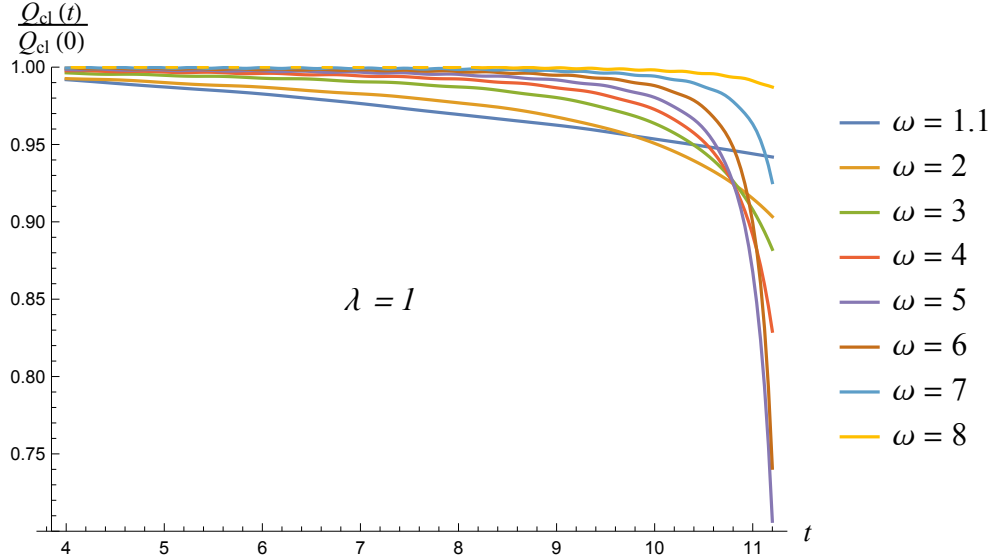


Figure 5.3: Time dependence of  $Q_{cl}$  normalized by the initial value for different frequencies  $\omega$ .

in a similar fashion. For completeness, in figure 5.2, the evolution of the quantum charge defined according to (3.70) is shown for the same set of  $\omega$ 's. As expected, because of the charge conservation of the system, it grows with time. Since the occupation number of different modes can be extracted from the propagator  $G$  (the way to extract occupation numbers can be found in [33]), we interpret the quantum breaking as a redistribution of such modes into a configuration where quantum fluctuations are no longer dynamically negligible according to the scheme suggested in Section 2.5.

The dependence of such “scrambling” on the frequency  $\omega$  is explicitly depicted in figures 5.4(a) and 5.4(b), where  $t_{qb}$  is defined according to the already discussed criterion (3.75). Independently of the coupling constant, two different features can be observed as the charge is varied. In the limit of small charge, displayed on the left side of figures 5.4(a) and 5.4(b), the quantum break time grows asymptotically. This is because, as  $\omega$  decreases, we approach the infinitely long-lived uncharged vacuum. In this limit, as the collective coupling becomes miniscule, the collective oscillatory period is closer and closer to that of free zero mode particles. Correspondingly, the propagator on top of the condensate is approximately the same as in the free theory one and the system basically consists of diluted quasi-free bosons on top of the unbroken vacuum.

Let me illustrate this using evaluation of the diagrams contributing to  $\Gamma_2[\phi, G]$  part of the 2PI effective action (3.18). One can understand the behaviour I talked about looking at the diagrammatic behaviour. Out of the two diagrams at  $\mathcal{O}(\hbar^2)$ , one is simply proportional

to the coupling constant (we restore  $m$  in this part for clarity)

$$\text{Diagram: a figure-eight loop with a central vertex and a label } \lambda \text{ above it} \sim \frac{\lambda}{m^2}. \quad (5.1)$$

Because the above is almost independent of the field expectation value, it is not the one responsible for the interaction between the degrees of freedom of the effective action, and, therefore, it is irrelevant for the breaking of the system. The reason I have said “almost independent” is that in spite of the diagram being dependent on the background field, there is still a propagator, which is the function of the background. But when  $\omega$  approaches  $m$ , the background field modulus  $v$  approaches 0, as one can see from (4.10). Hence, the propagator is almost the same as the propagator of the free theory.

The opposite is true for the second diagram, which is proportional to  $\lambda^2 \phi_a^2$ , non-local, and accounts for the interaction between  $\phi$  and  $G$ . Therefore, its relevance for the dynamics heavily depends on the value of  $\omega$ . In particular, in the limit of small charge (or  $\omega \approx m$ ), its cumulative effects leading to quantum breaking are additionally suppressed

$$\lambda\phi_a \text{ --- } \text{Diagram: a circle with a horizontal line through the center and two vertices on the line labeled } \lambda\phi_a \text{ and } \lambda\phi_b \text{ ---} \lambda\phi_b \sim \frac{\lambda^2}{m^4} \phi_a^2 = 4 \frac{\lambda}{m^2} \frac{\omega^2 - m^2}{m^2} \xrightarrow{\omega - m \ll m} 4 \frac{\lambda}{m^2} \frac{2(\omega - m)}{m} \ll \frac{\lambda}{m^2}.$$

In fact, in the exact free theory limit, this diagram vanishes, and the free theory propagators are recovered (with a self-energy like correction coming from the first diagram), and, due to the absence of a non-local diagram, no interesting dynamics leading to quantum breaking is observed at this loop order. Hence, this explains why  $t_{qb}$  increases as  $\omega$  decreases. Interestingly, but not surprisingly,  $t_{qb}$  grows also in the opposite, big charge, limit ( $\omega \gg m$ ) as it can be seen on the right side of figures 5.4(a) and 5.4(b). In this case, diagrammatically, the non local diagram seems to be enhanced; we have in fact:

$$\lambda\phi_a \text{ --- } \text{Diagram: a circle with a horizontal line through the center and two vertices on the line labeled } \lambda\phi_a \text{ and } \lambda\phi_b \text{ ---} \lambda\phi_b \sim \frac{\lambda^2}{m^4} \phi_a^2 = 4 \frac{\lambda}{m^2} \frac{\omega^2 - m^2}{m^2} \xrightarrow{\omega \rightarrow +\infty} 4 \frac{\lambda}{m^2} \frac{\omega^2}{m^2} \gg \frac{\lambda}{m^2},$$

Correspondingly, one would expect quantum breaking to happen even faster. This puzzle can be explained in the following way. The internal degrees of freedom in this case are very different from the free ones, due to the large charge and energy density. Consequently, one should also take into account the scaling of the propagator, and not just the field insertion, as it is done in the above estimate. This is hard to do analytically, however one can see that this contribution is small numerically. Moreover, the behaviour

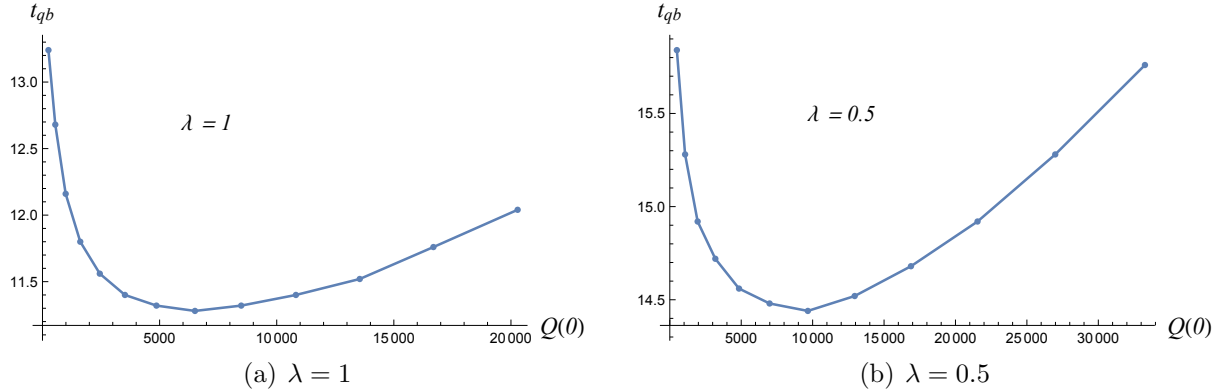


Figure 5.4: Quantum break-time as a function of the full charge

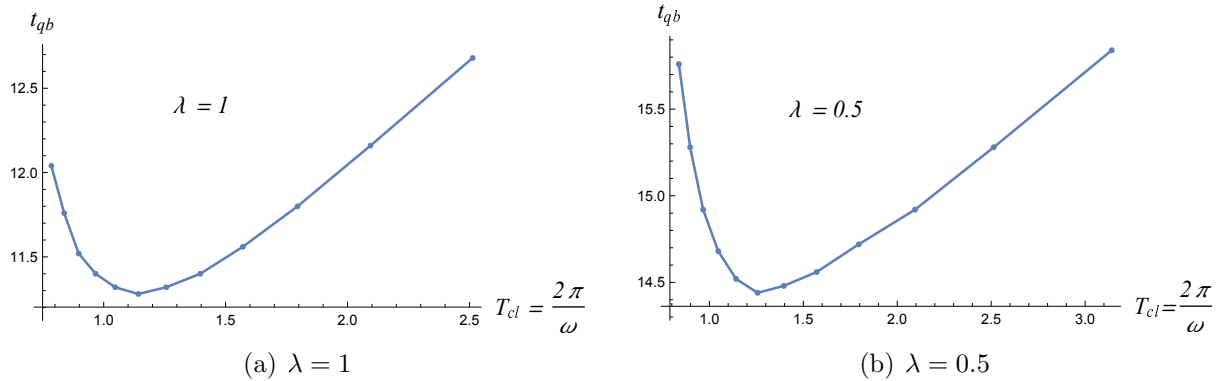


Figure 5.5: Quantum break-time as a function of period of initial classical oscillations

in the big charge regime is fully justified if one takes into account the fact that, in this limit, the system becomes highly classical, therefore ensuring a longer breaking.

Because  $t_{qb}$  grows in the opposite limits of small and large charge, there is a value of  $Q$  for which breaking happens the fastest.

Let us investigate this point in more details. In figures 5.4(a) and 5.4(b), the quantum break time is shown for the same set of frequencies, but for different charges (as the couplings are different). The minimum lies at two different charge values: at  $Q \sim 6 \cdot 10^3$  and at  $Q \sim 10^4$  respectively. However, if we check the dependence of the minimum on a more natural quantity, which is the classical period time  $T_{cl} = 2\pi/\omega$  as in figures 5.5(a) and 5.5(b), it is evident that the minimum occurs at approximately the same value i.e.  $T_{cl} \sim m^{-1}$ .

The attentive reader might wonder whether this minimum, as well as the big charge behaviour is indeed due to the high classicality of the system or to a failure of the perturbative  $\hbar$  expansion. The latter turns out not to be the case for the following reason. For the given  $\omega$  range, the qualitative behaviour we observe is the same as long as the coupling strength is kept weak, i.e.  $\lambda \leq 1$ . However, as  $\lambda \geq 1$ , the dependence was checked

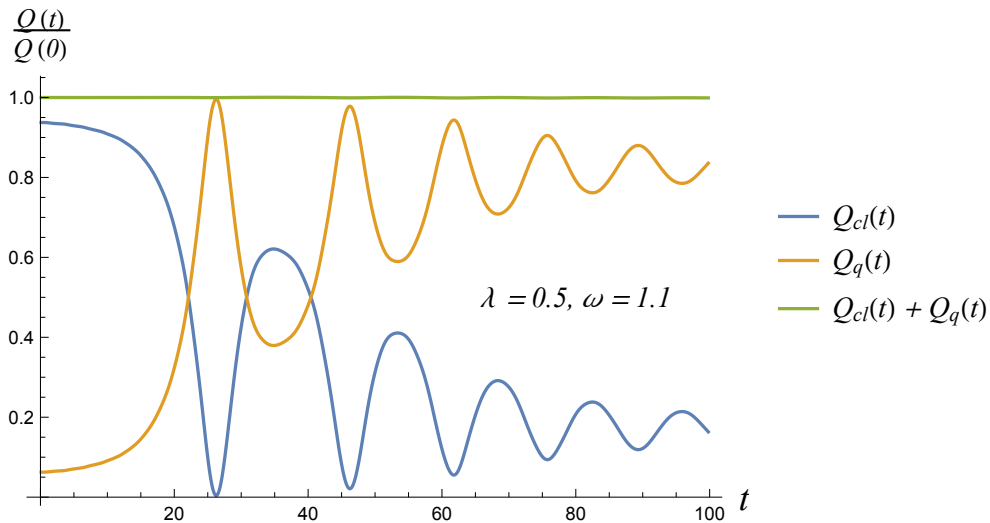


Figure 5.6: Behaviour of the classical and quantum charge for long time. Conservation of charge is showed. Here  $\omega = 1.1$ ,  $\lambda = 0.5$  .

to be totally different and, in particular, criterion dependent. If we define the quantum breaking criterion by the ratio  $a = Q_q(t_{qb})/Q_{cl}(t_{qb})$  in the region where  $Q_{cl}(t)$  monotonically decreases (and  $a \in (Q_q(0)/Q_{cl}(0), 1]^1$ ), the qualitative behaviour of  $t_{qb}$  as a function of  $\omega$  changes dramatically with  $a$  in the strong coupling regime. Contrarily, in the small coupling regime, the dependence is qualitatively unaffected by the choice of  $a$ .

Finally, the long-time dynamics is displayed in figure 5.6. As one can see, the evolution eventually becomes stationary, redistributing the total charge between  $\phi$  and  $G$ . It follows that, asymptotically, the solution approaches values far from the initial the one-loop stationary solution of the system (4.29), which form is given by ansatz (4.28). Indeed, we would like to stress that the evolution is reliable up to  $\mathcal{O}(\hbar^3)$  corrections. Since such effects, in principle, could be cumulative, it is unclear whether the plotted solution is reliable up to the very end of the simulation. Hence, we trust the evolution until the breaking happens, and after that the charge conservation ensures only the reliability of the numerical simulation, but does not accurately reflect physics. Using the scales introduced in Figure 5.6, we should trust the simulation until  $t \simeq 20 m^{-1}$ , where quantum breaking condition is fulfilled, namely  $Q_{cl}(t_{qb}) = Q_q(t_{qb})$ .

In the next section, I will make a comparison of the 2PI effective action approach, and the straightforward perturbative approach, where no resummation is used.

## 5.2 Comparison with the perturbative expansion

Once the results inferred from the solution of the stationary conditions of the 2PI effective action are delivered, and a non-trivial conclusion about the system actually undergoing

<sup>1</sup>when  $a = 1$  we recover (3.75)

quantum breaking is obtained, I would like to support the claim about the impotence of the ordinary methods to pick up this phenomenon, and exhibit fidelity at the long timescale. To do so, we will consider ordinary perturbation theory, and compute this perturbative evolution using closed time-contour.

The perturbative equations of motion in the coupling  $\lambda$  can be easily derived using the Schwinger-Keldysh formalism [98, 99] as done in [100] for a real scalar field. To do so, we define a density matrix  $\rho$  describing the system at  $t = 0$  evolving according to (in the interaction picture)

$$i \frac{\partial \rho(t)}{\partial t} = [H_I(t), \rho(t)],$$

whose formal solution is

$$\rho(t) = U_I(t, t_0) \rho(t_0) U_I^{-1}(t, t_0),$$

with  $U_I(t, t_0) = T_C \exp \left( -i \int_0^t dt' H_I(t') \right)$ ;  $T_C$  denoting the ordering with respect to the in-in contour.

The expectation value of the field is then given by

$$\phi(t) = \langle \Phi(t) \rangle = \frac{\text{Tr} \Phi \rho(t)}{\text{Tr} \rho(t)} = \text{Tr} \left[ \rho(t_0) T_C \left( \Phi(t)^+ \exp \left[ -i \int_0^t [H_I(t')^+ - H_I(t')^-] \right] \right) \right], \quad (5.2)$$

where  $\pm$  indicates on which branch the operators are to be evaluated.

The generating functional thus becomes

$$Z[J^+, J^-] = \int d\phi^+ d\phi^- \rho(\phi^+, \phi^-; t_0) \int_{bc} \mathcal{D}\Phi^+ \mathcal{D}\Phi^- \exp [i S[\Phi^+, \Phi^-, J^+, J^-]], \quad (5.3)$$

where the boundary conditions correspond to  $\Phi^+(0, x) = \phi^+(x)$ ,  $\Phi^-(0, x) = \phi^-(x)$  and  $\Phi^+(t, x) = \Phi^-(t, x)$  and

$$S[\Phi^\pm, J^\pm] = \int_0^t dt' \int dx [\mathcal{L}[\Phi^+] - \mathcal{L}[\Phi^-] + J^+ \Phi^+ - J^- \Phi^-].$$

To find the equations of motion we employ the tadpole method as in [100, 101]. Splitting the field into  $\Phi(t, x)^\pm = \phi(t) + \delta\phi(t, x)^\pm$  where  $\delta\phi(t, x)$  is a fluctuation, one can ask for which background  $\phi(t)$  the tadpole condition,

$$\langle \delta\phi(t, x)^\pm \rangle = 0, \quad (5.4)$$

is satisfied. Assuming that at  $t = 0$  the vacuum is the same as in the free theory (i.e.  $|0(t=0)\rangle = |0\rangle$ ) one obtains, from the path integral

$$\langle \delta\phi^+ \rangle = i \int_0^t dt' \int dx \left[ \left. \frac{\delta S^+}{\delta \Phi^+} \right|_{\phi(t')} G^{++}(t, t'; x, y) - \left. \frac{\delta S^-}{\delta \Phi^-} \right|_{\phi(t')} G^{+-}(t, t'; x, y) \right] + O(\hbar), \quad (5.5)$$

where  $G^{\pm\pm}(t, x; t', y) = \langle T_C (\Phi^\pm(t, x) \Phi^\pm(t', y)) \rangle$ . In particular  $G^{++}, G^{+-}, G^{-+}$  and  $G^{--}$  correspond to the Feynmann, the advanced, the retarded and Dyson propagator respectively. We see that in order for (5.5) to satisfy the tadpole condition (5.4) the background

field needs to be a stationary point of the classical action.

We now evaluate perturbatively in  $\lambda$  the tadpole condition for the fluctuations of (4.1), whose action is given by (from now on we restore  $m$ )

$$S[\delta\phi^+, \delta\phi^-] = \int d^2x \left( \frac{(\partial_\mu \phi_a^+)^2}{2} - \frac{m^2(\delta\phi_a^+)^2}{2} + \delta\phi_a^+ \left. \frac{\delta S}{\delta\varphi_a^+} \right|_{\varphi=\phi} - \frac{(\delta\phi_a^+)^2}{2} \left( m^2 + \frac{\lambda}{4}\phi_a^2 \right) - \frac{\lambda}{4}\delta\phi_a^+ \delta\phi_b^+ \phi_a \phi_b - \frac{\lambda}{16} [(\delta\phi_a^+)^4 + \phi_a^4] - \frac{\lambda}{4}\delta\phi_a^+ \delta\phi_b^2 \phi_a - (\delta\phi^+ \leftrightarrow \delta\phi^-) \right). \quad (5.6)$$

Up to  $\lambda^2$ , the tadpole condition schematically reads:

$$= 0, \quad (5.7)$$

where the dashed line corresponds to an insertion of the background field  $\phi_a$ . The first diagram is nothing but the tree level equation of motion as one can see from (5.5). The second diagram can be absorbed by a mass renormalization. Altogether they lead to

$$\left\{ \begin{array}{l} \ddot{\phi}_1 + m^2\phi_1 + \lambda(\phi_1^2 + \phi_2^2)\phi_1 - \frac{\lambda^2}{2}\phi_1 \int_0^t dt' (\phi_1(t')^2 + \phi_2(t')^2) \int \frac{dk}{2\pi} \frac{\sin[2\omega_k(t-t')]}{2\omega_k^2} \\ \quad - \lambda^2\phi_2 \int_0^t dt' \phi_1(t')\phi_2(t') \int \frac{dk}{2\pi} \frac{\sin[2\omega_k(t-t')]}{2\omega_k^2} = 0 \\ \ddot{\phi}_2 + m^2\phi_2 + \lambda(\phi_1^2 + \phi_2^2)\phi_2 - \frac{\lambda^2}{2}\phi_2 \int_0^t dt' (\phi_1(t') + \phi_2(t'))^2 \int \frac{dk}{2\pi} \frac{\sin[2\omega_k(t-t')]}{2\omega_k^2} \\ \quad - \lambda^2\phi_1 \int_0^t dt' \phi_1(t')\phi_2(t') \int \frac{dk}{2\pi} \frac{\sin[2\omega_k(t-t')]}{2\omega_k^2} = 0 \end{array} \right. \quad (5.8)$$

where the renormalization of the mass has already been taken into account by dropping the second diagram. Note that the choice of the time contour ensured the last term to be causal.

The comparison between the fully resummed 2-loop dynamics and the perturbative analysis to  $\lambda^2$  is shown in figure 5.7. To fix the initial conditions for the perturbative equation of motion (5.8) we considered the saddle point solution (4.7), where field amplitude is defined in eq/ (4.10).

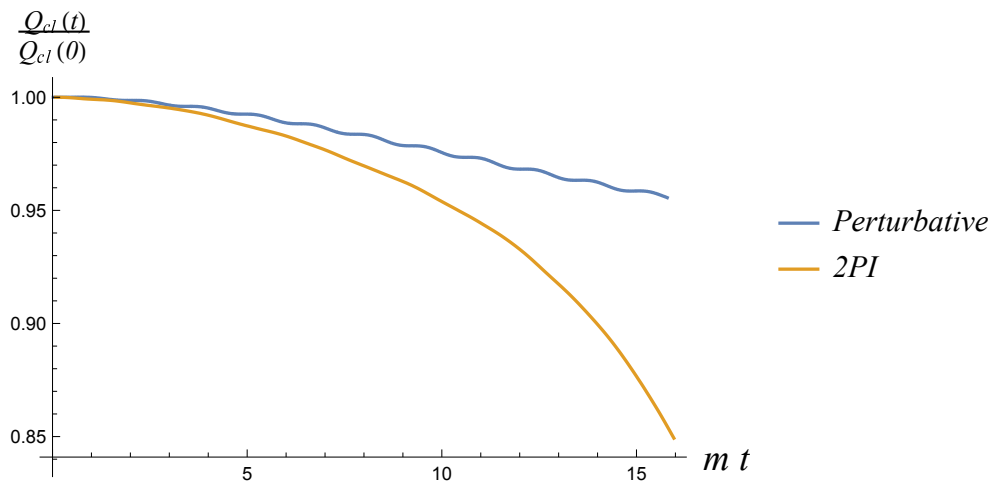


Figure 5.7: Perturbative expansion compared with fully resummed 2PI for  $\lambda = m^2$  and  $\omega = 1.1 m$ .

As it can be seen, the leading behaviour for small times is very similar. However, at later times, the 2PI solution breaks faster. For longer times (although not shown explicitly), the perturbative solution oscillates around  $Q_{cl}(0)$ . Clearly, on such time scales, the perturbative solution is no longer reliable and the leading behaviour of the breaking is captured by the 2PI effective action. So, one sees that perturbative expansion captures some deviation, but does not provide reliable approximation of the real physical evolution at a longer timescale.

Here, we finish studying of the classically stable condensate, and move to the case of the classically unstable condensate.





# Chapter 6

## Classically unstable condensate

### 6.1 Fast quantum breaking

Different system could exhibit various timescales associated with quantum breaking. But there is a class of systems that seems to exhibit breaking much faster than the others.

Namely, in [29] the connection between phenomena of quantum breaking and chaos was established, and it was argued that a many-body macroscopic system can undergo a maximally fast quantum breaking and become chaotic, provided it possesses a Lyapunov exponent  $\gamma$ , with the following formula for quantum break-time:

$$t_{qb} \sim \gamma^{-1} \log N, \tag{6.1}$$

where  $N$  is a certain macroscopic particle number (e.g., the number of off-shell gravitons in the black-hole case, or the particle number in a non-relativistic BEC). In [29], this equation was explicitly checked on an example of a 1 + 1 dimensional system with Lyapunov exponent, namely a non-relativistic unstable BEC. The above-mentioned quantity was derived by means of entanglement arguments. Moreover, it was also suggested that quantum breaking and chaos represent the microscopic mechanisms behind the so-called phenomenon of quantum information scrambling and that the existence of Lyapunov exponent is crucial for a system to saturate the logarithmic bound on the fast scrambling time proposed in [30]. It is argued that these kinds of systems are the ones which break the fastest<sup>1</sup>.

The results of [29] leave certain questions open. For example, it is unclear whether relativistic corrections would affect the above predicted timescale.

The purpose of the next chapter is therefore to study these relativistic effects and to employ an alternative method allowing to compute the quantum-corrected evolution of the semi-classical solution initially assembled as a coherent state within mean-field approximation. Due to the absence of particle conservation, it is rather natural to expect a similar behaviour under the replacement  $N \rightarrow Q$ , which is the conserved charge of the system in the relativistic case. This replacement is anyway absolutely not obvious, as the relativistic

---

<sup>1</sup>There are systems where  $t_{qb} \propto \hbar^{-1}$  c.f. [22], which is much longer than (6.1)

theory possesses a much wider spectrum. In this study, a law similar to (6.1) was found for a relativistic 1 + 1 - dimensional model endowed with  $U(1)$  symmetry and attractive self-interaction. Namely, it was verified that the quantum break time is given by

$$t_{qb} = \gamma^{-1} \log Q + \text{constant}, \quad (6.2)$$

where  $Q$  is the total charge of the configuration,  $\gamma$  is the Lyapunov exponent associated with the instability mode in the spectrum of linear perturbations that the condensate has, and the small constant presence will be shown to be related to the chosen criterion used to extract  $t_{qb}$ . Moreover, note how this timescale happens to be infinite in the semiclassical limit (namely as  $\hbar \rightarrow 0$ ,  $t_{qb} \rightarrow \infty$ ), therefore ensuring the captured effect to be genuinely quantum and not visible at the classical level.

One might ask, what is the relevance of the quantum breaking here, if the system is unstable, and is supposed to break at the classical level, due to the presence of the instability mode in the spectrum of the linear perturbation? The answer is straightforward, although, requires a little bit of fine-tuning.

The thing is that even if the instability is present in the spectrum of the small perturbations, nothing prevents us from evading dealing with this mode by excluding it from initial conditions. In other words, if we tune the system's initial state such that it does not pick up exponentially growing mode, then evolution is stable, and classically no breaking is happening. In this work, this is achieved by keeping the condensate homogeneous from the very beginning. And, the homogeneity of the solution during the evolution is then preserved because of translational invariance of the equations (3.45). Hence, the only way it could break is again by taking a route of quantum breaking!

From here, we proceed with the studying a case of the unstable condensate starting again from scrutinizing a classical theory, and gradually moving to the quantum one.

## 6.2 Classical theory

In this section, we introduce a classical scalar field theory with negative self-interaction, and analyse its spectrum.

Consider a real scalar field endowed with  $SO(2)$  global symmetry with attractive quartic self-interaction in a 1 + 1 dimensional finite box of size  $L$ . The action of this theory is:

$$S[\varphi_a] = \int_0^T dx^0 \int_0^L dx^1 \left( \frac{1}{2} (\partial_\mu \varphi_a)^2 - \frac{1}{2} m^2 \varphi_a^2 + \frac{\lambda}{16} (\varphi_a^2)^2 \right). \quad (6.3)$$

with  $\lambda > 0$ . As in the previous case, we impose periodic boundary condition upon the scalar field  $\phi_a(x)$ .

For convenience, we again list here two integrals of motion which are the most relevant

for our analysis. These are the classical energy

$$E^{(cl)} = \int_0^L dx^1 \left( \frac{1}{2} \left( \frac{\partial \varphi_a}{\partial t} \right)^2 + \left( \frac{\partial \varphi_a}{\partial x} \right)^2 + \frac{1}{2} m^2 \varphi_a^2 - \frac{\lambda}{16} (\varphi_a^2)^2 \right), \quad (6.4)$$

and the classical charge

$$Q^{(cl)} = \int_0^L dx^1 (\dot{\varphi}_1(x) \varphi_2(x) - \dot{\varphi}_2(x) \varphi_1(x)), \quad (6.5)$$

which is literally the same as the one given by (3.65), but we would like to underline that here the field is classical, while in (3.65)  $\phi_a(x)$  is the expectation value of the operator.

This theory enjoys plenty of classical stationary solutions. These solutions can be obtained by means of following ansatz

$$\varphi_a(t, x) = \sqrt{2} R(\omega t)_{ab} \tilde{f}_b(x), \quad (6.6)$$

where  $R(\theta)$  is the usual  $SO(2)$  rotation matrix and  $\omega$  is the integration constant parametrising all possible solutions. Using  $SO(2)$  covariance of the equations we can choose  $\tilde{f}_b(x) = (f(x), 0)^T$ . Then, two equations of motion are reduced to a single one:

$$\frac{d^2 f}{dx^2} + (\omega^2 - m^2) f + \frac{\lambda}{2} f^3 = 0. \quad (6.7)$$

We are going to look for all solutions satisfying periodic boundary conditions.

Two solutions to (6.7) can be found: namely a homogeneous one, the condensate, and a localized one, the bright soliton [62]. In the following, their relation with each other and stability are discussed.

### 6.2.1 Condensate

The condensate solution is given by the homogeneous configuration:

$$f(x) = \sqrt{\frac{2(m^2 - \omega^2)}{\lambda}}, \quad (6.8)$$

where frequency covers the range  $\omega \in (0, m)$ . This expression is identical to the expression (4.10) up to the substitution  $\lambda \rightarrow -\lambda$ . For this solution integrals of motion (6.4) and (6.5) are

$$E_{b.c.} = \frac{L}{\lambda} (m^4 + 2m^2\omega^2 - 3\omega^4), \quad (6.9)$$

$$Q_{b.c.} = \frac{4\omega L (m^2 - \omega^2)}{\lambda}, \quad (6.10)$$

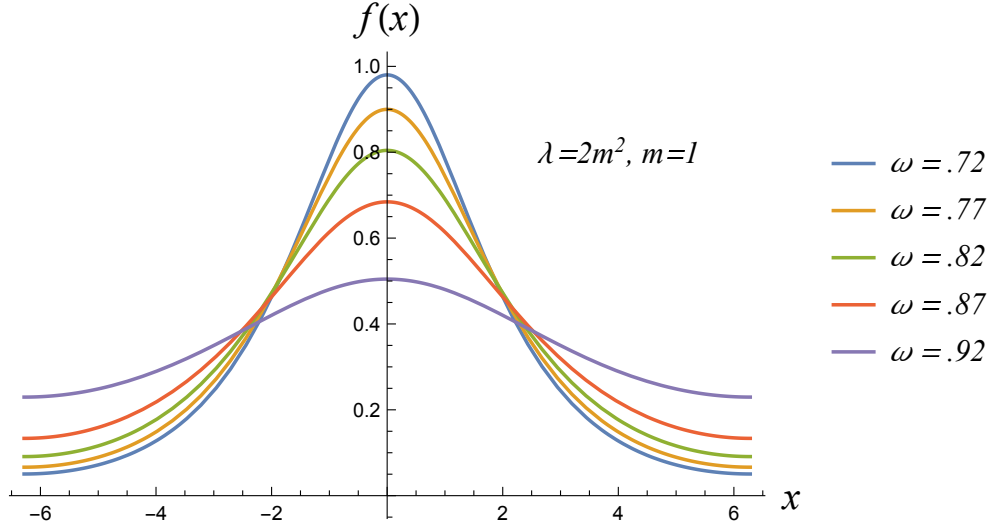


Figure 6.1: Bright soliton solution for different frequencies  $\omega$  and length  $L = 4\pi m^{-1}$ .

where subscript “*b.c.*” stands for Bose condensate.

Notice that for this attractive interaction, the energy of the configuration is lower than the one of free particles, i.e.  $E(\omega) \leq mQ(\omega)^2$ , which is opposite of the case of the stable condensate, where  $E_{b.c} > mQ$

### 6.2.2 Bright Soliton

The second solution arising here is the well-known bright soliton. In the non relativistic limit, the classical bright soliton was studied in [62] and [103]. Here we focus on the relativistic case.

The solution is showed for different  $\omega$ 's in Fig. 6.1 and is given by

$$f(x) = \frac{4K(\mu)}{L\sqrt{\lambda}} dn\left(2K(\mu) \frac{x}{L} \middle| \mu\right), \quad (6.11)$$

where  $K(\mu)$  is the elliptic integral of the first kind,  $dn(x|\mu)$  is the Jacobi elliptic function and  $\mu$  is fixed by the condition

$$4K(\mu)^2(2 - \mu) = L^2(m^2 - \omega^2), \quad (6.12)$$

for which the solution exists if  $\omega \in (0, \omega_{cr})$  and the critical frequency is given by

$$\omega_{cr} = \sqrt{m^2 - \frac{2\pi^2}{L^2}}. \quad (6.13)$$

<sup>2</sup>Here we mean by rest mass of the free particle the mass parameter in the Lagrangian, but one has to remember that if mass parameter is defined at infinite volume by means of conditions  $\Sigma(m^2) = 0$  and  $d\Sigma/dp^2(m^2) = 0$ , than in finite volume it gets modified [102]. But as long as mass acquires an exponentially small correction we don't bother ourselves considering it.

The integrals of motion (6.4) and (6.5) corresponding to the bright soliton are:

$$E_{b.s.}(\omega) = \frac{16(4(\mu-1)K(\mu)^4 + L^2(4\omega^2 + 2)K(\mu)E(\mu))}{3\lambda L^3}, \quad (6.14)$$

$$Q_{b.s.}(\omega) = \frac{32\omega}{L\lambda}E(\mu)K(\mu). \quad (6.15)$$

where subscript “b.s.” stands for bright soliton,  $E(\mu)$  is the elliptic integral of the second kind and  $\mu = \mu(\omega)$  is given by (6.12).

### 6.2.3 Classical stability as the reflection of an interplay between two solutions

We see that both the homogeneous Bose-Einstein condensate and the inhomogeneous bright soliton solutions depend on a single integration constant  $\omega$ . This integration constant defines their charge and energy. Therefore we have several branches of solutions parametrized by  $\omega$ . Let us focus first on the blue branch in Fig. 6.2, representing the condensate solution for different values of  $\omega$  and correspondingly for different charges. We note that  $\omega$  varies from 0 to  $m$ , where values closer to  $m$  have smaller charges. The orange branch instead represents the bright soliton configurations with different  $\omega$ . For the bright soliton we have  $\omega \in (0, \omega_{cr})$ , from which it follows that for  $\omega \in [\omega_{cr}, m)$  the homogeneous solution minimizes energy. As frequency decreases and crosses  $\omega_{cr}$ , the condensate localizes and the bright soliton appears. Therefore,  $\omega_{cr}$  turns out to be the branching point at which  $E_{b.s.}(\omega_{cr}) = E_{b.c.}(\omega_{cr})$  and  $Q_{b.s.}(\omega_{cr}) = Q_{b.c.}(\omega_{cr})$ . The reason behind the emergence of this point is exactly the stability of the classical BEC solution.

Since the potential for this model is unbounded from below<sup>3</sup>, it is natural to question the classical stability of the system. This can be done by means of expanding fields in small perturbations around a given solution of classical equations in the same way we did in Section 4.1.2, namely,

$$\phi_a(x) \rightarrow \phi_a^{(cl)}(x) + \delta\phi_a(x), \quad (6.16)$$

where  $\phi_a^{(cl)}(x)$  is the classical solution and  $\delta\phi_a(x)$  are the small perturbations. Then equations for  $\delta\phi_a(x)$  follow as

$$\int d^2y \left. \frac{\delta^2 S[\phi]}{\delta\phi_a(x)\delta\phi_b(y)} \right|_{\phi=\phi_{cl}} \delta\phi_b(y) = 0, \quad (6.17)$$

or in the explicit form

$$\left( \left( \partial^2 + m^2 - \frac{\lambda}{4}\phi_a^{(cl)2}(t) \right) \delta_{ab} - \frac{\lambda}{2}\phi_a^{(cl)}(t)\phi_b^{(cl)}(t) \right) \delta\phi_b(x) = 0 \quad (6.18)$$

---

<sup>3</sup>This plays no role in our analysis, because the field amplitude is lower than  $2m/\sqrt{\lambda}$  and we do not enter the domain when boundlessness can not be ignored anymore. In the general case, of course the theory can be made bounded by means of inclusion of higher order terms.

Then, again we get rid of the time-dependence by the substitution

$$\delta\bar{\phi}_a(x) = R_{ab}(\omega t) \delta\phi_b(x), \quad (6.19)$$

and get to

$$\left( (\partial^2 - \omega^2 - \frac{\lambda}{4}v^2)\delta_{ab} + 2\omega\epsilon_{ab}\partial_t - \frac{\lambda}{2}v^2 e_a e_b \right) \delta\bar{\phi}_b(t, x) = 0. \quad (6.20)$$

And, as the final step we employ the ansatz (4.20), and find eigenvalues  $\gamma$ , that are

$$\gamma_+(p_n) = \sqrt{p_n^2 + 3\omega^2 - m^2 + \sqrt{m^4 - 6m^2\omega^2 + 4p_n^2\omega^2 + 9\omega^4}}, \quad (6.21)$$

$$\gamma_-(p_n) = \sqrt{p_n^2 + 3\omega^2 - m^2 - \sqrt{m^4 - 6m^2\omega^2 + 4p_n^2\omega^2 + 9\omega^4}}, \quad (6.22)$$

where

$$p_n = \frac{2\pi n}{L}, \quad n \in \mathbb{Z}. \quad (6.23)$$

Note that for solution (6.8), one perturbation mode is classically gapless, i.e.  $\gamma_-(0) = 0$ . Therefore, to analyse the instability, we focus on the non-zero modes. In particular, from (6.22), we see that the first mode turning imaginary, as  $\omega$  decreases, is  $p_1$  and it happens when  $\omega$  becomes less than  $\omega_{cr}$

$$\omega < \omega_{cr} = \sqrt{m^2 - \frac{2\pi^2}{L^2}}. \quad (6.24)$$

We therefore conclude that the condensate solution is classically stable for  $\omega \in [\omega_{cr}, m)$  and unstable otherwise<sup>4</sup>.

In view of this analysis the meaning of the branching point is clear. In fact, the frequency at which the solitonic solution appears in the spectrum is exactly the same frequency (6.13) for which the first momentum mode (and therefore the condensate) becomes unstable. It follows that at  $\omega_{cr}$  the spectrum splits into two branches of classical solutions for smaller frequencies (bigger charges): stable ones, namely bright solitons, and unstable ones - BEC's. We refer to the imaginary part of this frequency  $\text{Im}(\gamma_-(p_1))$  as Lyapunov exponent, because it shows the rate of exponential growth of this mode.

To sum up, we have the following situation: for  $\omega \in [\omega_{cr}, m)$  the condensate solution is classically stable and unique for equation (6.7). In this region, the collective coupling, proportional to  $(\lambda/m^2)f^2$ , increases as  $\omega$  decreases. Upon reaching  $\omega_{cr}$  a phase transition takes place. In this sense, the collective coupling is strong enough as to allow for a localization of the solution. Correspondingly, the fluctuations on top of the condensate display at least an unstable mode indicating the fact that, for a given fixed charge, there exists a classical configuration with lower energy (as it can be seen from comparing (6.9) and (6.14)).

The above statement can easily be deduced from Fig. 6.2. As it is possible to see, the

---

<sup>4</sup>This situation reflects the presence of a Jeans instability and as size gets bigger more modes become unstable. It occurs successively, namely, a given mode  $p_n$  becomes unstable at  $\omega_{cr}(p_n) = \sqrt{m^2 - 2\pi^2 n^2 / L^2}$ . Therefore we deduce that for fixed size  $L$  there will be  $\lfloor mL/\sqrt{2\pi} \rfloor$  unstable modes

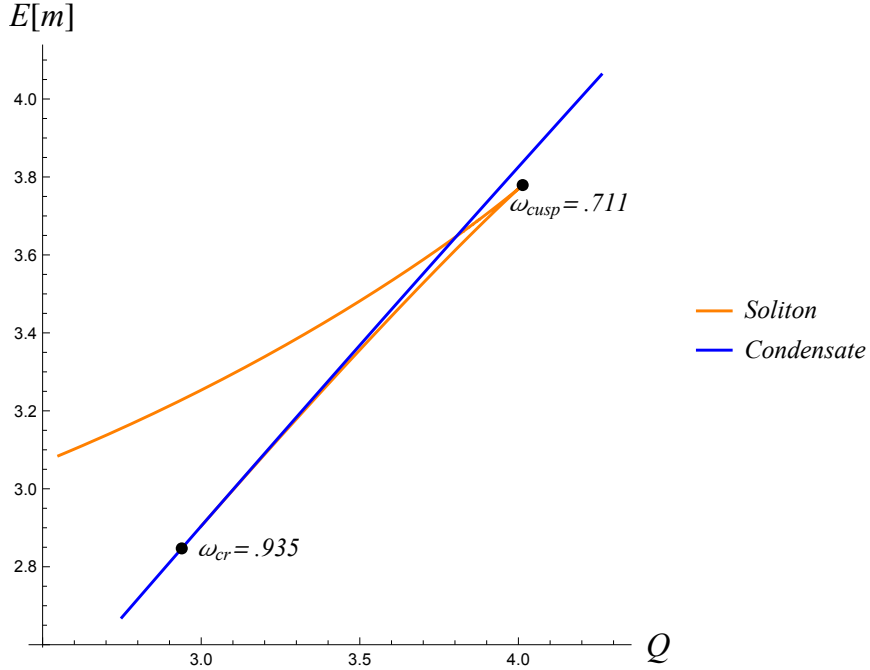


Figure 6.2: Energy versus charge behaviour of condensate and soliton. Here  $L = 4\pi m^{-1}$  and  $\lambda = 2m^2$ .

soliton trajectory emerges from the branching point  $\omega_{cr}$ . Moreover, as  $\omega$  decreases (and the collective coupling increases), the soliton configuration localizes more and more up to the point where it becomes classically unstable (this does not happen in the classical theory). This happens in correspondence of  $\omega_{cusp}$  which is the value for which the known instability condition is fulfilled [104, 105]:

$$\left. \frac{dQ_{cl}}{d\omega} \right|_{\omega=\omega_{cusp}} < 0. \quad (6.25)$$

For lower  $\omega$ 's, the soliton solution corresponds to the points of the upper branch of Fig. 6.2.

Before moving forward it is important mentioning that although the potential is unbounded from below for the condensate (soliton), one can easily see from (4.10) ((6.11)), that the only source of classical instability under small perturbations is given by (6.13) ((6.25)). Moreover, notice that tunnelling phenomena are not relevant in our quantum study as they are exponentially suppressed, while we will see that quantum breaking happens exponentially fast.

#### 6.2.4 Saddle-point solution as the initial condition

Appropriate initial conditions to numerically simulate (3.45) are necessary. Our goal is clear: we wish to study how the classical unstable condensate evolves as quantum fluctuations are dynamically taken into account. Therefore, a natural choice is to consider, at

$t = 0$ , the classical condensate solution, but in this case we will not consider the one-loop approximation of the 2PI as we did in Section 4.2, because of the instability. Instead, we take just the saddle-point solution. That means that, initially, the field  $\phi$  is fixed by the stationarity condition

$$\frac{\delta S[\phi]}{\delta \phi_a} = 0 \quad (6.26)$$

while, for the propagator  $G$ , we need to invert the following operator

$$G_{ab}^{-1}(x, y) = i \left( \left( \partial^2 + m^2 - \frac{\lambda}{4} \phi_a^2 \right) \delta_{ab} - \frac{\lambda}{2} \phi_a \phi_b \right) \delta^{(2)}(x - y). \quad (6.27)$$

In the same fashion, as in Section 4.2, we go to the fourier space to compute initial propagator

$$\begin{aligned} \tilde{G}_{ab}(x - y) &= \frac{1}{L} \int \frac{d\gamma}{2\pi} \sum_{n=-\infty}^{+\infty} e^{-i\gamma(x^0 - y^0) + ip_n(x^1 - y^1)} \tilde{G}_{ab}(\gamma, p_n) \Big|_{p_n = \frac{2\pi n}{L}}, \\ \tilde{G}_{ab}(\gamma, p_n) &= \frac{i \left( \left( \omega^2 + \gamma^2 - p_n^2 - m^2 + \frac{\lambda}{4} f_d^2 \right) \delta_{ac} + 2i\omega\gamma\epsilon_{ac} + \frac{\lambda}{2} f_a f_c \right)}{\left( \gamma^2 - \gamma_+^2(p_n) + i0 \right) \left( \gamma^2 - \gamma_-^2(p_n) + i0 \right)}, \end{aligned} \quad (6.28)$$

where the relation between  $G$ ,  $\tilde{G}$  and  $\phi$ ,  $f$  is given by

$$\begin{cases} \phi_a(x) = R_{ab}(\omega x^0) f_b \\ G_{ab}(x, y) = R_{ac}(\omega x^0) R_{bd}(\omega y^0) \tilde{G}_{cd}(x - y) \end{cases} \quad (6.29)$$

with  $R_{ab}(\theta) \in SO(2)$  the standard rotational matrix,  $f$  amplitude fixed by condition (6.8) and  $\gamma_+(p)$  and  $\gamma_-(p)$  are defined in (6.21) and (6.22). Since for the tree level solution  $\gamma_-(0)$  is gapless and  $\gamma_-(p_1)$  has imaginary part, in order to specify initial conditions for  $F$  from (6.28), at  $t = 0$ , the zeroth and first momentum modes of the statistical propagator were removed. This corresponds to a little shift away from the saddle point, anyway, without affecting the dynamics in a relevant way. The mapping of the initial conditions between  $G$  and  $F$  and  $\rho$  is explicitly derived at the end of the Section 4.2, and given by (4.37) and (4.39), where  $F^0$  now computed using (6.28). Let me remind here again that all initial conditions are derived with the use of the periodic boundary conditions in space, which are preserved during evolution due to the translational invariance of the equations (3.45).

### 6.3 Numerical Simulations

In the following, we discuss the numerical results of the simulation for the case of the unstable condensate.



Figure 6.3: Time dependence of the classical charge for different frequencies in the strong coupling regime.

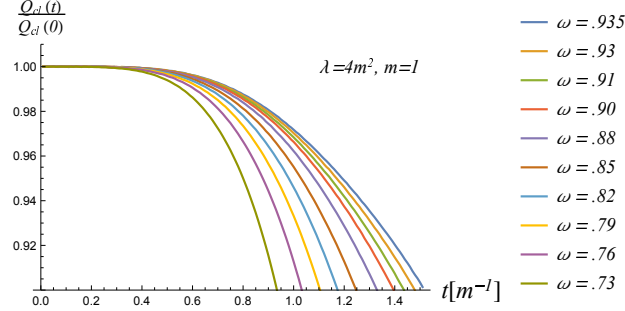
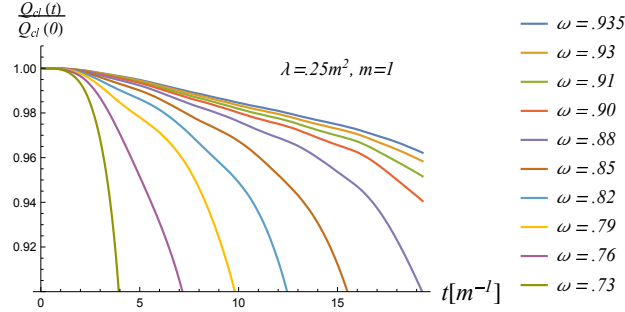


Figure 6.4: Time dependence of the classical charge for different frequencies in the weak coupling regime.



Equations (3.45) have been solved numerically using the Crank-Nicolson finite difference scheme for derivatives, and a trapezoidal rule for memory integrals. Moreover, since we are interested in the region where the classical spectrum is split between the condensate and the bright soliton, the study is confined to the range  $\omega \in (\omega_{cusp}, \omega_{cr})$ <sup>5</sup>. In this region, the choice of initial conditions, namely the unstable condensate solution, leads to the presence of one imaginary mode. As  $L$  is increased, more and more modes display such behaviour in the above-mentioned  $\omega$  range, as it can be easily seen from (6.22). Therefore, the size of the box is purely dictated by reasons of simplicity: first of all the box size should be much bigger than the constituent's Compton wavelength  $\omega^{-1}$  and, secondly, the numerical analysis simplifies a lot if only one instability mode shows up in the explored  $\omega$ 's range. In view of this, the box size is set to be  $L = 4\pi m^{-1}$ , for which  $\omega_{cusp} \simeq 0.71m$ ,  $\omega_{cr} \simeq 0.94m$  and only one instability mode is present, namely the first one  $\gamma_-(p_1)$ . In all the simulations it is set  $m = 1$ .

The general behaviour of the quantum breaking is displayed for different  $\omega$ 's in Figures 6.3 and 5.3 for strong and weak coupling. The behaviour is very reminiscent to the one observed for the quantum breaking in the repulsive case for a stable condensate [106],

<sup>5</sup>To avoid confusion I have to mention that for fixed  $\omega$ , the charges of soliton and condensate are different, and they have, correspondingly, different energies (as it can be seen from (6.10) and (6.15)), though they coincide at the critical point  $Q_{b.s.}(\omega_{cr}) = Q_{b.c.}(\omega_{cr})$

although much faster. However, even if not shown explicitly, one can notice the following feature: for all the simulations in the strong coupling regime, the total charge (3.72) varies on the displayed timescales by approximately the 1% i.e.  $Q(m^{-1})/Q(0) \sim 0.99$ . This is comparable to the change in classical charge displayed in fig. 6.3. However, due to the coupling being strong, we do not expect the resulting simulation to approximate appropriately the true quantum evolution anyway. The situation is qualitative different in the weak coupling regime displayed in Figure 6.4. There, even though the coupling is weak, as  $\omega$  is decreased (and the collective coupling is increased), there is a violation of the conservation of the total charge. This is, however, practically negligible (at least 100 times smaller and slightly growing with the collective coupling). This is no longer the case as we look at the simulation for longer times. For example, when  $Q_{cl}(t) \approx 0.5 Q_{cl}(0)$  we generically notice an increasing violation of the total charge conservation. This underlies a failure of the chosen numerical scheme, as the exponential growth of  $Q_q$  is so fast that it can no longer be well approximated after certain timescales. We now proceed with the discussion of the two main results of the analysis of the evolution of the unstable condensate.

### 6.3.1 Evolution along the BEC trajectory

The first result I want to comment upon is the evolution of the unstable condensate.

I will introduce here two notions for the energy, as it was done for the charge. So, in full analogy with  $Q_{cl}(t)$  and  $Q_q(t)$  defined in (3.65) and (3.70) I define

$$E_{cl}(x^0) = \int_0^L dx^1 \left( \frac{1}{2} (\partial_{x^0} \phi_a)^2 + \frac{1}{2} (\partial_{x^1} \phi_a)^2 + V(\phi_a) \right) \quad (6.30)$$

and quantum part which I will not write explicitly here.

The sum of two is a conserved quantity

$$\frac{d(E_{cl}(t) + E_q(t))}{dt} = 0. \quad (6.31)$$

During the evolution both classical charge and energy diminish while full integrals of motion are conserved. In Figure 6.6 the evolution of this classical quantities is shown for different  $\omega$ 's (different colours) and compared w.r.t. the branch of classical condensate solutions (blue line).

The points in the plot are numerical evaluations of the classical energy (6.30) and charge (6.10) at different times. Different colours there correspond to different initial configurations, namely different initial  $\omega$ . Therefore, looking the dots of particular colour, which coordinates at the plot are  $(Q_{cl}(t), E_{cl}(t))$ , one can see how the classical energy and classical charge of this configuration evolve with time. In Fig. 6.5 one can see how the numerical simulations fully evolve along the classical condensate trajectory. The reader might wonder why no deviations are seen, although lower energy configurations (at similar

Figure 6.5: Time evolution of the classical energy  $E_{cl}(t)$  as a function of  $Q_{cl}(t)$  for different  $\omega \in (.90, \omega_{cr})$  (each with a different marker). Here the evolution follows the classical condensate trajectory.

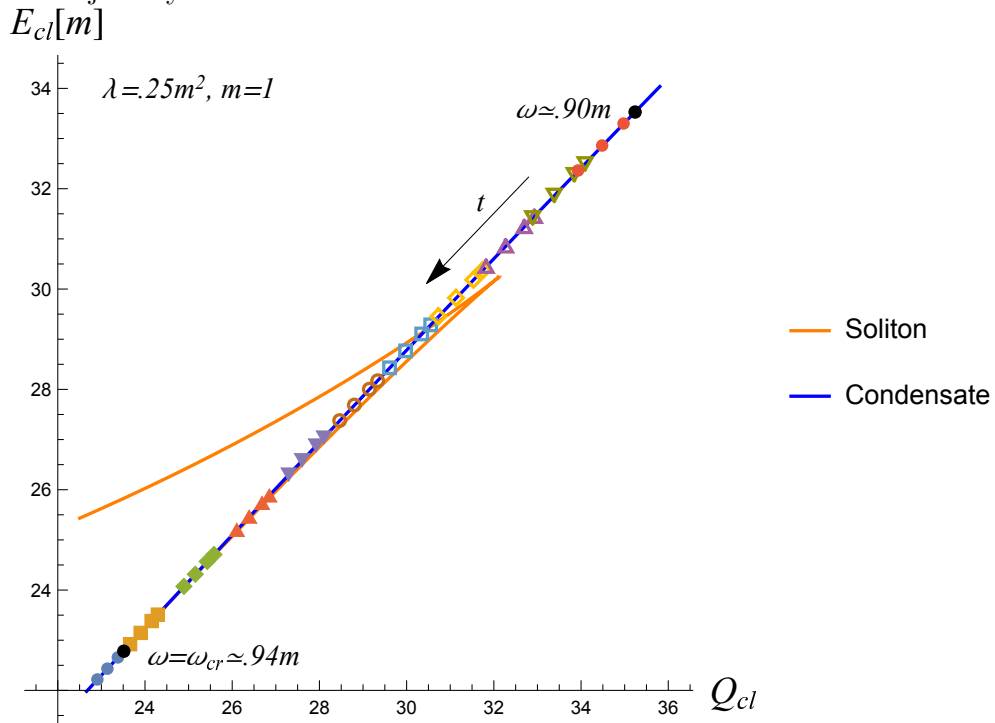
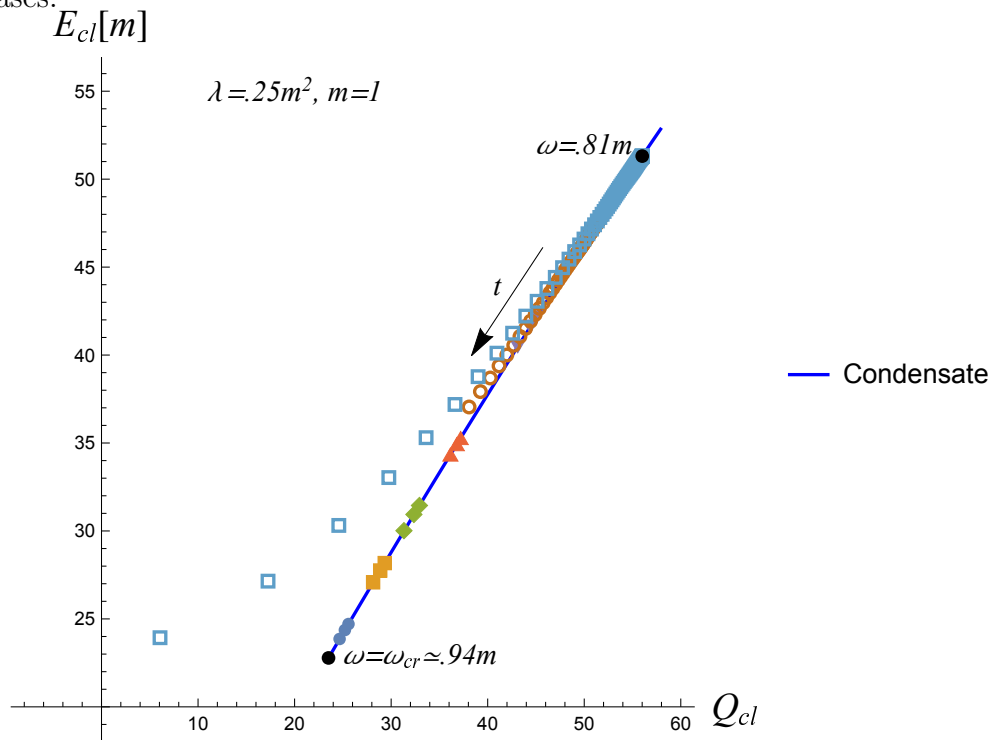


Figure 6.6: Time evolution of the classical energy  $E_{cl}(t)$  as a function of  $Q_{cl}(t)$  for different  $\omega \in (.81, \omega_{cr})$  (each with a different marker). The failure of the simulation is apparent as  $\omega$  decreases.



charge), namely the soliton (orange line), are present. The reason is that the bright soliton is a localized configuration, and therefore, due to the homogeneity of our initial conditions, the system in principle can only evolve into a superposition of such solutions. I must admit that here it is actually not known how to understand whether the initial homogeneous configuration is tending to approach a superposition of solitons or not, but there is a clear qualitative picture explaining the condensate evolution along the BEC  $E_{cl}(Q_{cl})$  line.

In total analogy with the Q-balls case, one can deduce the following relation between classical energy and charge of the BEC

$$\frac{dE_{cl}}{d\omega} = \omega \frac{dQ_{cl}}{d\omega}. \quad (6.32)$$

Therefore, one can conclude that if classical charge is getting changed by some small amount  $\delta Q_{cl}$ , which in the considered case the part carried out by fluctuations, then the next homogeneous configuration stationarizing the local part of the energy is given by

$$E_{cl}(\delta t) \simeq E_{cl}(0) + \omega \delta Q_{cl}(\delta t), \quad (6.33)$$

which means that during quantum evolution, the preferable directions in the phase space is the one stationarizing the classical part as long as classical quantities remain dynamically dominant. This is true as long as  $Q_{cl} \gg Q_q$ , but in the end, upon reaching  $t_{qb}$ , this approximate relation does not need to hold, as well as the  $\hbar$  perturbative expansion, and evolution might deviate from this curve. Anyway, you will see in the next paragraph how the presence of a lower energy configuration affects the speed at which the system rolls along the BEC  $E_{cl}(Q_{cl})$  trajectory.

The situation is different in Fig. 6.6 where the behaviour of simulations is shown for lower  $\omega$ 's. As one can see, some simulations (blue squares) start deviating from the condensate-like evolution. Such deviations increase as  $\omega$  decreases. Such phenomenon is analogue to the one observed for the strong coupling case. Namely, the exponential growth becomes so fast, as to lead to a failure of the numerical scheme. In fact, correspondingly with these deviations, non-negligible – yet very small violations of total charge emerge. However, it should be noted that for small timescales, the evolution of these simulations is still reliable.

### 6.3.2 Quantum break-time

In order to capture the rate at which the system evolves along the condensate trajectory (c.f. Figure 6.6), I use the criterion (3.75) to obtain  $t_{qb}$ . Moreover, because of the above-mentioned numerical issues, the quantum break-time is fixed as the time such that  $Q_q(t_{qb}) = 0.1 Q_{cl}(t_{qb})$ . In this way, on the obtained quantum breaking timescales, most of the simulations have a very well conserved charge (within .1% deviations). The dependence of  $t_{qb}$  on  $\log Q/\text{Im}(\gamma_-(p_1))$  is explicitly shown in Figure 6.7, where the quantum breaking time is shown w.r.t.  $\omega$ . One can see how in this coupling region i.e.  $\lambda \leq 0.1 m^2$ , the breaking time is indeed captured by the relation

$$t_{qb} \simeq \frac{\log Q}{\text{Im}(\gamma_-(p_1))} + \text{constant} \quad (6.34)$$

where  $\text{Im}(\gamma_-(p_1))$  is the Lyapunov exponent, therefore confirming (6.2) mentioned in the introduction. Let us discuss this relation and the corresponding physics in more details.

Firstly, it is very important to stress that such a logarithmic behaviour is controlled by the Lyapunov exponent, which sets the system instability. As long as a homogeneous solution exhibits this form of instability, the leading initial time behaviour is apparently governed by this mode arising in the Green's function. Therefore, we can roughly say that for  $\delta t \sim 1/\text{Im}(\gamma_-(p_1))$

$$Q_{cl}(\delta t) \simeq Q_{cl}(0) + A (1 - e^{\text{Im}(\gamma_-(p_1))\delta t}) \quad (6.35)$$

and we can infer from this, that using our quantum breaking criterion  $Q_{cl}(t_{qb})/Q_{cl}(0) \simeq r$ , we obtain (6.34). Indeed, the aforementioned constant in (6.34) depends only on the chosen criterion  $r$  and is almost independent on any parameters of the model.

From the quantum point of view, this law means that to undergo quantum breaking, the system has to wait for a significant amount of quanta to decay, which leads to logarithmic dependence of quantum break-time on charge. This mechanism is in contrast with the classical picture, where departure from stationary solution is set by inhomogeneities introduced by means of initial classical perturbations. To clarify this difference, let us briefly recap how the decay due to classical perturbations takes place. In fact, for this to happen, the inhomogeneous perturbation spectrum needs to include an unstable mode, which, in the system under consideration, corresponds with the first momentum mode. In turn, the presence of such a mode leads to the development of inhomogeneities in the system on a timescale fixed by the Lyapunov exponent as  $1/\text{Im}(\gamma_-(p_1))$ , leading to the localization of the soliton. Thus, we see that departure occurs almost immediately, independently of the initial configuration itself (namely the amount of quanta comprising the initial state). This kind of transitions were clearly demonstrated for unstable Q-balls (Q-clouds) as they are perturbed and, after a timescale set by the instability, they move to a stable configuration, dropping some charge along the process [107]. In addition, I must stress again, that not all the perturbations can destroy BEC classically, but only those which contain the unstable mode. This is totally different from what happened in this case as the evolution is driven by quantum effects preserves translational invariance. In fact, we saw in Figure 6.5 that classical quantities evolve along the classical homogeneous BEC trajectory, although the growth of the unstable mode within the Green's function being present (note that at  $t = 0$  we input this unstable mode to be zero). Therefore, we see that quantum and classical process are significantly different. In particular, the quantum decay is more general, as it takes place independently whether homogeneity is preserved by initial conditions.

One clear feature of Fig. 6.7 is the deviation from the logarithmic scaling as the coupling is increased. I believe this to be due to the above discussed failure of the numerical scheme.

At this point, after stating the last result deduced from the studying of quantum evolution of the unstable condensate, it is time to wrap up and summarize all together the results that were obtained, and compare it with the other ones discovered previously.

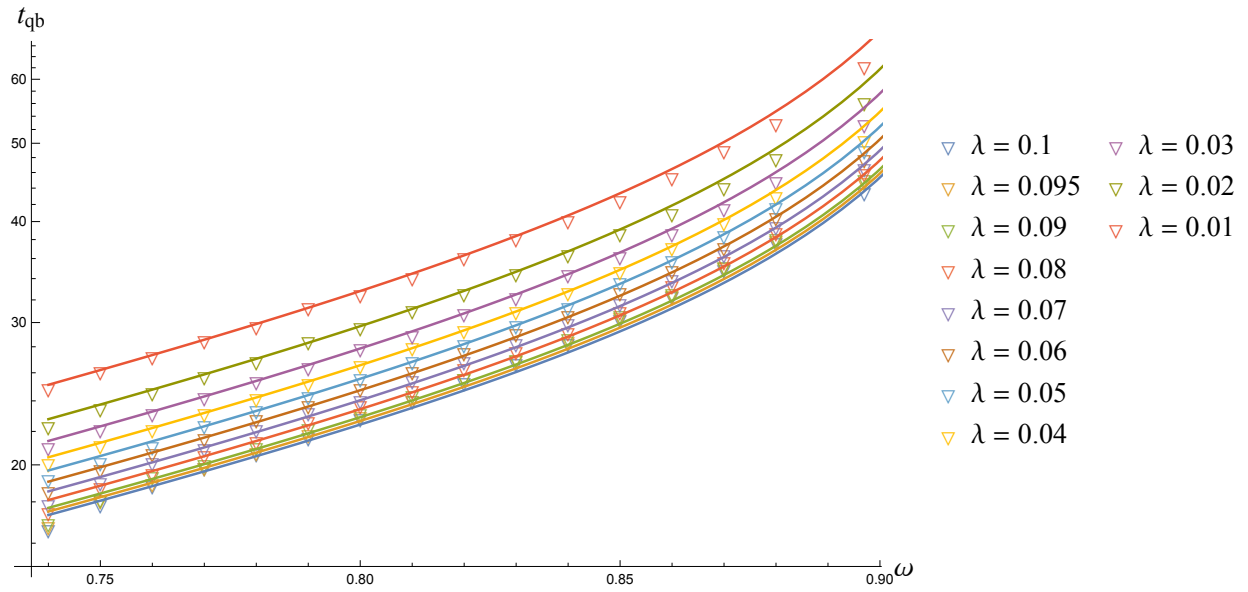


Figure 6.7: Quantum breaking time dependence on  $\omega$  compared to analytical estimation. Solid lines are functions  $\log Q(\omega, \lambda)/\text{Im}(\gamma_-(p_1))$  for different couplings and triangles are quantum breaking times extracted from simulations





# Conclusion

The main goal of this was to investigate the quantum breaking phenomenon, which describes the deviation of the true quantum evolution of a semi-classical system from its evolution prescribed by classical physics. The quantum breaking phenomenon appears to be a very generic one, as the nature is filled by the objects of semi-classical origin, and it is quite apparent that most of these objects can not remain the same eternally. Nevertheless, the less evident thing is the speed at which each of these semi-classical objects will transform into something else. Therefore, even if the quantum breaking is very generic, it happens with the different speed for different objects of such kind. This poses the question: *which kind of systems have a reasonable quantum break-time to pay attention to?*

We have already discussed that for the quantum breaking to happen fast enough, a system must obtain strong collective coupling, or in other words, all the constituents must interact with each other with equal strength to sustain collective interaction, hence, when collective coupling defined in (2.2) is strong enough we can expect quantum breaking to happen at the relatively short timescale.

Another issue that pops up is of mathematical nature, because we have to identify the timescale associated with the quantum breaking. In the previous literature, various methods were used, but these were accustomed to the peculiarities of the particular system under consideration. For instance, quantum breaktime of cosmic axion was computed by means of perturbative estimation of the scattering processes [27], and in [29] the non-relativistic was studied, and the specific method was used to diagonalize it and compute exact evolution of the system by considering only three momentum modes with  $p = -2\pi/L, 0, 2\pi/L$ .

Thus, it seemed to be natural to try to look for some more general approach, which would not rely on the special features of the system one is considering, but solely on the general knowledge of semi-classicality. It turned out that methods developed already in the out-of-equilibrium quantum field theory are quite handy [33]. The method that was used in this work is the method of 2-particle irreducible effective action. The 2PI effective action is the functional that depends on two variables: the field expectation value  $\phi(x) = \langle \hat{\phi}(x) \rangle$ , and the connected 2-point correlation function  $G(x, y) = \langle \hat{T} \{ \hat{\phi}(x) \hat{\phi}(y) \} \rangle$ . Every other correlator can be computed by means of functional derivatives with respect to these two functions. Of course, if one is capable of computing the exact functional, then it gives nothing more than the usual effective action. However, it is impossible to do, and the reason we use 2PI effective action instead of ordinary 1PI is that it gives a better approximation by the resummation of all two-particle irreducible Feynman diagrams. Another ingredient coming

from out-of-equilibrium QFT is the Schwinger-Keldysh or “*in-in*” time-contour that allows to compute real-time evolution of the system. As a result, combined both tools lead to extremely powerful framework well-approximating true quantum evolution, and leading to capturing effects, that can not be picked up by ordinary perturbative approach (see Section 5.2). Thus, one can see that the formalism presented here is well-suited to study the evolution of the quantum system. Moreover, it is applicable to any QFT a relativistic and non-relativistic one, which makes it in impeccable tool to study the deviations from the semi-classical evolution.

This method also allows defining the criterion for identifying timescale associated with quantum breaking quite naturally. We saw that the formalism considers evolution of both the background field  $\phi$ , and connected two-point function  $G$ , and takes into account their mutual influence contrary to the 1PI effective action where we just compute propagator as the function of the background field. This splitting of two parts of the two-point correlator allows us to identify the quantum break-time, when contributions coming from both parts start to contribute equally to the physical observables as charge or energy (see Sec. 2.4 and 2.5), I will repeat it here for illustrative purposes.

The full charge can be inferred from the full two-point correlator by computing (here I put  $d\vec{x}$  for generality, but this work is for 1+1 dimensional system, so, the integral is actually just  $dx^1$ )

$$Q = \int d\vec{x} \lim_{y \rightarrow x} \epsilon_{ab} \partial_{x^0} \left\langle \hat{\phi}_a(x) \hat{\phi}_b(y) \right\rangle \Big|_{x^0 > y^0} = \int d\vec{x} \lim_{y \rightarrow x} \epsilon_{ab} \partial_{x^0} \left( \langle \hat{\phi}_a(x) \rangle \langle \hat{\phi}_b(y) \rangle + \left\langle \hat{\phi}_a(x) \hat{\phi}_b(y) \right\rangle_{\text{connected}} \right),$$

which in terms of the 2PI variables  $\phi$  and  $G$  becomes

$$Q = \int d\mathbf{x} \lim_{y \rightarrow x} \epsilon_{ab} \partial_{x^0} \left( \phi_a(x) \phi_b(y) + G_{ab}(x, y) \right),$$

where classical part of the charge is the part coming from the product of two one-point correlators

$$Q_{cl}(x^0) = \int d\vec{x} \lim_{y \rightarrow x} \epsilon_{ab} \partial_{x^0} \phi_a(x) \phi_b(y),$$

and the quantum part of the charge comes from connected part of the two-point function

$$Q_q(x^0) = \int d\vec{x} \lim_{y \rightarrow x} \epsilon_{ab} \partial_{x^0} G_{ab}(x, y).$$

All together, they make up each other to conserved in time full charge of the system.

$$Q = Q_{cl}(x^0) + Q_q(x^0).$$

Initial conditions are fixed such that

$$Q_{cl}(0) \gg Q_q(0),$$

which is a consequence of the semi-classicality. But when time goes by both contributions could become comparable, and when this happens, and condition

$$Q_{cl}(t_{qb}) = Q_q(t_{qb})$$

is fulfilled, we claim that quantum breaking took place, because the evolution is no more can be approximated by the mean field. Only zero-momentum modes overoccupation of which leads to condensation makeup disconnected part of the Green's function, but with time more and more non-zero momentum modes are getting excited, and background is steadily getting destroyed.

This criterion was used to determine the time of the quantum breakdown of the Bose-Einstein condensate emerging in the complex scalar field theory (or, in other words, in the theory of two real scalar fields) for two cases. In the first case, the quartic self-interaction of the scalar field was positive that ensured classical stability of the condensate, and in the second case, it was negative, which makes it unstable.

Let me summarize the results that were obtained for the stable condensate first.

The main results show the way that breaking happens in the Figures 5.3 and 5.2 exposing mutual change of the two charges, while total charge is conserved as it depicted in Figure 5.1. This is indeed “*quantum breaking*”, because we have explicitly seen that the system is classically stable!

As the result of the numerical simulations, dependence of the quantum break-time on the total charge of the system was computed. It turned out that in two opposite limits  $Q \rightarrow 0$  and  $Q \rightarrow \infty$  the quantum break time grows, as one can see in Figures 5.4(a) and 5.4(b). It is hard to infer an analytical dependence here, because the tails are not long enough. Unfortunately, even for the cases that are exhibited in these plots, the time of simulations was rather long, and attempts to get a quantum break-time for longer timescales seemed not very reasonable, because the initial purpose was just to capture the breaking. The estimated time for simulation of the condensate evolution with larger charges, or with very small ones was counted in months, so, my colleague and I rejected the possibility to proceed with this. However, as very rough approximation we can interpolate quantum break-time dependence on charge depicted in 5.4(a) and 5.4(b), as

$$t_{qb} \sim \frac{C_1}{Q} + C_2 Q,$$

where  $C_1$ , and  $C_2$  are just some constants. So, in the domain of charges where it was possible to compute the  $t_{qb}(Q)$  dependence one case see that it's at least polynomial, which doesn't contradict with the results in [27].

Despite the fact that we can't extract analytical dependences with good precision, we can still observe some interesting features there. As I have already mentioned, there are two different asymptotic behaviours, namely, that quantum break-time grows for the very large charges, and for the small ones. This is due to two different trends. For small charge the configuration is closer to its true vacuum and, correspondingly, the effects breaking the configuration are suppressed. In the big charge limit, the theory is highly classical

and, consequently, more rescattering events are necessary for the effects to be dynamically relevant. The minimal quantum break-time between these two regimes was found.

In view of these results, some interesting remarks can be made. First, one can question the saddle point approximation used in most of the computations of a BEC condensate when considering processes which have a typical timescale (or length scale) of order of the breaking that was observed. This might lead to erroneous conclusions, as quantum breaking is jeopardizing the reliability of the background. Moreover, I believe that the corrections that were observed might be relevant, and should be taken into account in order to better approximate the quantum evolution of physical condensates. It is worth mentioning that within a full proper treatment, quantum and thermal fluctuations appear on equal footing. Hence, quantum effects are dominant only if thermal fluctuations are negligible. If this is not the case, a statistical description of the system must be taken into account.

As we have managed to observe the quantum breaking in the stable system, the next step was to inspect the system, which contains the classical instability. Again, I allow myself to remind the reader that in spite of the instability, classical break-down doesn't have to happen if we evade exciting exponentially growing mode in the spectrum of the linear perturbations.

During the analysis of the evolution of the unstable condensate it was found that the quantum break-time, namely the moment when departure from the classical solution become significant, scales logarithmically with dimensionless charge  $Q$  and is controlled by the Lyapunov exponent  $\gamma$  characterizing the classical instability of the system, namely

$$t_{qb} = \gamma^{-1} \log Q + C, \quad (6.36)$$

with  $C$  a small constant caused by the way the quantum break-time was extracted numerically  $t_{qb}$ . This result for quantum break-time is similar to the one derived in [29] (see eq. (6.2)). However, being our study in the relativistic regime, we see that the number of constituents is replaced with charge  $N \rightarrow Q$  (compare (6.36) with (1.2)). These two results need not be similar, as the spectrum of the relativistic model is much broader. However, as it follows from the analysis, (6.36) is indeed the natural extension of the result of [29] in the relativistic regime.

Another interesting result of this work is related to the breaking trajectory of the condensate. In fact, the evolution takes place along the branch of classical solution  $E_{cl}(Q_{cl})$  as long as charge is steadily getting carried away by quantum fluctuations according to (6.32) and (6.33) (see Fig. 6.6). There, the classical part of the energy w.r.t. classical charge evolves along the branch of classical solutions given by (6.9) and (6.10). This is due to the fact that homogeneity is preserved in the equations of motion (3.45). In fact, as discussed above, there is a preferable direction in the phase space of classical configurations set by (6.32). Indeed, as soon as quantum breaking takes place, we do not expect this kind of relation to hold and the system might evolve differently from there onward. Further investigation of this issue, although interesting, is beyond the scope of this work. Moreover, it can be seen that as either the coupling or the collective coupling is increased, deviations

from such trajectory are observed in Fig. 6.6. The possible reason for this to happen is due to a failure of the numerical scheme. Therefore, these simulations were excluded when studying the functional dependence of the quantum break-time.

One can see that the method developed here is powerful and has a wide range of the applicability for any system that can be described at the semi-classical level. The results obtained by this method are in agreement with the previous ones discovered in literature, which is the argument in favour of this approach, as it can be used regardless the peculiarities of particular system, and relies solely on the semi-classicality. Therefore, it could be interesting to probe other systems like solitons, or systems in the dimension higher than  $1 + 1$ , or to compute quantum break-time in more realistic settings, e.g., for the models that can be experimentally simulated.

Another prospect is to improve the expansion scheme, and go further by accounting higher order graphs, or using  $1/N$  expansion for a larger symmetry group, which would allow carrying the numerical integration further at lower expense compared to full inclusion of higher order graphs. Also, another interesting question is how the system evolves when considering as initial conditions the bright soliton configuration (see Fig. 6.2). In fact, exploring its evolution might help us to deepen our knowledge regarding the back-reaction properties of localized objects.



# Acknowledgment

First and foremost, I would like to thank my supervisor Gia Dvali, who was helping me during all these four years. I'm grateful that I had a possibility to learn from him, get to know his approach to the different phenomena, and gain a lot of knowledge due to his enormous expertise and very broad views on the concepts of contemporary physics.

Another thank belongs to my colleague and dear friend Michael Zantedeschi, with whom we developed this work, and spent countless hours discussing, hanging out, and drinking tons of coffee. I'm happy that I had an opportunity to meet him, and become friends.

Also, I would like to thank Juan Sebastian Valbuena Bermúdez, who is another friend and colleague of mine. Me, Juan and Michael were in the same office, and it was a great pleasure to have this company for the fruitful work, discussions, and idle conversations.

My next thank is to Otari Sakhelashvili, Max Warkentin, Andrea Giugno, Oleg Kaikov, Georgios Karananas, Emmanouil Koutsangelas and Lasha Berezhiani, with whom we have also spent a good time chatting about science and working together.

And last, but not the least, my gratitude is to the Max-Planck Institute for Physics and IMPRS, that gave an outstanding opportunity to do my research there.





# Bibliography

- [1] N. P. Bhatia and G. P. Szegő, *Stability theory of dynamical systems*. Springer Science & Business Media, 2002.
- [2] R. Feynman, R. Leighton, and M. Sands, *The Feynman Lectures on Physics, Vol. II: The New Millennium Edition: Mainly Electromagnetism and Matter*. The Feynman Lectures on Physics, Basic Books, 2011.
- [3] A. M. Lyapunov, “The general problem of the stability of motion,” *International Journal of Control*, vol. 55, no. 3, pp. 531–534, 1992.
- [4] H. Groenewold, “On the principles of elementary quantum mechanics,” *Physica*, vol. 12, no. 7, pp. 405–460, 1946.
- [5] J. Zinn-Justin, *Path Integrals in Quantum Mechanics*. Published to Oxford Scholarship Online, 02 2005.
- [6] S. Coleman, “Fate of the false vacuum: Semiclassical theory,” *Phys. Rev. D*, vol. 15, pp. 2929–2936, May 1977.
- [7] C. G. Callan and S. Coleman, “Fate of the false vacuum. ii. first quantum corrections,” *Phys. Rev. D*, vol. 16, pp. 1762–1768, Sep 1977.
- [8] H. J. W. Müller-Kirsten, *Introduction to Quantum Mechanics*. WORLD SCIENTIFIC, 2nd ed., 2012.
- [9] A. Belavin, A. Polyakov, A. Schwartz, and Y. Tyupkin, “Pseudoparticle solutions of the yang-mills equations,” *Physics Letters B*, vol. 59, no. 1, pp. 85–87, 1975.
- [10] G. 't Hooft, “Computation of the quantum effects due to a four-dimensional pseudoparticle,” *Phys. Rev. D*, vol. 14, pp. 3432–3450, Dec 1976.
- [11] E. Gildener and A. Patrascioiu, “Instanton Contributions to the Energy Spectrum of a One-Dimensional System,” *Phys. Rev. D*, vol. 16, pp. 423–430, 1977. [Erratum: *Phys.Rev.D* 16, 3616 (1977)].
- [12] C. Callan, R. Dashen, and D. Gross, “The structure of the gauge theory vacuum,” *Physics Letters B*, vol. 63, no. 3, pp. 334–340, 1976.

- [13] R. Jackiw and C. Rebbi, “Vacuum periodicity in a yang-mills quantum theory,” *Phys. Rev. Lett.*, vol. 37, pp. 172–175, Jul 1976.
- [14] R. Feynman, A. Hibbs, and D. Styer, *Quantum Mechanics and Path Integrals*. Dover Books on Physics, Dover Publications, 2010.
- [15] Y. Yang, *Solitons in Field Theory and Nonlinear Analysis*. Springer Monographs in Mathematics, Springer New York, 2013.
- [16] V. I. Yukalov, “Basics of Bose-Einstein Condensation,” *Phys. Part. Nucl.*, vol. 42, pp. 460–513, 2011.
- [17] C. J. Pethick and H. Smith, *Bose–Einstein Condensation in Dilute Gases*. Cambridge University Press, 2 ed., 2008.
- [18] N. Manton and P. Sutcliffe, *Topological Solitons*. Cambridge Monographs on Mathematical Physics, Cambridge University Press, 2004.
- [19] E. J. Weinberg, *Classical Solutions in Quantum Field Theory: Solitons and Instantons in High Energy Physics*. Cambridge Monographs on Mathematical Physics, Cambridge University Press, 2012.
- [20] T. Lee and Y. Pang, “Nontopological solitons,” *Physics Reports*, vol. 221, no. 5, pp. 251–350, 1992.
- [21] E. Nugaev and A. Shkerin, “Review of nontopological solitons in theories with  $u(1)$ -symmetry,” *Journal of Experimental and Theoretical Physics*, vol. 130, pp. 301–320, 02 2020.
- [22] G. Dvali and C. Gomez, “Black Hole’s Quantum N-Portrait,” *Fortsch. Phys.*, vol. 61, pp. 742–767, 2013.
- [23] G. Dvali and C. Gomez, “Black hole macro-quantumness,” *arXiv preprint arXiv:1212.0765*, 2012.
- [24] G. Dvali and C. Gomez, “Black hole’s  $1/n$  hair,” *Physics Letters B*, vol. 719, no. 4-5, pp. 419–423, 2013.
- [25] G. Dvali and C. Gomez, “Quantum compositeness of gravity: black holes, ads and inflation,” *Journal of Cosmology and Astroparticle Physics*, vol. 2014, no. 01, p. 023, 2014.
- [26] G. Dvali, C. Gómez, and S. Zell, “Quantum break-time of de sitter,” *Journal of Cosmology and Astroparticle Physics*, vol. 2017, no. 06, p. 028, 2017.
- [27] G. Dvali and S. Zell, “Classicality and Quantum Break-Time for Cosmic Axions,” *JCAP*, vol. 07, p. 064, 2018.

- [28] G. Dvali and C. Gomez, “Black Holes as Critical Point of Quantum Phase Transition,” *Eur. Phys. J. C*, vol. 74, p. 2752, 2014.
- [29] G. Dvali, D. Flassig, C. Gomez, A. Pritzel, and N. Wintergerst, “Scrambling in the black hole portrait,” *Physical Review D*, vol. 88, no. 12, p. 124041, 2013.
- [30] P. Hayden and J. Preskill, “Black holes as mirrors: quantum information in random subsystems,” *Journal of high energy physics*, vol. 2007, no. 09, p. 120, 2007.
- [31] L. P. Kadanoff, “More is the Same: Phase Transitions and Mean Field Theories,” *J. Statist. Phys.*, vol. 137, p. 777, 2009.
- [32] J. Rammer, *Quantum Field Theory of Non-equilibrium States*. Cambridge University Press, 2007.
- [33] J. Berges, “Introduction to nonequilibrium quantum field theory,” in *AIP Conference Proceedings*, vol. 739, pp. 3–62, American Institute of Physics, 2004.
- [34] J. M. Luttinger and J. C. Ward, “Ground-state energy of a many-fermion system. ii,” *Phys. Rev.*, vol. 118, pp. 1417–1427, Jun 1960.
- [35] G. Baym and L. P. Kadanoff, “Conservation laws and correlation functions,” *Phys. Rev.*, vol. 124, pp. 287–299, Oct 1961.
- [36] C. De Dominicis and P. C. Martin, “Stationary entropy principle and renormalization in normal and superfluid systems. ii. diagrammatic formulation,” *Journal of Mathematical Physics*, vol. 5, no. 1, pp. 31–59, 1964.
- [37] C. de Dominicis and P. C. Martin, “Stationary Entropy Principle and Renormalization in Normal and Superfluid Systems. I. Algebraic Formulation,” *J. Math. Phys.*, vol. 5, pp. 14–30, 1964.
- [38] G. Baym, “Self-consistent approximations in many-body systems,” *Phys. Rev.*, vol. 127, pp. 1391–1401, Aug 1962.
- [39] J. M. Luttinger, “Fermi surface and some simple equilibrium properties of a system of interacting fermions,” *Phys. Rev.*, vol. 119, pp. 1153–1163, Aug 1960.
- [40] J. M. Cornwall, R. Jackiw, and E. Tomboulis, “Effective Action for Composite Operators,” *Phys. Rev. D*, vol. 10, pp. 2428–2445, 1974.
- [41] J. Berges and J. Cox, “Thermalization of quantum fields from time reversal invariant evolution equations,” *Phys. Lett. B*, vol. 517, pp. 369–374, 2001.
- [42] G. Aarts and J. Berges, “Nonequilibrium time evolution of the spectral function in quantum field theory,” *Phys. Rev. D*, vol. 64, p. 105010, 2001.

- [43] J. Berges, “Controlled nonperturbative dynamics of quantum fields out-of-equilibrium,” *Nucl. Phys. A*, vol. 699, pp. 847–886, 2002.
- [44] G. Aarts and J. Berges, “Classical aspects of quantum fields far from equilibrium,” *Phys. Rev. Lett.*, vol. 88, p. 041603, 2002.
- [45] A. Einstein, *Quantentheorie des einatomigen idealen Gases*, pp. 237–244. John Wiley & Sons, Ltd, 2005.
- [46] Bose, “Plancks Gesetz und Lichtquantenhypothese,” *Zeitschrift fur Physik*, vol. 26, pp. 178–181, Dec. 1924.
- [47] C. C. Bradley, C. A. Sackett, J. J. Tollett, and R. G. Hulet, “Evidence of bose-einstein condensation in an atomic gas with attractive interactions,” *Phys. Rev. Lett.*, vol. 75, pp. 1687–1690, Aug 1995.
- [48] M. Schick, “Two-dimensional system of hard-core bosons,” *Phys. Rev. A*, vol. 3, 03 1971.
- [49] M. H. Anderson, J. R. Ensher, M. R. Matthews, C. E. Wieman, and E. A. Cornell, “Observation of bose-einstein condensation in a dilute atomic vapor,” *Science*, vol. 269, no. 5221, pp. 198–201, 1995.
- [50] L. Berezhiani, G. Dvali, and O. Sakhelashvili, “de Sitter space as a BRST invariant coherent state of gravitons,” *Phys. Rev. D*, vol. 105, no. 2, p. 025022, 2022.
- [51] S.-J. Sin, “Late time cosmological phase transition and galactic halo as Bose liquid,” *Phys. Rev. D*, vol. 50, pp. 3650–3654, 1994.
- [52] C. G. Boehmer and T. Harko, “Can dark matter be a Bose-Einstein condensate?,” *JCAP*, vol. 06, p. 025, 2007.
- [53] A. M. Gavrilik, M. V. Khelashvili, and A. V. Nazarenko, “Bose-einstein condensate dark matter model with three-particle interaction and two-phase structure,” *Phys. Rev. D*, vol. 102, p. 083510, Oct 2020.
- [54] P.-H. Chavanis, “Jeans instability of dissipative self-gravitating bose–einstein condensates with repulsive or attractive self-interaction: Application to dark matter,” *Universe*, vol. 6, no. 12, 2020.
- [55] F. Briscese, “Self-interacting complex scalar field as dark matter,” *AIP Conference Proceedings*, vol. 1396, no. 1, pp. 176–180, 2011.
- [56] L. Berezhiani, “On Corpuscular Theory of Inflation,” *Eur. Phys. J. C*, vol. 77, no. 2, p. 106, 2017.

- [57] L. Feng, L. W. Clark, A. Gaj, and C. Chin, “Coherent inflationary dynamics for bose–einstein condensates crossing a quantum critical point,” *Nature Physics*, vol. 14, no. 3, pp. 269–272, 2018.
- [58] S. Das, “Bose–einstein condensation as an alternative to inflation,” *International Journal of Modern Physics D*, vol. 24, no. 12, p. 1544001, 2015.
- [59] A. Bishop, J. Krumhansl, and S. Trullinger, “Solitons in condensed matter: A paradigm,” *Physica D: Nonlinear Phenomena*, vol. 1, no. 1, pp. 1–44, 1980.
- [60] K. R. Subbaswamy and S. E. Trullinger, “Complex scalar fields in one dimension with fourfold phase anisotropy: Solitary-wave solutions,” *Phys. Rev. A*, vol. 19, pp. 1340–1349, Mar 1979.
- [61] L. D. Carr, C. W. Clark, and W. P. Reinhardt, “Stationary solutions of the one-dimensional nonlinear schrödinger equation. i. case of repulsive nonlinearity,” *Phys. Rev. A*, vol. 62, p. 063610, Nov 2000.
- [62] L. D. Carr, C. W. Clark, and W. P. Reinhardt, “Stationary solutions of the one-dimensional nonlinear schrödinger equation. ii. case of attractive nonlinearity,” *Phys. Rev. A*, vol. 62, p. 063611, Nov 2000.
- [63] A. Kovtun and M. Zantedeschi, “Breaking BEC,” *JHEP*, vol. 07, p. 212, 2020.
- [64] A. Kovtun and M. Zantedeschi, “Breaking BEC: Quantum evolution of unstable condensates,” *Phys. Rev. D*, vol. 105, no. 8, p. 085019, 2022.
- [65] N. N. Bogolyubov, “On the theory of superfluidity,” *J. Phys. (USSR)*, vol. 11, pp. 23–32, 1947.
- [66] S. Barnett, K. Burnett, and J. Vaccaro, “Why a condensate can be thought of as having a definite phase,” *Journal of Research of the National Institute of Standards and Technology*, vol. 101, 03 1997.
- [67] V. Chernyak, S. Choi, and S. Mukamel, “Generalized coherent state representation of bose-einstein condensates,” *Physical Review A*, vol. 67, no. 5, p. 053604, 2003.
- [68] J. Klauder and B. Skagerstam, *Coherent States*. WORLD SCIENTIFIC, 1985.
- [69] J. Mayers, “Bose-einstein condensation and two fluid behavior in  $^4\text{He}$ ,” *Phys. Rev. B*, vol. 74, p. 014516, Jul 2006.
- [70] L. Berezhiani, G. Cintia, and M. Zantedeschi, “Background-field method and initial-time singularity for coherent states,” *Phys. Rev. D*, vol. 105, no. 4, p. 045003, 2022.
- [71] J. Berges, S. Borsányi, U. Reinosa, and J. Serreau, “Nonperturbative renormalization for  $2\pi$  effective action techniques,” *Annals of Physics*, vol. 320, no. 2, pp. 344–398, 2005.

- [72] M. Planck, “Ueber das gesetz der energieverteilung im normalspectrum,” *Annalen der Physik*, vol. 309, no. 3, pp. 553–563, 1901.
- [73] M. Planck, “Nobel lecture: The genesis and present state of development of the quantum theory,” 1920.
- [74] A. Aharoni, *Introduction to the Theory of Ferromagnetism*. International Series of Monographs on Physics, Clarendon Press, 2000.
- [75] W. Heisenberg, “Zur theorie des ferromagnetismus,” *Zeitschrift für Physik*, vol. 49, no. 9, pp. 619–636, 1928.
- [76] H. Bethe, “Zur theorie der metalle,” *Zeitschrift für Physik*, vol. 71, no. 3, pp. 205–226, 1931.
- [77] R. Baxter, *Exactly Solved Models in Statistical Mechanics*. Dover books on physics, Dover Publications, 2007.
- [78] R. F. Dashen, B. Hasslacher, and A. Neveu, “Nonperturbative methods and extended-hadron models in field theory. i. semiclassical functional methods,” *Phys. Rev. D*, vol. 10, pp. 4114–4129, Dec 1974.
- [79] R. F. Dashen, B. Hasslacher, and A. Neveu, “Nonperturbative methods and extended-hadron models in field theory. ii. two-dimensional models and extended hadrons,” *Phys. Rev. D*, vol. 10, pp. 4130–4138, Dec 1974.
- [80] A. Neveu, *Semiclassical Quantization Methods in Field Theory*. Boston, MA: Springer US, 1976.
- [81] J.-L. Gervais and B. Sakita, “Extended particles in quantum field theories,” *Physical Review D*, vol. 11, no. 10, p. 2943, 1975.
- [82] C. G. Callan Jr and D. J. Gross, “Quantum perturbation theory of solitons,” *Nuclear Physics B*, vol. 93, no. 1, pp. 29–55, 1975.
- [83] R. D. Peccei and H. R. Quinn, “CP conservation in the presence of pseudoparticles,” *Phys. Rev. Lett.*, vol. 38, pp. 1440–1443, Jun 1977.
- [84] P. Sikivie and Q. Yang, “Bose-Einstein Condensation of Dark Matter Axions,” *Phys. Rev. Lett.*, vol. 103, p. 111301, 2009.
- [85] O. Erken, P. Sikivie, H. Tam, and Q. Yang, “Cosmic axion thermalization,” *Phys. Rev. D*, vol. 85, p. 063520, 2012.
- [86] P. Sikivie, “The emerging case for axion dark matter,” *Phys. Lett. B*, vol. 695, pp. 22–25, 2011.

- [87] S. Jeon, “Hydrodynamic transport coefficients in relativistic scalar field theory,” *Phys. Rev. D*, vol. 52, pp. 3591–3642, Sep 1995.
- [88] S. Jeon and L. G. Yaffe, “From quantum field theory to hydrodynamics: Transport coefficients and effective kinetic theory,” *Phys. Rev. D*, vol. 53, pp. 5799–5809, May 1996.
- [89] B. Mihaila, J. F. Dawson, and F. Cooper, “Order  $1/n$  corrections to the time-dependent hartree approximation for a system of  $n+1$  oscillators,” *Physical Review D*, vol. 56, no. 9, p. 5400, 1997.
- [90] L. M. A. Bettencourt and C. Wetterich, “Time evolution of correlation functions for classical and quantum anharmonic oscillators,” 5 1998.
- [91] J. Berges, S. Borsanyi, U. Reinosa, and J. Serreau, “Renormalized thermodynamics from the 2PI effective action,” *Phys. Rev. D*, vol. 71, p. 105004, 2005.
- [92] R. Jackiw, “Functional evaluation of the effective potential,” *Phys. Rev. D*, vol. 9, pp. 1686–1701, Mar 1974.
- [93] H. van Hees and J. Knoll, “Renormalization in selfconsistent approximations schemes at finite temperature. 1. Theory,” *Phys. Rev. D*, vol. 65, p. 025010, 2002.
- [94] H. Van Hees and J. Knoll, “Renormalization of selfconsistent approximation schemes. 2. Applications to the sunset diagram,” *Phys. Rev. D*, vol. 65, p. 105005, 2002.
- [95] H. van Hees and J. Knoll, “Renormalization in selfconsistent approximation schemes at finite temperature. 3. Global symmetries,” *Phys. Rev. D*, vol. 66, p. 025028, 2002.
- [96] J.-P. Blaizot, E. Iancu, and U. Reinosa, “Renormalization of Phi derivable approximations in scalar field theories,” *Nucl. Phys. A*, vol. 736, pp. 149–200, 2004.
- [97] J. Berges, S. Borsanyi, U. Reinosa, and J. Serreau, “Nonperturbative renormalization for 2PI effective action techniques,” *Annals Phys.*, vol. 320, pp. 344–398, 2005.
- [98] J. Schwinger, “Brownian motion of a quantum oscillator,” *Journal of Mathematical Physics*, vol. 2, no. 3, pp. 407–432, 1961.
- [99] L. V. Keldysh, “Diagram technique for nonequilibrium processes,” *Zh. Eksp. Teor. Fiz.*, vol. 47, pp. 1515–1527, 1964.
- [100] D. Boyanovsky, H. J. de Vega, R. Holman, D.-S. Lee, and A. Singh, “Dissipation via particle production in scalar field theories,” *Phys. Rev. D*, vol. 51, pp. 4419–4444, Apr 1995.
- [101] S. Weinberg, “Gauge and global symmetries at high temperature,” *Phys. Rev. D*, vol. 9, pp. 3357–3378, Jun 1974.

- [102] M. Luscher, “Volume Dependence of the Energy Spectrum in Massive Quantum Field Theories. 2. Scattering States,” *Commun. Math. Phys.*, vol. 105, pp. 153–188, 1986.
- [103] R. Kanamoto, H. Saito, and M. Ueda, “Quantum phase transition in one-dimensional bose-einstein condensates with attractive interactions,” *Physical Review A*, vol. 67, no. 1, p. 013608, 2003.
- [104] N. Vakhitov and A. A. Kolokolov, “Stationary solutions of the wave equation in the medium with nonlinearity saturation,” *Radiophysics and Quantum Electronics*, vol. 16, no. 7, pp. 783–789, 1973.
- [105] R. Friedberg, T. Lee, and A. Sirlin, “Class of scalar-field soliton solutions in three space dimensions,” *Physical Review D*, vol. 13, no. 10, p. 2739, 1976.
- [106] A. Kovtun and M. Zantedeschi, “Breaking bec,” *arXiv preprint arXiv:2003.10283*, 2020.
- [107] A. Panin and M. Smolyakov, “Classical behaviour of Q-balls in the Wick–Cutkosky model,” *Eur. Phys. J. C*, vol. 79, no. 2, p. 150, 2019.